DOI: 10.1002/anie.200601780

Nanoelectronics

Insulated Molecular Wires

*Michael J. Frampton and Harry L. Anderson**

Keywords:
conjugated polymers · cyclodextrins · cyclophanes · dendrimers · rotaxanes

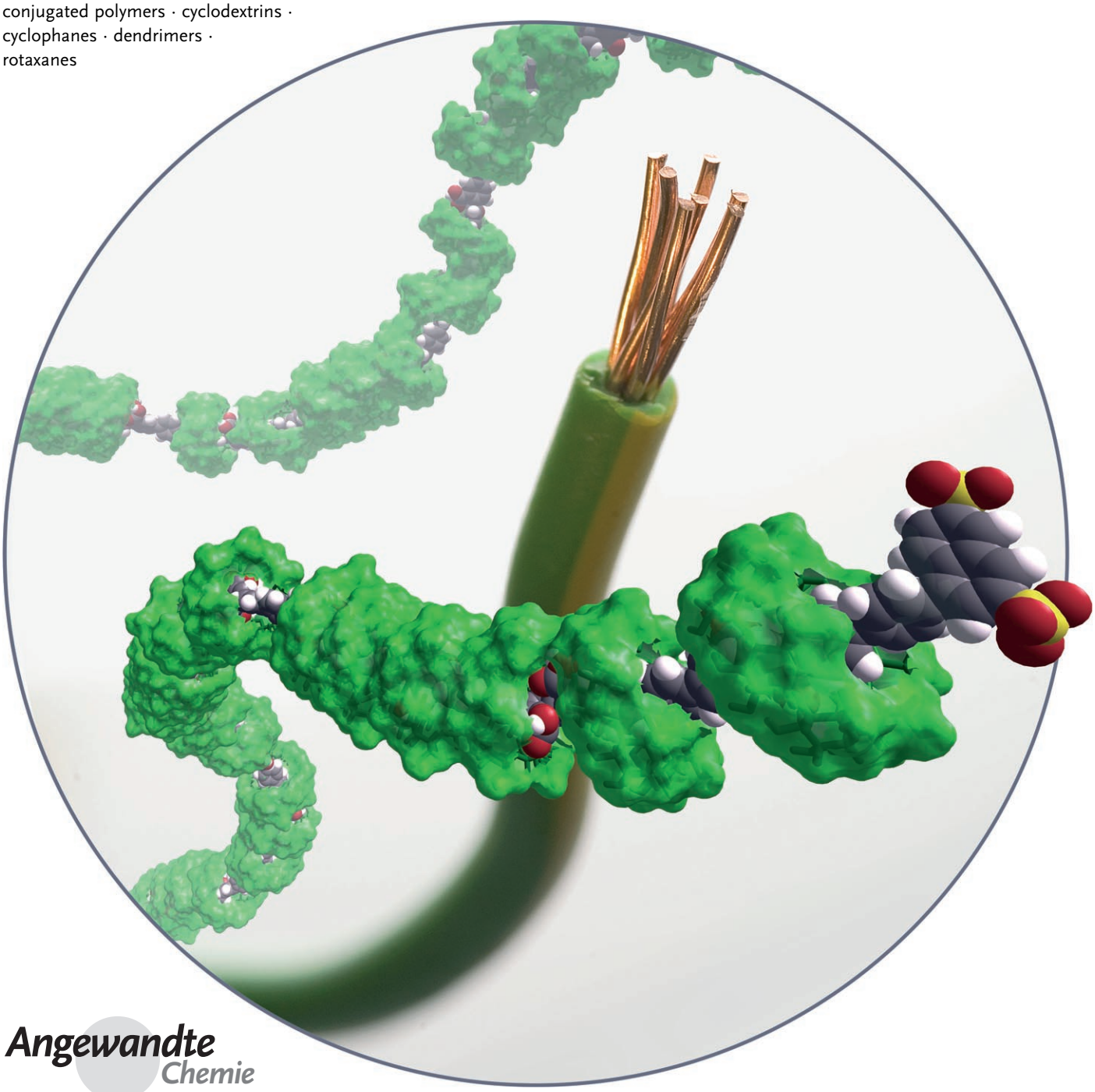

An astonishing assortment of structures have been described as "insulated molecular wires" (IMWs), thus illustrating the diversity of approaches to molecular-scale insulation. These systems demonstrate the scope of encapsulation in the molecular engineering of optoelectronic materials and organic semiconductors. This Review surveys the synthesis and structural characterization of IMWs, and highlights emerging structure–property relationships to determine how insulation can enhance the behavior of a molecular wire. We focus mainly on three IMW architectures: polyrotaxanes, polymer-wrapped π systems, and dendronized polymers, and compare the properties of these systems with those of conjugated polymers threaded through mesoporous frameworks and zeolites. Encapsulation of molecular wires can enhance properties as diverse as luminescence, electrical transport, and chemical stability, which points to applications in electroluminescent displays, sensors, and the photochemical generation of hydrogen.

From the Contents

1. Introduction

Two great discoveries have shaped research on organic semiconductors: the demonstration of metallic conductivity in doped polyacetylene by Shirakawa, MacDiarmid, Heeger, and co-workers in 1977,[1] and the demonstration of electroluminescence in undoped conjugated polymers by Friend, Holmes, and co-workers in 1990.[2] However, interest in "molecular wires" started long before these breakthroughs. During the 1940s it was widely believed that the π–π* energy gaps of long conjugated polyenes of the type *trans*-H(CH=CH)$_n$H would decrease continually with increasing chain length (n), reaching zero in polyacetylene ($n=\infty$) and resulting in metallic conductivity along the polymer backbone.[3] This inspirational misconception was dispelled by experimental work on the absorption spectra of polyenes,[4] and by developments in molecular orbital theory,[5] which led to the concept of Peierls distortion (that is, alternation of the bond lengths in polyacetylene).[6] Enthusiasm for molecular wires was rekindled in the 1960s by the discovery of metallic conductivity in polysulfurnitride $(SN)_n$,[7] and by Little's proposal that polyacetylenes substituted with cyanine dyes might be superconductors.[8]

Today, conjugated polymers are gaining commercial importance in light-emitting diodes,[2,9,10] thin-film field-effect transistors,[11] photovoltaic cells,[12] and sensors.[13] High charge mobility along individual polymer chains is critical to most of these applications, so these polymers are called "molecular wires",[14] even though a single molecule can never behave like a macroscopic strand of metal.[15] The term "molecular wire" is used interchangeably with "conjugated polymer" or "conjugated oligomer" when considering such systems at the molecular scale. A macroscopic sample of a conjugated polymer can be viewed as a mass of molecular wires.

The description of conjugated polymers as molecular wires immediately suggests that it would be worth exploring *insulated* molecular wires (IMWs), to prevent cross-talk or short-circuits, by using a protective cylindrical sheath.[16] Interchain interactions modify the optical and electronic behavior of conjugated polymers, so it is useful to be able to block these interactions. Encapsulation of a single conjugated molecule can also have dramatic effects on the chemical stability and luminescence efficiency. Chemical reactivity—and the lack of operational stability under environmental conditions—is a common problem with organic semiconductors, and solving this problem is a compelling motivation for investigating IMWs.

A wide variety of structures have been described as "insulated" or "encapsulated" molecular wires, thus illustrating the broad appeal of this concept. Some of the first examples were conjugated polymers threaded through zeolites and mesoporous hosts, as pioneered by Bein and co-workers[17–19] as well as others.[20–25] For example, the conjugated polymer MEH-PPV can thread into mesoporous silica as depicted in Figure 1.[20] Silicate and aluminosilicate frameworks provide ideal linear channels for isolating polymer chains. The polymer can be synthesized in the host or incorporated after polymerization.[21] However, one of the main advantages of organic semiconductors, compared to their inorganic counterparts, is solution processability, and this advantage is lost when the polymer is threaded into a solid host. This Review focuses on IMWs in which the molecularity of the wire is preserved. Zeolite and clathrate-type IMWs, which can only exist in the solid state, have been

[*] Dr. M. J. Frampton, Prof. H. L. Anderson
Department of Chemistry
University of Oxford
Chemistry Research Laboratory
12 Mansfield Road, Oxford, OX1 3TA (UK)
Fax: (+44) 1865-285-002
E-mail: harry.anderson@chem.ox.ac.uk
Homepage: http://users.ox.ac.uk/~hlagroup/

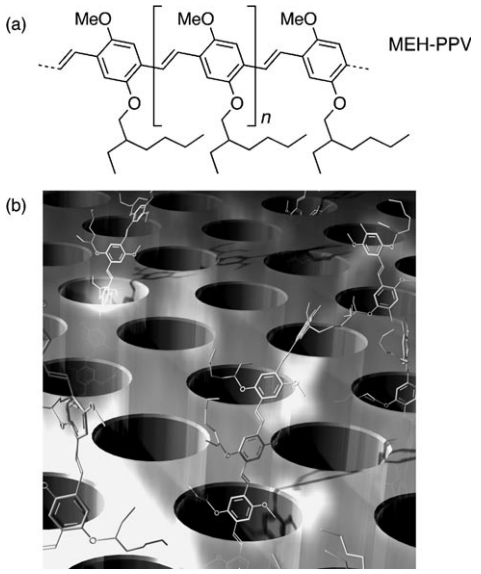

Figure 1. a) Structure of the conjugated polymer poly[2-methoxy-5-(2′-ethylhexyloxy)-1,4-phenylenevinylene] (MEH-PPV). b) Schematic representation of chains of MEH-PPV threaded into the channels of mesoporous silica. Each pore has a diameter of 22 Å, which is large enough to accommodate just one MEH-PPV chain. (Reprinted from Ref. [20]. Picture: Daniel Schwartz, D.I.S.C. Corporation.)

comprehensively reviewed previously,[22] and are only discussed here for comparison with other types of IMWs. Another class of materials sometimes described as IMWs is that of column discotic stacks. These materials can exhibit high charge mobilities along the stack axis, even though they lack a covalent backbone.[26] Here we focus on three types of IMWs, all with covalent conjugated backbones: 1) polyrotaxanes, in which the conjugated π system is encapsulated by threading through a series of macrocycles; 2) polymer–polymer complexes in which one polymer strand wraps round the other; and 3) dendronized conjugated polymers, in which the insulation is covalently grafted to the wire. Sections 2–4 summarize the various approaches to the synthesis and structural characterization of these three types of IMWs, then Section 5 analyzes how insulation modifies the properties of molecular wires in these diverse systems.

The structural authentication of supramolecular polymers, such as conjugated polyrotaxanes, polymer–polymer complexes, and dendronized polymers, poses particular challenges. The first questions to ask are: 1) Does the conjugated backbone have the purported covalent structure? 2) What is the level of threading, wrapping, or dendronization? What is the stoichiometry between the "conducting" and "insulating" parts of the structure? 3) How long is the conjugated backbone and what is the molecular-weight distribution? In the case of polyrotaxanes, one must also ask about the polymer end groups. The determination of the molecular weight is problematic with many of these systems. The most commonly employed method of determining the number-average molecular weight $\bar{M}_n$ and the mass-average molecular weight $\bar{M}_w$ is GPC analysis with polystyrene standards. This method can give inaccurate results with polymers that do not resemble polystyrene: Shape-persistent rodlike polymers tend to give erroneously high molecular weights by GPC,[27] whereas compact polymers, such as dendrimers, give erroneously low values.[28] In this Review we have attempted, wherever possible, to give quantitative estimates of the polymer chain length in terms of a number-average degree of polymerization $\bar{n}_n$, which is simply $\bar{M}_n$ divided by the mass of the repeat unit. In many cases these $\bar{n}_n$ values may be inaccurate by more than a factor of 2, but we believe that it is vital to keep in mind even a crude estimate of $\bar{n}_n$, otherwise one risks concluding that a high value of $\bar{M}_n$ or $\bar{M}_w$ indicates a high degree of polymerization when it may only reflect the huge mass of the polymer repeat unit.

2. Rotaxane, Polyrotaxane, and Pseudopolyrotaxane IMWs

One strategy for insulating a molecular wire is to thread it through a series of insulating macrocycles to form a pseudopolyrotaxane or polyrotaxane (Figure 2). A variety of macrocyclic receptors form inclusion complexes with rodlike guests; when the guest is long enough to protrude from both ends of the macrocycle these inclusion complexes are called pseudorotaxanes. The presence of bulky substituents at both ends of the guest results in a rotaxane structure, in which the dumbbell-shaped guest is trapped inside the cavity of the macrocycle. If the guest is threaded through several macrocycles, this leads to a main-chain pseudopolyrotaxane or polyrotaxane architecture.[29]

Investigation of short monodisperse conjugated oligomers, as model compounds, can provide valuable insights into the corresponding polymers. These oligomers have the tremendous advantage that they can be purified and charac-

Michael Frampton studied at Oxford University and completed his DPhil at Oxford with Dr Paul Burn on electroluminescent dendrimers (2002). He then worked as a research chemist at Cambridge Display Technology Ltd (and previously at Opsys Ltd) on the design of organic electroluminescent materials. He is currently a Postdoctoral Research Fellow exploring the synthesis of insulated molecular wires for optoelectronic applications.

Harry Anderson completed his PhD at Cambridge University with Prof. Jeremy Sanders. After postdoctoral work with Prof. François Diederich (ETH Zürich) he was appointed to a lectureship in Oxford in 1994. His research concerns the design and synthesis of molecular and supramolecular materials for optoelectronic applications, with particular emphasis on conjugated porphyrin oligomers and rotaxane architectures. In 2001 he was awarded a Corday–Morgan Medal from the Royal Society of Chemistry.

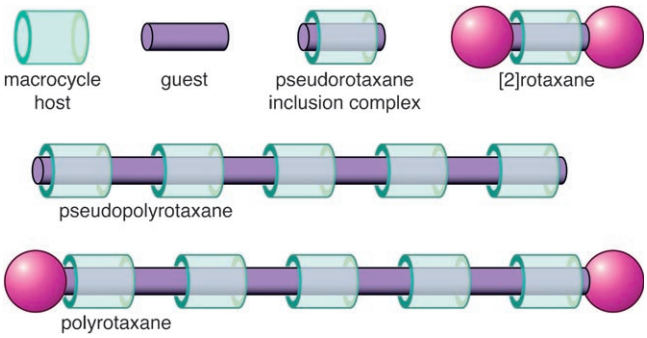

Figure 2. An introduction to polyrotaxane terminology. In this example, the polyrotaxane is actually a [6]rotaxane.

terized more rigorously. The evolution of their properties with increasing chain length can be extrapolated to those of long polymers.[30] This "oligomer approach" is particularly pertinent to conjugated polyrotaxanes because of the difficulty of characterizing and understanding such complex architectures. Thus, the following sections include discussion of [2]rotaxanes and [3]rotaxanes with conjugated cores, such as encapsulated dyes,[31] as well as polyrotaxanes.

2.1. Cyclophane Systems

2.1.1. Metal-Directed Threading

The first issue to consider when planning the synthesis of a rotaxane is how to make one molecule thread through another. The same issue applies equally to the synthesis of catenanes, where the linear thread is subsequently cyclized. The field of catenane synthesis was revolutionized in 1983 when Sauvage showed that a metal cation can be used as a template to direct the threading process.[29a,32] Lehn and co-workers applied this metal-directed strategy to the synthesis of a "rack-type" [4]pseudorotaxane $[\mathbf{1}\cdot Cu_3\subset\mathbf{2}_3]^{3+}$ (Scheme 1).[33] Two molecules of macrocycle **2** are unable to coordinate with the copper(I) ions to form a $[\mathbf{2}_2\cdot Cu]^+$ complex, so when a stoichiometric amount of copper is added, the only way of satisfying all the binding sites is to form a threaded complex. The structure of $[\mathbf{1}\cdot Cu_3\subset\mathbf{2}_3]^{3+}$ was confirmed by NMR spectroscopic studies and by comparison with related compounds (which were characterized by X-ray crystallography) including a shorter [4]pseudorotaxane with pyridazine–metal binding units.[33]

Swager and co-workers have applied this strategy to synthesize conjugated pseudopolyrotaxanes by the electropolymerization of thiophene-terminated monomers; in this case copper(I) and zinc(II) ions were used as templates (Scheme 2).[34,35] The polymer $[\mathbf{4}\cdot Zn_n\subset\mathbf{2}_n]^{2n+}$ is formed as an insoluble film on the anode, but it can be demetalated by treatment with diaminoethane. This conjugated pseudopolyrotaxane $\mathbf{4}\subset\mathbf{2}_n$ binds reversibly to Zn^{2+} and Cu^{2+} ions, which alters its conductivity and suggests potential applications in sensors (see Section 5.7). In this case, the insolubility of the polymer prevents loss of the macrocycle. The metal-binding properties of this pseudopolyrotaxane are a consequence of

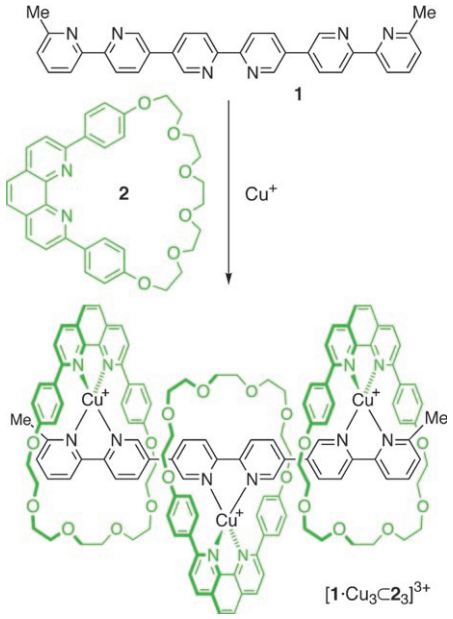

Scheme 1. Metal-directed formation of a [4]pseudorotaxane.[33]

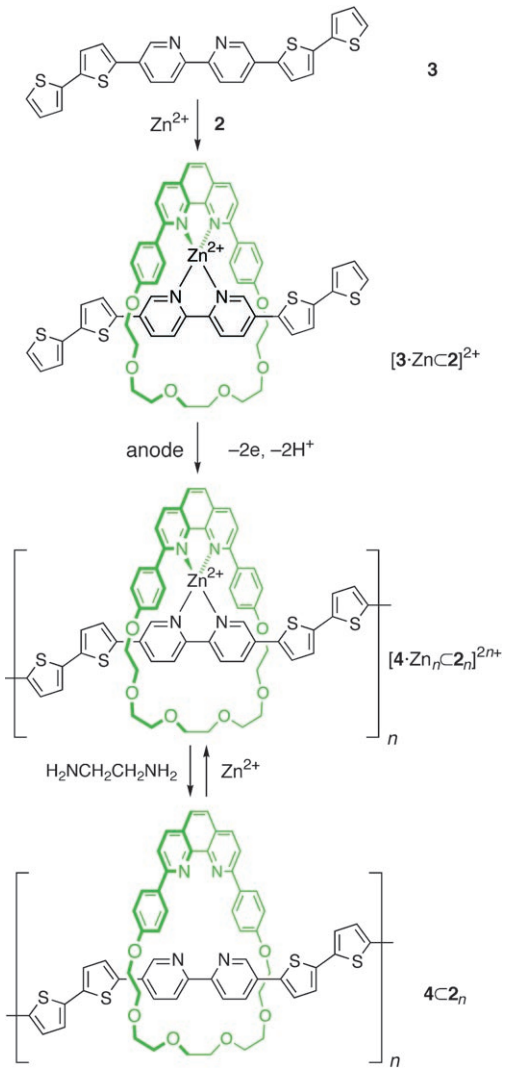

Scheme 2. Metal-directed synthesis of a pseudopolyrotaxane.[34]

its threaded structure, and are not exhibited by the unthreaded polymer **4**.

Related pseudopolyrotaxanes were investigated by Sauvage and co-workers. In the case of $[\mathbf{5}\cdot Cu_n\subset\mathbf{2}_n]^{n+}$, it is only

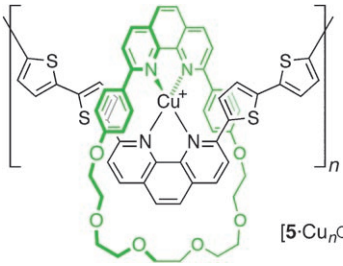

possible to reincorporate a Cu^+ ion if the Li^+ center is added during removal of the copper(I) template to give $[\mathbf{5}\cdot Li_n\subset\mathbf{2}_n]^{n+}$. The topology of the coordination sites seems to be lost irreversibly in the metal-free polymer $\mathbf{5}\subset\mathbf{2}_n$.[36] In another system, substitution of the phenanthroline ligand was used to control the reversibility of the metalation.[37]

Metal-directed self-assembly has also been used to synthesize a conducting triple-strand ladder polymer (Scheme 3).[38] Oxidative electropolymerization of $[\mathbf{3}\cdot Cu\subset\mathbf{6}]^+$ was carried out in two stages: first macrocycle **6**, which has a short electron-rich 3,4-(ethylenedioxy)thiophene (EDOT) end group, was polymerized to give strands of **7** by cycling the potential from −0.5 to +0.55 V (versus Fc/Fc^+). Higher potentials were then applied to polymerize the longer threaded component **3** to generate strands of **4**, thereby giving the ladder polymer $[\mathbf{4}_2\cdot Cu_{2n}\subset\mathbf{7}]^{2n+}$. Zinc(II) ions can also be used as a template in this synthesis. Each step in the polymerization was monitored electrochemically, but the product is completely insoluble and amorphous, so it is difficult to evaluate how well the product matches the idealized triple-strand structure.

Metallo-pseudopolyrotaxanes can exhibit remarkably high conductivities when the redox potential of the metal matches the oxidation potential of the π system, thus leading to potential applications in chemoresistive sensors (Section 5.7).[39]

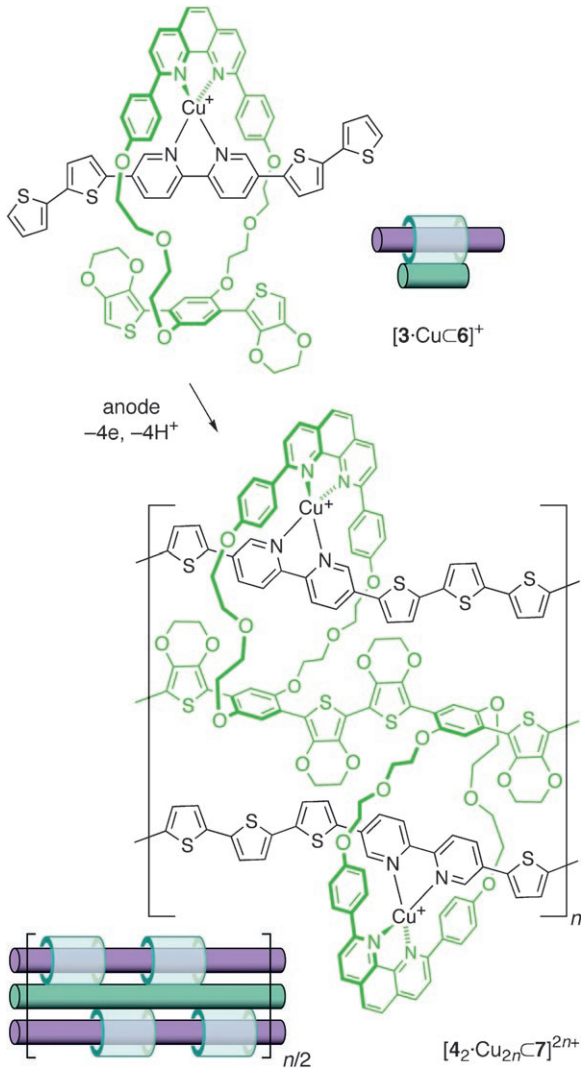

Scheme 3. Synthesis of a triple-strand conducting ladder polymer. The anodic electropolymerization is carried out in two stages: first the electron-rich central chain **7** is formed, then the two outer strands **4**.[38]

2.1.2. Hydrophobic Cyclophanes

Although metal coordination provides a precise and predictable way of directing the synthesis of IMWs, it has the disadvantage that metal binding sites need to be built into both the wire and the insulation. Hydrophobic binding is an alternative way of directing the threading process, and it avoids the need for specific binding sites because most conjugated molecules are hydrophobic. The challenge is to design a system which is sufficiently soluble in water, and to control the expression of this inherently less selective—and less predictable—form of molecular recognition. There are many examples of water-soluble macrocycles with hydrophobic cavities, such as cyclophanes[40] and cyclodextrins (see Section 2.2), which bind suitably shaped hydrocarbons in aqueous solution.

The most thoroughly studied synthetic water-soluble macrocycles are the cyclophanes developed by Diederich and co-workers; an example of these compounds is $\mathbf{8}^{2+}\cdot 2\,Cl^-$,

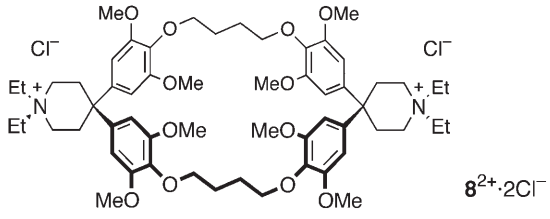

which features a hydrophobic box defined by four aromatic sidewalls.[40] The quaternary ammonium centers make these chloride salts water soluble, while preserving the hydrophobicity of the cavity. Cyclophane $\mathbf{8}^{2+}$ forms inclusion complexes with many *para*-disubstituted aromatic compounds in aqueous solution; for example our research group

found that it forms a 1:1 complex with the alkyne $\mathbf{9}^{2+}$ (Scheme 4) with an association constant of $4 \times 10^4\,\text{M}^{-1}$, despite the fact that both species are dications. Glaser coupling of this $[\mathbf{9}\subset\mathbf{8}]^{4+}$ complex in water gives a [3]rotaxane $[\mathbf{10}\subset\mathbf{8}_2]^{8+}$ with a long conjugated core as the main product, together with the [2]rotaxane $[\mathbf{10}\subset\mathbf{8}]^{6+}$ and the dumbbell $\mathbf{10}^{4+}$.[41] A neutral version of [3]rotaxane $[\mathbf{10}\subset\mathbf{8}_2]^{8+}$ was also synthesized with sulfonated stoppers (Section 5.5).[42] This study represented the first synthesis of rotaxanes with long π-conjugated cores. Attempts to extend this methodology to longer poly(phenylenebutadiynylene) polyrotaxanes by polymerization of 1,4-diethynylbenzene in the presence of cyclophane $\mathbf{8}^{2+}$ and stopper $\mathbf{9}^{2+}$ failed as a result of aggregation and precipitation of the conjugated oligomer intermediates.[41] A similar principle has been implemented successfully by polymerizing 1,4-diethynylbenzene inside a mesoporous MCM-41 silica host that had been functionalized with a copper(II) complex to catalyze the Glaser coupling reaction inside the silica channels.[25]

2.2. Cyclodextrin-Based IMWs

2.2.1. Introduction to Cyclodextrin-Threaded Structures

Cyclodextrins are naturally occurring molecular tubes (Figure 3).[43] The commonest forms are α- and β-cyclodextrin, with six and seven α-1,4-linked glucopyranose units, respectively, and minimum internal van der Waals diameters of 4.3 and 6.0 Å, respectively (calculated from the H-5 polygon).[44,45] Larger cyclodextrins are also available, such as γ-CD with eight glucose units (internal minimum van der Waals diameter 7.4 Å from the H-5 polygon).[46] The rim-to-rim tube length is about 8.7 Å, but this dimension varies with the conformation, and cyclodextrins often pack more closely than this in the solid state through hydrogen-bonding interactions to form channel structures[47] with head-to-tail or head-to-head arrangements (Figure 4).[48] The crystal structures of these hydrogen-bonded channels enable the maximum possible packing density of cyclodextrins along a polyrotaxane to be estimated. The length of a cyclodextrin unit in a channel with a head-to-tail, head-to-head, and head-to-tail/head-to-head packing arrangement is 8.2, 7.8, and 7.7 Å, respectively.

Native cyclodextrins are soluble in water, as well as in polar organic solvents such as DMSO, DMF, and pyridine.

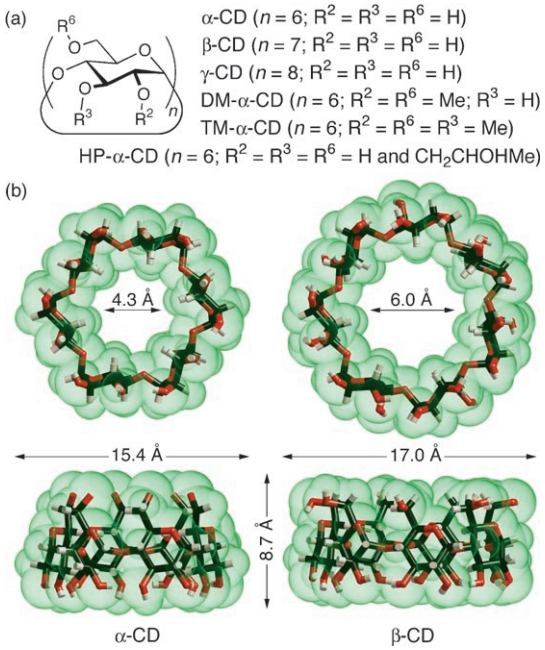

Figure 3. a) Structures of α-, β-, and γ-cyclodextrin, as well as some of their common derivatives. b) Examples of crystallographic conformations of α- and β-cyclodextrin,[44,45] showing the dimensions of the van der Waals surface. The projections down the cavity (top) show the wider 2,3-rim at the front and the side views (bottom) have the narrower 6-rim at the top. Internal and external diameters are calculated from the H-5 and H-2 polygons, respectively; the tube length (8.7 Å) is estimated from the mean distance of the O-6 atoms from the mean plane of the O-3 polygon.

Common cyclodextrin derivatives include the 2,3,6-tri-*O*-methyl cyclodextrins (TM-α/β-CD) and the 2,6-di-*O*-methyl cyclodextrins (DM-α/β-CD).[49] These methylated cyclodextrins are soluble in most solvents, from hexane to water. 2-Hydroxypropylcyclodextrins (HP-α/β-CD) are widely used because of their high solubility in water, although these materials are complex mixtures, generally with an average of about 0.6 substituents per glucose unit.

Cyclodextrins form inclusion complexes with a wide variety of organic guests in aqueous solution and in the solid state.[50] The stability of these complexes in solution mainly comes from hydrophobic interactions, and they generally dissociate in organic solvents. The first cyclodextrin-threaded polymers to be thoroughly investigated were

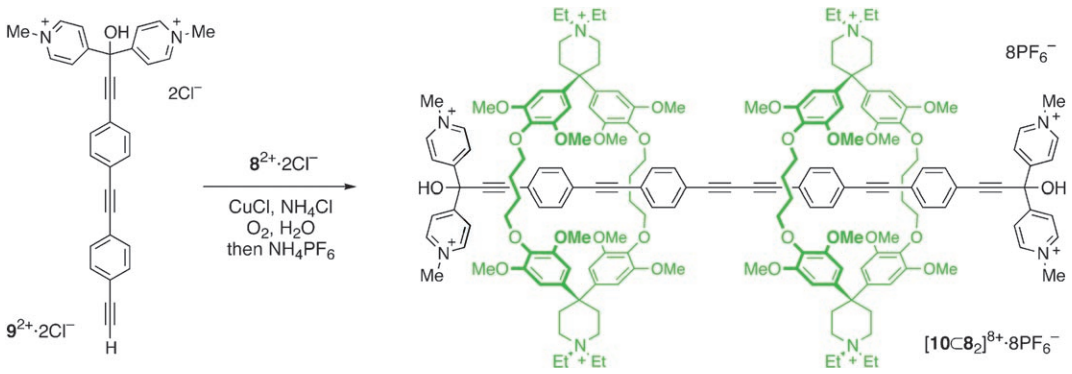

Scheme 4. Synthesis of a conjugated [3]rotaxane by Glaser coupling in water.[41]

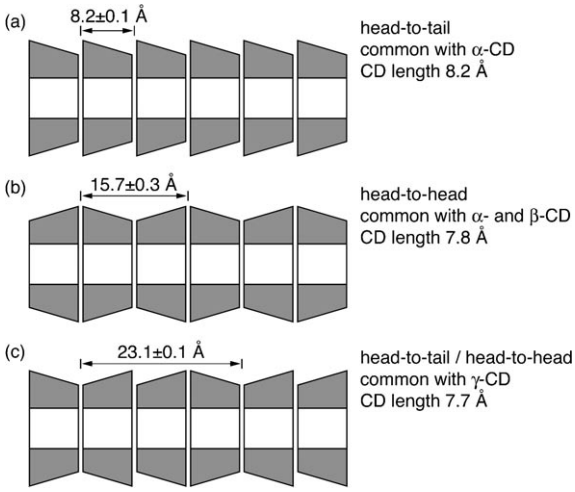

Figure 4. Cyclodextrins form three types of hydrogen-bonded channel structures in the solid state. The repeat distances shown here (which are averages from many crystal structures found in the Cambridge Crystallographic Database)[48] enable the maximum number of cyclodextrins that might thread onto a polymer of a given length to be estimated.

reported independently by Harada and Kamachi[51] and by Wenz and Keller.[52] These studies provided the first demonstration that polymers can thread through cyclodextrins to generate pseudopolyrotaxanes. The two systems provided a powerful inspiration for the synthesis of cyclodextrin-threaded molecular wires,[53] and they have become archetypes of two distinct classes of pseudopolyrotaxanes.

Harada and Kamachi prepared a pseudopolyrotaxane as a crystalline precipitate by adding polyethylene glycol (PEG) to an aqueous solution of α-CD. These PEG⊂α-CD complexes are essentially insoluble in water, but dissolve with dissociation in DMSO and DMF. They have stoichiometries of approximately two ethylene glycol repeat units per α-CD, which implies that the cyclodextrins are tightly packed along the PEG chain through formation of hydrogen-bonded channels. Comparison of the powder X-ray diffraction pattern of this material with those of other α-CD inclusion complexes led to the conclusion that the cyclodextrins are packed in a head-to-head arrangement. If the PEG adopts a fully extended all-*anti* conformation then the length of the -O-CH_2-CH_2- repeat unit is (3.50 ± 0.05) Å,[54] thus a channel length per cyclodextrin of (7.8 ± 0.1) Å (Figure 4b) corresponds to a theoretical stoichiometry of 0.45 CD molecules per repeat unit.

Wenz and Keller investigated the threading of cyclodextrins onto cationic polyelectrolytes.[52] The ammonium groups slow down the threading process, so that in some cases it takes weeks or even years to reach equilibrium at room temperature. The ammonium centers also prevent the cyclodextrins from packing tightly together along the chain, so that the relative orientation of neighboring cyclodextrin units is probably random. The most dramatic difference between this system and PEG⊂α-CD is that the cationic pseudopolyrotaxanes are soluble in water. This probably reflects the greater flexibility of these polyrotaxanes, which arises from the lack of a rigid hydrogen-bonded channel structure, as well as the presence of ionic charge.

Many cyclodextrin-based rotaxanes and polyrotaxanes have been reported, and the field has been recently reviewed.[55] Here we provide a critical analysis of the small fraction of this field relevant to IMWs.

2.2.2. *Azo-Dye Rotaxanes*

Many azo dyes form complexes with cyclodextrins. These inclusion complexes were first investigated by Cramer et al. when they reported in 1967 that methyl orange **11** forms a 1:1 complex with α-cyclodextrin in water.[56] Although the 1:1 complex is formed in solution (stability constant $1.1 \times 10^4\ M^{-1}$), the material crystallizes as the 1:2 complex **11**⊂$(\alpha\text{-CD})_2$, in which the chromophores sit head-to-tail in continuous tubes of hydrogen-bonded head-to-tail cyclodextrins (Figure 5).[57] This channel structure points to the possibility of creating long IMWs.

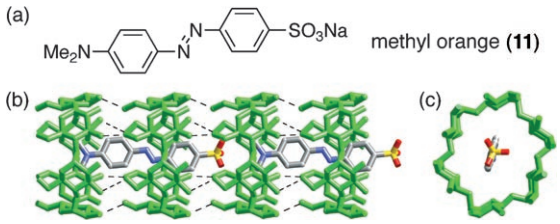

Figure 5. a) Structure of methyl orange. b, c) Two orthogonal views of the methyl orange–(α-CD) complex **11**⊂$(\alpha\text{-CD})_2$ in the solid state.[57] The cyclodextrins form continuous head-to-tail hydrogen-bonded tubes. Dashed lines indicate O6···O3 hydrogen bonds between neighboring α-CD rings. The repeat distance of the α-CD along the axis of the channel is 8.30 Å (see Figure 4a).

Azo dyes are generally prepared by azo coupling, and this reaction proceeds well in water, so that hydrophobic binding can be used to direct the formation of azo-dye rotaxanes, as illustrated with bisdiazonium salt **12** in Scheme 5.[58] In this example, the phenol stopper **13** gives a [3]rotaxane **14**⊂$(\alpha\text{-CD})_2$ as the main product. If the coupling of **12** and **13** is carried out in the presence of one equivalent of α-CD, the [3]rotaxane **14**⊂$(\alpha\text{-CD})_2$ still predominates over the [2]rotax-

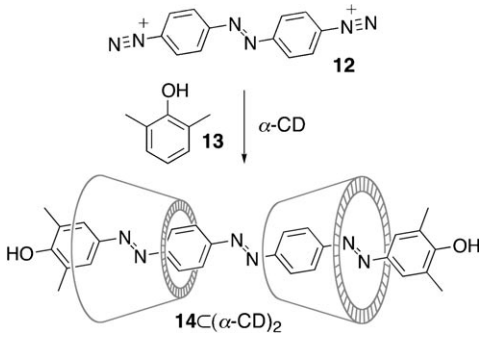

Scheme 5. Rotaxane synthesis by azo coupling (in aqueous solution at pH 9).[58] The α-CD is represented by a truncated cone which is narrower at the 6-rim.

ane **14**⊂α-CD, thus indicating that there is a favorable hydrogen-bonding interaction between the two threaded cyclodextrins. An NMR spectroscopic analysis has shown that the [3]rotaxane is formed exclusively as one stereoisomer, with the primary 6-OH rims at the center (NOE interactions are observed from the methyl protons to H-3 of the cyclodextrin).

Although azo coupling is a convenient reaction for synthesizing azo-dye rotaxanes, there does not seem to be space for the reaction to occur in the cavity of a cyclodextrin. Thus rotaxanes are often formed with at least one azo group exposed to the external environment. We prepared azo-dye rotaxanes such as **15**⊂TM-α-CD,[59] in which the azo chromophore is permanently locked inside the cavity of a cyclodextrin, by using chlorotriazine. These rotaxanes exhibit dramatically enhanced chemical stability and photostability (Section 5.1). Other examples of azo-dye rotaxanes have been synthesized by using pyridine alkylation[60] and Suzuki coupling.[61]

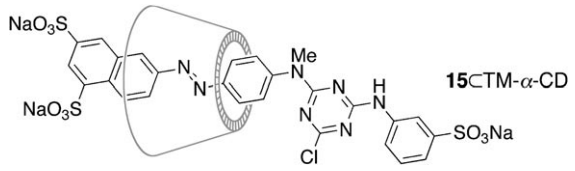

2.2.3. *Cyanine Rotaxanes*

Cyanine dyes consist of an amine electron donor linked to an iminium electron acceptor through a π-conjugated polymethine bridge. They have important applications as fluorescent probes, near-IR dyes, and nonlinear optical materials.[64] These chromophores played a key role in the development of a theoretical understanding of molecular wires and electronic conjugation because their absorption spectra shift to longer wavelengths as the π system is extended, much as would be expected for a simple one-dimensional "electron in a box" model (Figure 6). The large reduction in the S_0–S_1 gap with increasing chain length reflects the efficient π overlap and the lack of bond-length alternation. It has been shown that longer cyanine dyes do undergo the expected Peierls distortion,[65] thus limiting the reduction in the S_0–S_1 gap that can be achieved simply by increasing the length of the π system. The longer cyanines become increasingly unstable under ambient conditions, as a result of the reactivity of the polymethine bridge, and provide a motivation for the synthesis of rotaxanes in which this vulnerable region of the molecule is shielded from the environment. We have found that cyanine rotaxanes can be synthesized by aqueous Knoevenagel reactions, as illustrated in Scheme 6.[66,67] Both stereoisomers of the [2]rotaxane A-**16**⊂α-CD and B-**16**⊂α-CD are formed in this reaction, and were separated by chromatography. The chemical stability of the cyanine dye is enhanced in these rotaxanes (Section 5.1).

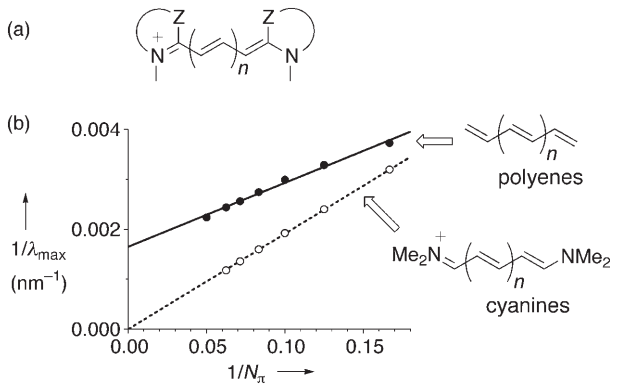

Figure 6. a) General structure of a cyanine dye. b) Plot of $1/\lambda_{max}$ for the absorption band with the longest wavelength versus the reciprocal of the number of π electrons for simple polyenes and cyanines (polyene data in isooctane;[62] cyanine data for perchlorate salts in dichloromethane[63]).

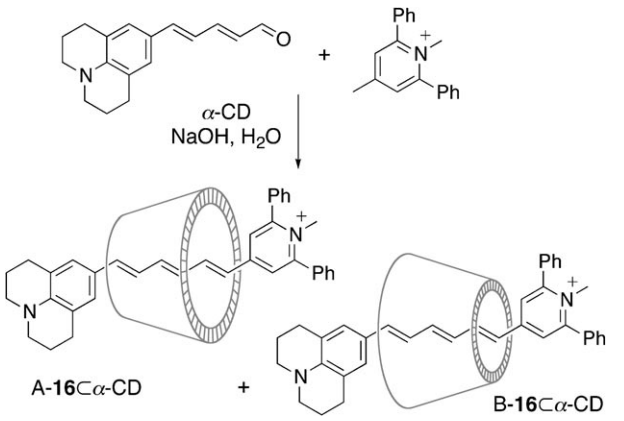

Scheme 6. Synthesis of a separable mixture of two stereoisomers of a cyanine rotaxane.[66,67]

2.2.4. *Biphenyl- and Stilbene-based Rotaxanes and Polyrotaxanes*

Suzuki coupling is one of the most widely used methods for the synthesis of conjugated polymers. The palladium-catalyzed coupling of a boronic acid $R^1B(OH)_2$ with an organic halide R^2X leads to the formation of biphenyl or stilbene derivatives R^1-R^2 (R^1 and R^2 are generally aryl or vinyl groups).[68] The reaction works well in water, and we have used this approach to synthesize [2]rotaxanes such as **17**⊂α-CD and **18**⊂α-CD (Figure 7).[69,70] The solid-state structures of both these [2]rotaxanes have been determined by single-crystal X-ray analysis. It is interesting to compare their structures with those of the only other two crystallographically characterized cyclodextrin rotaxanes **19**⊂α-CD and **20**⊂α-CD.[71,72] All four structures have an α-cyclodextrin clasped round the waist of a stilbene unit, and the cyclodextrin does not appear to have any significant affect on the conformation of the stilbene π system. All four structures feature π–π stacking interactions between the ends of the dumbbell units, thus leading to infinite one-dimensional strands (Figure 7) and suggesting a mechanism for long-range charge transport in a bulk material made up of longer polyrotaxane IMWs (Sections 5.6 and 5.7).

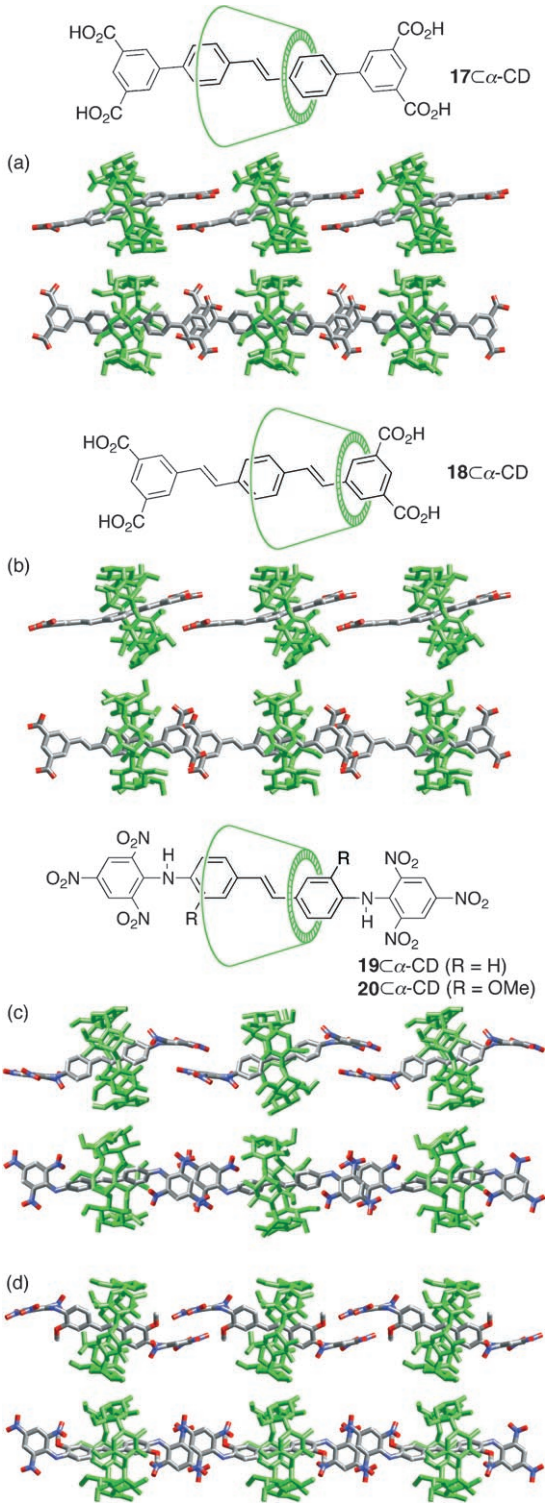

Figure 7. [2]Rotaxane molecules stack in a π–π arrangement into infinite strands in the crystal structures of **17**⊂α-CD (a),[69] **18**⊂α-CD (b),[70] **19**⊂α-CD (c), and **20**⊂α-CD (d).[71] In each case two orthogonal views of the π-stacked strand are shown.

We have used Suzuki coupling to synthesize conjugated polyrotaxanes from a diboronic acid and a water-soluble diiodide with a small amount of a bulky mono-iodide stopper, as illustrated by the synthesis of the threaded poly(*para*-phenylene) **PPP1**⊂β-CD (Scheme 7).[73] We also used this method to prepare polyrotaxanes with cores based on polyfluorene (**PF1**⊂β-CD), poly(4,4′-diphenylenevinylene)

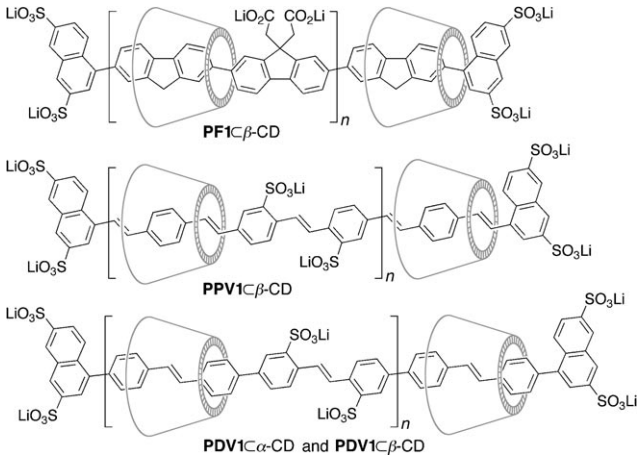

(**PDV1**⊂α-CD and **PDV1**⊂β-CD), as well as poly(phenylenevinylene) (**PPV1**⊂α-CD and **PPV1**⊂β-CD).[70,73] These polyrotaxanes have some resemblance to the pseudopolyrotaxanes developed by Wenz and Keller,[52] in that they are very soluble in water and DMSO. The cyclodextrin rings are separated by polar ionic residues, so that there is probably no interaction between them along the chain. ^{1}H NMR spectroscopic analysis of these polyrotaxanes allows the number of threaded cyclodextrins to be determined (Figure 8). This value can be quantified by the threading ratio $y = x/(n+1)$. In some cases it is also possible to integrate the proton resonances of the stopper units, and thus to estimate the degree of polymerization. Excess cyclodextrin and low-molecular-weight impurities are readily removed by dialysis, and this experiment provides a good test for the integrity of the polyrotaxane: if the ends of the chain are not capped with bulky stoppers then the cyclodextrin gradually slips off the chains. This property can be illustrated by the plots of threading ratio (determined from NMR apectroscopic analysis) as a function of the volume of water eluted through the ultrafiltration cell (Figure 8). At the start of the experiment, when no water has been eluted through the ultrafiltration membrane, the apparent threading ratio determined by integration of the ^{1}H NMR signals is very high, because of the presence of free cyclodextrin. In the case of the pseudopolyrotaxane **PPP2**⊂β-CD with small end groups, all the cyclodextrin is washed off during dialysis, whereas with **PPP1**⊂β-CD the threading ratio does not fall below a value of about 1.1.

The molecular weights of these polyrotaxanes, as determined by equilibrium ultracentrifugation, agree well with the values determined by NMR spectroscopic quantification of the end groups and with those predicted from the mole ratio of monofunctional iodide used in the polymerization reactions. In general, the average degree of polymerization is intentionally limited to $\bar{n}_n = 10$, by adjusting the polymerization stoichiometry, to minimize accidental termination, but reasonable agreement between expected and experimental

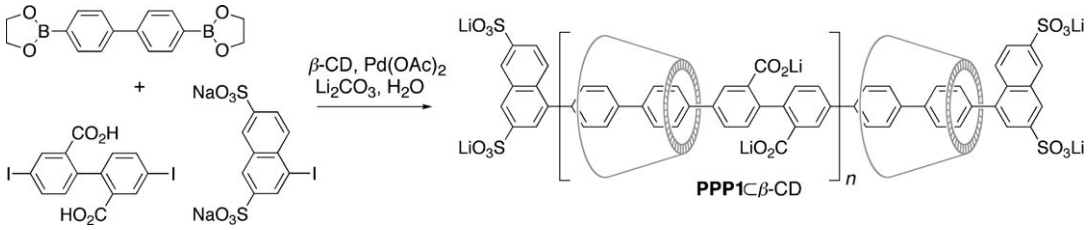

Scheme 7. Synthesis of a poly(*para*-phenylene) polyrotaxane.[73]

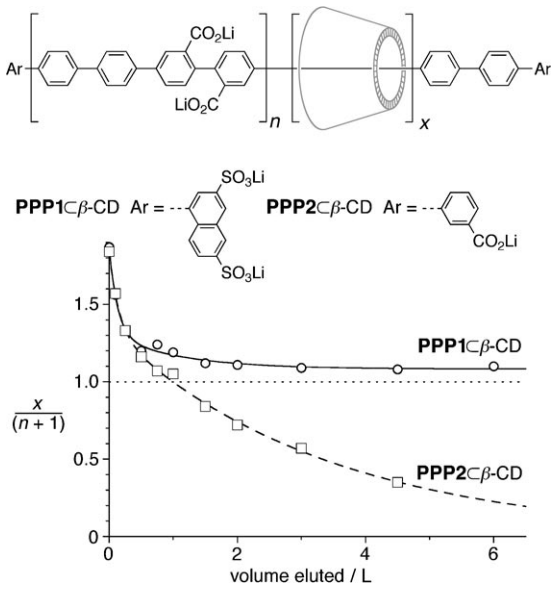

Figure 8. Dialysis of polyrotaxane **PPP1**⊂β-CD and pseudopolyrotaxane **PPP2**⊂β-CD (both with $\bar{n}_n = 10$) through a 5-kDa NMWCO membrane. The threading ratio [$\bar{y}_{NMR} = x/(n+1)$], determined by integration of the ^{1}H NMR signals, is plotted versus the volume of water eluted.[73]

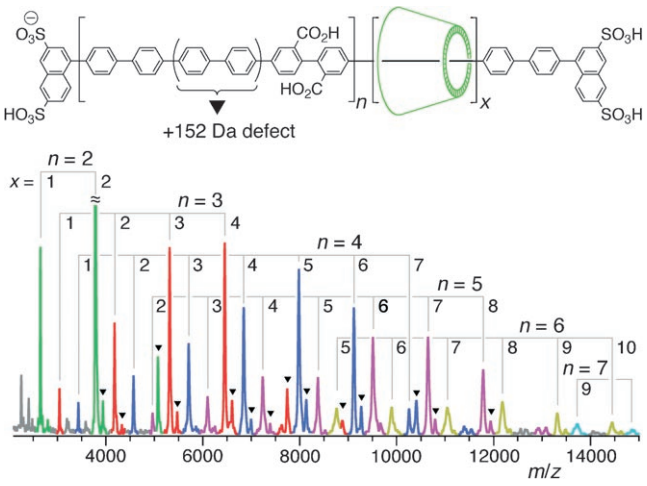

Figure 9. MALDI-TOF mass spectrum of **PPP1**⊂β-CD ($\bar{n}_n = 10$), with α-cyano-4-hydroxycinnamic acid used as the matrix (negative mode). Triangles indicate molecular ions corresponding to chains with one extra biphenyl unit. Color code: $n = 2$ (green), $n = 3$ (red), $n = 4$ (blue), $n = 5$ (purple), $n = 6$ (mustard), and $n = 7$ (turquoise).[73]

molecular weights is maintained up to $\bar{n}_n = 20$. (In this case an average chain contains 84 benzene rings and the mean contour length is 36 nm.) Further insights into the structure of these polyrotaxanes are provided by mass spectra. Figure 9 shows such a spectrum for **PPP1**⊂β-CD, which reveals families of signals of species with different numbers of threaded cyclodextrins for each number of repeat units. All the main signals in this spectrum fit with the expected species, but there are also some minor signals with *m*/*z* values 152 Da higher (marked with triangles in Figure 9) which are due to oxidative homocoupling of the diboronic acid monomer. These minor signals are generally associated with an extra threaded cyclodextrin, thus reflecting the hydrophobicity of the unsubstituted biphenyl group.

Whereas NMR spectroscopy gives a measure of the average number of cyclodextrins threaded on each polyrotaxane (for example, a threading ratio of $\bar{y} = 1.1$), mass spectrometry reveals the distribution of the threading ratios: it is evident that some chains are sparsely covered while others have much higher threading ratios, with more than one cyclodextrin per unsubstituted biphenyl unit. The length of the polymer repeat units of **PPP1**⊂β-CD, **PF1**⊂β-CD, **PPV1**⊂β-CD, and **PDV1**⊂β-CD are 17.3, 16.8, 20.0, and 21.9 Å, respectively, so the maximum numbers of cyclodextrins that could be accommodated in Harada–Kamachi structures (Figure 4) are 2.2, 2.2, 2.6, and 2.8 β-CDs per repeat unit, respectively.

These polyrotaxanes have been imaged by tapping mode AFM.[74] Figure 10 shows the image obtained using **PPP1**⊂β-CD with a nominal degree of polymerization of $\bar{n}_n = 30$ (calculated from the ratio of the reactants in the polymerization), so the polyrotaxanes should have number-average contour lengths of about 50 nm. The observed structures have roughly the expected width and height for a cyclodextrin (after correction for the tip dimensions), but they are surprisingly long, with contour lengths in the region of 100 nm. This observation probably reflects the selective adsorption of longer chains onto the mica surface during spin-coating. It is interesting that, while individual **PPP1**⊂β-CD polyrotaxane molecules can be imaged reproducibly by AFM, it is not possible to image individual molecules of unthreaded **PPP1** (Section 5.8).

This section has focused on systems prepared by Suzuki coupling because this methodology has led to rapid progress in the synthesis of IMWs. Several biphenyl- and stilbene-based cyclodextrin rotaxanes have been synthesized using other types of chemistry.[75] The synthesis of an anthracene-terminated β-cyclodextrin–polyfluorene polyrotaxane by Yamamoto coupling has also been reported.[76]

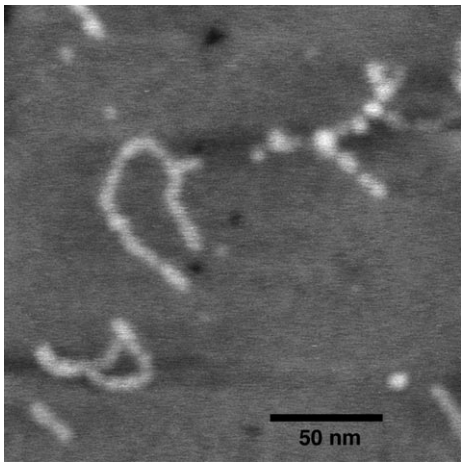

Figure 10. Tapping mode AFM image of **PPP1**⊂β-CD ($\bar{n}_n = 30$), spin-coated from aqueous solution onto mica. The corrected dimensions of a rod are estimated to be about 1.6 nm (width) and (0.4 ± 0.1) nm (height).[74]

2.2.5. *Polythiophene Polyrotaxanes*

Polythiophenes are one of the most widely studied family of organic semiconductors, and there have been several investigations into the synthesis of pseudopolyrotaxanes consisting of polythiophenes threaded through cyclodextrins.[76–83] 2,2′-Bithiophene (**2T**) forms strong 1:1 complexes with β-CD, DM-β-CD, and HP-β-CD in aqueous solution. The stability constants of the β-CD and HP-β-CD complexes are 3.8×10^3 and $3.6 \times 10^3\,\text{M}^{-1}$, respectively.[77,78] A crystal-structure analysis of the $(\mathbf{2T})_3{\cdot}(\beta\text{-CD})_2$ complex has also been reported.[79] The cyclodextrins pack into a hydrogen-bonded head-to-head channel structure (Figure 4b), with one **2T** molecule in the cavity of each CD, and a third **2T** molecule sitting between the 2,3-rims of two β-CD units. Lagrost et al. have shown that **2T** can be electropolymerized in aqueous solution in the presence of HP-β-CD to form a pseudopolyrotaxane (Scheme 8).[78]

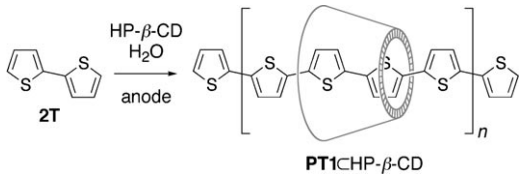

Scheme 8. Synthesis of a polythiophene pseudopolyrotaxane.[78] A similar product can be obtained by chemical oxidation with $FeCl_3$.[79]

HP-β-CD was used rather than native β-CD to increase the solubility of the cyclodextrin and its complex with **2T**. The pseudopolyrotaxane is deposited as a film on the anode surface, and is almost completely insoluble, although its solubility in DMF (ca. $1\,\text{g}\,\text{L}^{-1}$) is greater than that of ordinary unthreaded polythiophene of the same chain length. UV/Vis, Raman, FTIR, and XPS analysis of solid films of the pseudopolyrotaxane confirmed the presence of the polythiophene and cyclodextrin components, and indicated a ratio of 0.03–0.23 cyclodextrins per thiophene unit (depending on the synthesis conditions). Harada and co-workers prepared a similar pseudopolyrotaxane, as a purple precipitate, by oxidizing aqueous solutions of **2T**⊂β-CD and **2T**⊂DM-β-CD with $FeCl_3$.[79] The mechanism of these aqueous oxidative polymerizations has been investigated in solution by using flash photolysis,[80] and on anode surfaces by using a quartz microbalance.[81] The reaction seems to proceed by diffusion-controlled dimerization of radical cations, followed by threading of cyclodextrins onto the nascent polythiophene chains. Yamaguchi et al. have shown that polythiophene slowly forms inclusion complexes with aqueous β-CD.[82] A water-soluble pseudopolyrotaxane forms after stirring polythiophene with β-CD for about three weeks in water. Further threading of cyclodextrin leads to precipitation of a pseudopolyrotaxane with about 0.1 cyclodextrins per thiophene unit, which implies that large regions of the polymer remain uncovered.

Hadziioannou and co-workers have recently reported the synthesis of an anthracene-terminated polythiophene polyrotaxane **PT2**⊂β-CD by nickel-catalyzed Yamamoto coupling

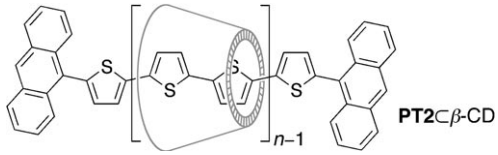

in DMF.[76] Small-angle neutron-scattering data indicate that this polyrotaxane has a degree of polymerization of about $\bar{n}_n = 12$ and an average of 0.6 β-CDs per bithiophene repeat unit (the length of this repeat unit is 7.8 Å, so the polymer could accommodate up to 1.0 β-CD per repeat unit).

Polypyrrole is closely related to polythiophene, but to the best of our knowledge, the synthesis of cyclodextrin–polypyrrole polyrotaxanes has yet to be achieved, although a few relevant experiments have been reported.[84]

2.2.6. *Polyaniline Pseudopolyrotaxanes*

Polyaniline (PANI) is an unusual type of conjugated polymer in that it can be doped by protonation, as well as by oxidation (Scheme 9). The conductivity increases by 10 orders of magnitude to around $10^2\,\text{S}\,\text{cm}^{-1}$ when the emeraldine base is protonated to give the emeraldine salt.[85] Polyaniline is also easy to synthesize, by oxidation of aniline, and it has several applications: in rechargeable batteries, sensors, electromagnetic screening fabrics, and electrochromic devices.[85]

IMWs consisting of polyaniline threaded through cyclodextrins were first investigated by Ito and co-workers by using frequency-domain electric birefringence (FEB) spectroscopy and scanning tunneling microscopy (STM).[86] The FEB technique probes molecular optical and electric anisotropy, so rodlike molecules give strong electric birefringence whereas isotropic species, such as coiled polymer chains, give no response. Addition of a large excess of β-CD to a solution of emeraldine base in *N*-methyl-2-pyrrolidinone

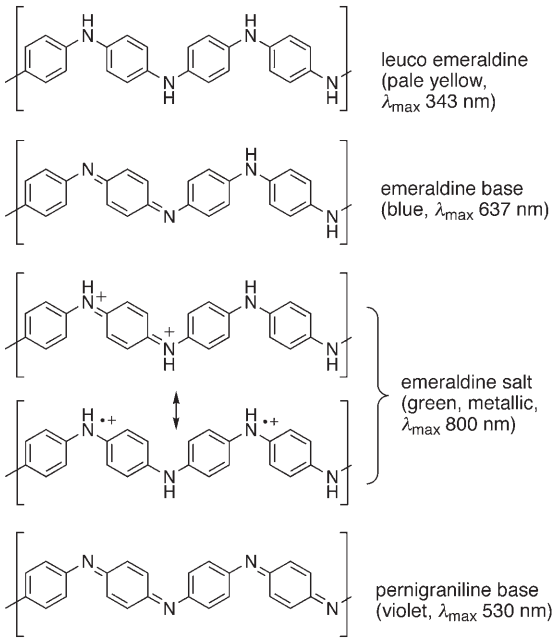

Scheme 9. The redox/protonation states of polyaniline (PANI).[85]

(NMP) at temperatures below 275 K gives a strong increase in the FEB signal, apparently resulting from a change in the polymer conformation (Figure 11).

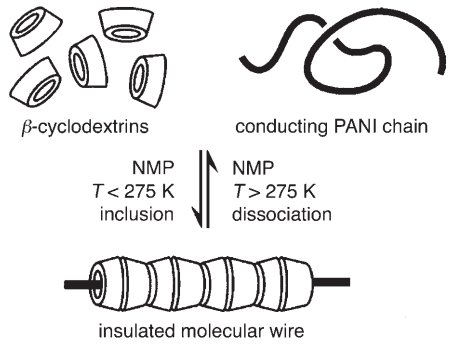

Figure 11. Schematic representation of the complexation of polyaniline with β-CD. Adapted with permission from Ref. [86]. Copyright 2005 American Chemical Society.

No FEB response is observed under these conditions in the absence of β-CD, nor in the presence of β-CD at temperatures above 275 K. The strong temperature dependence of the binding process was attributed to the loss of conformational entropy in the polyaniline, and to the loss of translational entropy in the many threaded cyclodextrin molecules. The stoichiometry of this polymer inclusion complex has not been determined, but it is assumed that the cyclodextrins are closely packed along the polyaniline chain—in a structure resembling PEG⊂α-CD—because otherwise it is difficult to see how the presence of threaded macrocycles could have such a strong influence on the conformation of the polymer backbone. A computational study[87] of PANI⊂β-CD concluded that the threaded cyclodextrin favors a more conjugated planar conformation for the π system, and that a structure with 1.0 β-CD per aniline unit (packed head-to-head) is likely. However, the length of the aniline repeat unit projected onto the polymer backbone axis is only 5.1 Å (from crystal structures of short oligomers[88]), so the cyclodextrin channel parameters (Figure 4) imply that the polymer could not accommodate more than 0.65 β-CDs per aniline unit.

Complexation of β-CD and emeraldine base was also observed at room temperature in water/NMP mixed solvent systems. Under these conditions the inclusion complex falls out of solution as a crystalline blue precipitate.[86,89] No complexation was observed with α-CD. STM images of the β-CD polyaniline complex spin-coated onto highly oriented pyrolytic graphite (HOPG) revealed rodlike structures with lengths matching the contour length of the polyaniline (300 nm) and heights corresponding approximately to the external diameter of a cyclodextrin.[86] It was not possible to image strands of the unthreaded polyaniline, presumably because it adopts a compact coiled conformation or aggregates. Similar PANI⊂β-CD inclusion complexes have been prepared by the oxidative polymerization of *N*-phenyl-1,4-phenylenediamine or aniline in the presence of aqueous β-CD, although the material produced by in situ polymerization of aniline contains only 0.07 cyclodextrins per aniline repeat unit.[90]

Ito and co-workers have also shown that polyaniline emeraldine base forms inclusion complexes with cross-linked α-cyclodextrin nanotubes.[91,92] These nanotubes are prepared by covalently linking α-CDs together, through formation of ether links with epichlorohyrin, on a PEG template.[93] It is interesting that polyaniline binds strongly to these α-CD-based nanotubes in aqueous NMP without requiring a large excess of the nanotubes, whereas it does not bind native α-CD. AFM images of these inclusion complexes, spin-coated onto mica, show long rodlike structures (Figure 12). The length of the individual nanotubes is around 25 nm (by STM), so several nanotubes fit onto a polyaniline strand with a contour length of around 300 nm. The distribution of contour lengths for the nanotube inclusion complexes (Figure 12c) indicates that some strands consist of several polyaniline chains spliced end-to-end by nanotubes (Figure 12b).[92]

Complexation of polyaniline hinders oxidative doping with iodine,[94] but it does not prevent protonic doping; acidification of the nanotube complexes results in a strong red-shift in their absorption, as a result of formation of the emeraldine salt.[95] Single-molecule conductivity measurements on these IMWs have been reported recently (Section 5.7).[95]

2.2.7. *Schiff Base Polyazomethine Polyrotaxanes*

The idea of making IMW-type polyrotaxanes by imine formation has been pioneered by Farcas and Grigoras.[96] They investigated the acid-catalyzed condensation of 1,4-phenylenediamine with terephthalaldehyde in the presence of β-CD in hot DMF, with 4-triphenylmethylaniline used as a bulky stopper (Scheme 10). The product of this reaction, **PAM1**⊂β-CD, is rather insoluble, which made characterization difficult. The ^{1}H NMR spectrum (in [D_6]DMSO at 70 °C)

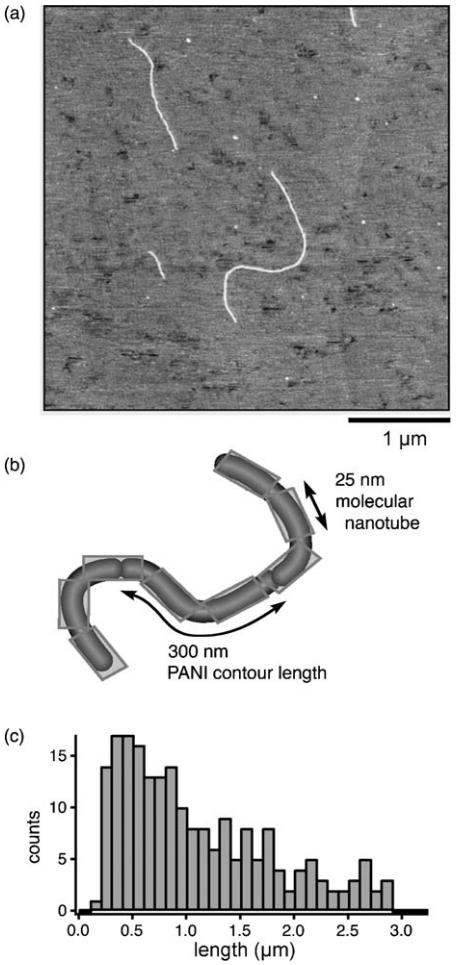

Figure 12. a) AFM image of polyaniline threaded through α-CD-based molecular nanotubes on a cleaved mica substrate (4 μm × 4 μm); b) schematic representation of an IMW formed by molecular nanotubes linking some polyaniline chains; c) contour-length histogram from 210 AFM images of these IMWs. Reprinted with permission from Ref. [92]. Copyright 2002 American Institute of Physics.

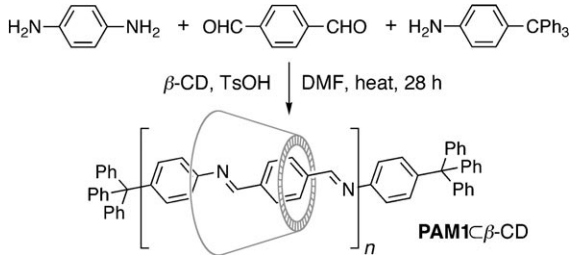

Scheme 10. Synthesis of a polyazomethine polyrotaxane.[96]

shows aromatic and sugar resonances, and GPC analysis in DMF using polystyrene standards gives a number-average molecular weight $\bar{M}_n$ of 18600 g mol^{-1}, which corresponds to an average degree of polymerization $\bar{n}_n$ of 13, assuming one β-CD per polymer repeat unit. The amount of threaded cyclodextrin was not determined, and no evidence was provided for incorporation of the trityl end groups. A similar material was also obtained using α-CD.

Farcas and Grigoras also prepared polyrotaxanes **PAM2**⊂β-CD and **PAM3**⊂β-CD, by treating *N*-butyl-3,6-

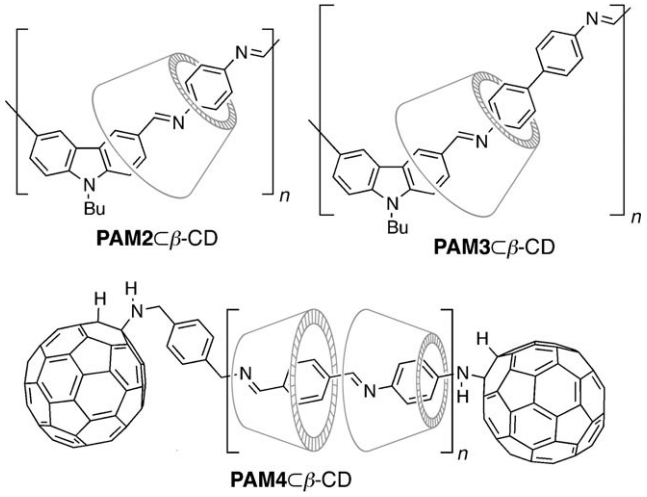

diformylcarbazole with 1,4-phenylenediamine and 4,4′-diaminobiphenyl, respectively, under similar reaction conditions.[97,98] The combined effect of the nonlinear backbone, butyl sidechains, and threaded cyclodextrins make these pseudopolyrotaxanes soluble in methanol, DMSO, and DMF (but they remain insoluble in water), whereas the corresponding polymers **PAM2** and **PAM3** without threaded cyclodextrins are insoluble in methanol and only sparingly soluble in DMF. ^{1}H NMR analysis of **PAM2**⊂β-CD and **PAM3**⊂β-CD in [D$_6$]DMSO indicates that the numbers of β-CDs per repeat unit are about 0.6 and 1.0, respectively, thus reflecting stronger binding on the biphenyl residue. GPC analysis of **PAM2**⊂β-CD and **PAM3**⊂β-CD in DMF with polystyrene standards gave $\bar{M}_n$ values of 16200 and 22500 g mol^{-1}, respectively ($\bar{n}_n = 16$ and $\bar{n}_n = 14$, respectively).

Geckeler and co-workers have synthesized a fullerene-terminated polyrotaxane **PAM4**⊂β-CD, in essentially the same manner as the synthesis of **PAM1**⊂β-CD by Farcas and Grigoras, by terminating the polymerization with 1,4-xylylenediamine followed by C_{60}.[99] The length of the polymer repeat unit of **PAM4**⊂β-CD is the same as that of **PAM1**⊂β-CD (12.6 Å),[54] so if the cyclodextrins form a close-packed channel (Figure 4) there would be 1.6 β-CDs per repeat unit. This theoretical maximum threading ratio agrees quite well with the ^{1}H NMR results (in [D$_6$]DMSO), which indicate that there are two cyclodextrins per repeat unit. GPC analysis gave a number-average molecular weight $\bar{M}_n$ of 82400 g mol^{-1} (compared to polystyrene standards) which implies a degree of polymerization $\bar{n}_n$ of 33 (assuming 2 β-CDs per repeat unit). The polyrotaxane was characterized by ^{13}C NMR, IR, UV/Vis, and fluorescence spectroscopy as well as TGA and cyclic voltammetry. However, it is not clear how closely it matches the proposed structure for **PAM4**⊂β-CD, and the observation that the material is soluble in water seems counter to expectations.

Recently Liu et al. reported the synthesis of **PAM5**⊂β-CD.[100] They used essentially the same polycondensation

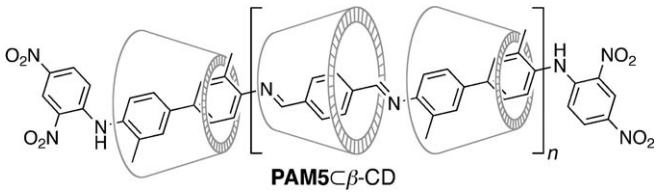

conditions as Geckeler and co-workers, except that the chains were terminated by adding 2,4-dinitrofluorobenzene. This end group is not large enough to prevent β-CD from unthreading, so the material is a pseudopolyrotaxane. In practice, unthreading may not be a problem because **PAM5**⊂β-CD is so insoluble. It is too insoluble in DMF for solution-phase NMR or GPC analysis, so its composition was determined by hydrolysis in [D_6]DMSO/DCl, which generated a mixture of *o*-tolidine, terephthalaldehyde, β-CD, and the *o*-tolidine-2,4-dinitrobenzene adduct (1.00:1.09:1.80:0.13 from ^{1}H NMR integration). This is approximately the expected ratio of components if one assumes 2 β-CDs per repeat unit and $\bar{n}_n = 4$ (calculated ratio: 1.00:0.80:1.80:0.40). This composition is consistent with the amount of nitrogen from combustion analysis. The proposed structure was supported by ^{13}C cross-polarization magic-angle-spinning solid-state NMR spectroscopy. STM images of **PAM5**⊂β-CD on HOPG revealed long straight strands; the diameter of these strands (1.5 nm) matches that of β-CD, but their length is greater than 100 nm, whereas a degree of polymerization of $n = 4$ should give a length of about 8 nm. This discrepancy was ascribed to an end-to-end association of pseudopolyrotaxane units, but it is difficult to envisage why they should associate in this way.

All the cyclodextrin-threaded polyazomethines discussed here were synthesized in anhydrous DMF, whereas most cyclodextrin-threaded systems are prepared in water.[101] Of course the reason for this is that polyazomethines are hydrolyzed by water. The binding of guests to cyclodextrins in organic solvents has not been thoroughly investigated, but in the few previous cases where strong binding was observed ($K > 100\,\text{M}^{-1}$) it was attributed to hydrogen bonding, and a nonthreaded "lid-type" equatorial geometry was postulated.[102] So it is remarkable that Geckeler and co-workers report that β-CD binds 1,4-phenylenediamine and terephthalaldehyde in DMF at 25 °C to form 1:1 complexes with association constants of (740 ± 300) and $(860 \pm 300)\,\text{M}^{-1}$, respectively.[97] Liu et al. report similar association constants of (570 ± 30) and $(740 \pm 40)\,\text{M}^{-1}$ for *o*-tolidine and terephthalaldehyde, respectively, under identical conditions.[100] Another puzzling feature of this chemistry is that all three research groups found that polyrotaxanes were formed most effectively by using the isolated β-CD inclusion complexes of the starting materials, rather than by allowing β-CD to bind to the stating materials in situ during polymerization. One might have expected the monomer–β-CD binding process to reach equilibrium within a few seconds, but Farcas and Grigoras report that it takes 6–8 h at 50 °C to form the β-CD inclusion complexes of 1,4-phenylene diamine and 4,4′-diaminobiphenyl in DMF.[98] Many aspects of this chemistry are not well understood, but it provides an intriguing route to conjugated polyrotaxanes.

2.2.8. Polysilane Peudopolyrotaxanes

Polysilanes have Si-Si linked backbones and behave like π-conjugated polymers, in that their UV absorption bands shift to longer wavelength with increasing chain length and they can be doped with oxidants to produce semiconducting materials. This property leads to the concept of "σ conjugation". Harada and co-workers have synthesized inclusion complexes of polydimethylsilane Me(SiMe$_2$)$_n$Me (where $\bar{n}_n = 5$–13) with γ-CD, as crystalline precipitates by stirring the solid polymer with an aqueous solution of cyclodextrin.[103] The stoichiometry of these complexes, determined from ^{1}H NMR spectra recorded in [D_5]pyridine, indicates that there is one γ-CD per three SiMe$_2$ repeat units, and X-ray powder diffraction data support a head-to-head channel structure (Figure 13). Crystallographic data on (SiMe$_2$)$_n$ oligomers[104] shows that the length of the Si–Si bond

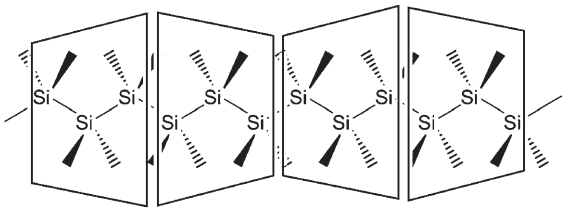

Figure 13. Proposed structure of the γ-CD–polydimethylsilane inclusion complex.[103]

projected onto the polymer axis for an extended all-*anti* (SiMe$_2$)$_n$ chain is 1.94 Å, so it seems unlikely that the polymer chain could accommodate more than one γ-CD for each 4.0 SiMe$_2$ units if the cyclodextrins form a close-packed channel (7.7 Å per γ-CD; Figure 4c).[48] β-Cyclodextrin does not form complexes with these polysilanes but it does bind short oligomers Me(SiMe$_2$)$_n$Me, where $n = 1$–5. See Section 3.2 for a discussion of related schizophyllan glucan complexes.

2.3. Threaded Cucurbiturils

The cucurbit[*n*]urils (CB[*n*], $n = 5$–10) are a family of pumpkin-shaped macrocycles derived from glycoluril and formaldehyde.[105–109] CB[6] has been known since 1905 and its binding behavior has been explored by Mock and co-workers since the 1980s.[105] The other members of this family only became available recently as a consequence of studies by the

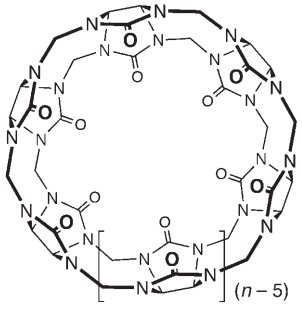

CB[*n*] (*n* = 5 to 10)

research groups of Kim and Day,[110] which has led to a flurry of activity during the last few years. Cucurbiturils are often regarded as cyclodextrin analogues, and the cavity sizes of CB[6], CB[7], and CB[8] roughly correspond to those of α-, β-, and γ-CD, respectively, although their guest affinities are often very different.[111] The central cavity of a cucurbituril is hydrophobic, like that of a cyclodextrin, but the rims of a cucurbituril are lined with convergent carbonyl groups, which leads to strong charge–dipole interactions with cationic guests, as well as hydrogen-bonding interactions with organic ammonium ions. Thus cucurbiturils generally bind cationic and neutral guests, but not anions. CB[5] accommodates small molecules such as N_2; CB[6] binds protonated α,ω-diaminoalkanes $^{+}NH_3(CH_2)_nNH_3^{+}$ ($n = 4$–7, $K = 10^5$–$10^6\ M^{-1}$ in aqueous formic acid)[106] as well as neutral species such as THF; CB[7] forms 1:1 complexes with larger cations, such as methyl viologen (MV^{2+}, $K = 2 \times 10^5\ M^{-1}$ in aqueous buffer),[112] and neutral molecules such as ferrocene; CB[8] has such a large cavity that it is able to simultaneously accommodate two aromatic guests the size of (*E*)-diaminostilbene.[113] The poor solubilities of cucurbiturils can be a critical factor limiting their use. Most binding studies are performed in aqueous acid as cucurbiturils are insoluble in most organic solvents. Several routes to functionalized cucurbiturils have been pursued to overcome this problem, particularly with CB[5] and CB[6],[114] but efficient routes to soluble derivatives of CB[7] and CB[8] have yet to be developed.

Many cationic dyes form stable 1:1 inclusion complexes with CB[7] in aqueous solution (association constants $K > 10^5\ M^{-1}$).[115] Complexation generally enhances the photostability of the dye, as with cyclodextrin complexes (Section 5.1). The remarkably low polarizability inside the cucurbituril cavity extends the fluorescence lifetimes of the encapsulated dyes.[116] Many cucurbituril-based rotaxanes, polyrotaxanes, and pseudopolyrotaxanes have been reported.[106,117,118] None of these systems feature long conjugated threaded π systems, but the recent explosion of interest in CB[7] and CB[8], together with their strong affinities for aromatic guests, lead us to suspect that cucurbiturils will soon make an important contribution to the field of IMWs.

2.4. Conclusions on the Synthesis of Polyrotaxane IMWs

Many polyrotaxane and pseudopolyrotaxane IMWs have been synthesized from both cyclophane and cyclodextrin macrocycles. All of these syntheses use noncovalent interactions to drive the threading process. Often these reactions are carried out in water, so that hydrophobic interactions favor threading, but some cyclodextrin polyrotaxanes can be synthesized in organic solvents (Sections 2.2.6 and 2.2.7). Metal coordination provides the most predictable way of positioning a conjugated π system through the cavity of a macrocycle (Section 2.1.1). Solubility is often a critical issue, and there are many examples of insoluble cyclodextrin- and cyclophane-based pseudopolyrotaxanes, which limits the scope for structural characterization or device fabrication. Excellent solubility can be achieved by using a charged polymer backbone (Section 2.2.4), but the ionic nature of these polyelectrolyte IMWs complicates their behavior in optoelectronic devices (Section 5.6). Charged substituents tend to prevent the macrocycles from packing closely along the chain, thereby leading to gaps in the insulating sheath. One of the main themes in our current research is the development of efficient routes to soluble nonpolar neutral polyrotaxane IMWs with closely packed threaded macrocycles. Most of the common types of conjugated polymers have now been threaded through macrocycles, but there are still many challenges in the engineering of these materials at the molecular level. Perhaps one day it will be possible to insulate any type of molecular wires in a sheath of specified dielectric constant, wall-thickness, persistence length, and solubility by synthesizing a polyrotaxane.

3. Polymer-Wrapped IMWs

Another strategy for encapsulating a molecular wire is to wrap it with a polymer, so that it becomes the guest inside the axial cavity of a helix. There is probably scope for threading molecular wires inside the axial cavities of many helical polymers, but so far most examples involve just two natural polysaccharides: amylose, which has a α-1,4-D-glucose backbone, and schizophyllan glucan (SPG), a branched polysaccharide based on β-1,3-D-glucose units.

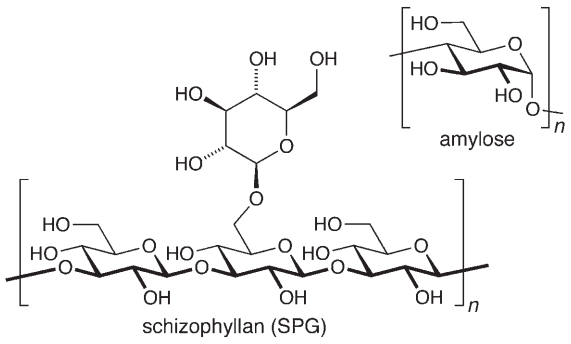

3.1. Amylose-Encapsulated Molecular Wires

Amylose is the main component of starch, where it is found along with the branched polysaccharide amylopectin. Amylose generally adopts helical conformations, as shown by crystallographic studies on the pure polymer[119–123] and on its blue iodine inclusion complex.[124] In nature, amylose occurs as two main polymorphs, A[120] and B[121] which are found in cereals and potatoes, respectively, both of which are double-strand parallel helix structures. A single-helical V polymorph is formed from solutions of amylose in solvents such as DMSO.[122] All these polymorphs have six glucose residues per helical turn, with a pitch that varies from about 8 Å in the V form to about 21 Å in the A and B forms. When viewed down the helix axis (Figure 14a), V-amylose presents an axial cavity which is very similar to that of α-cyclodextrin (Figure 3b), and the structures of amylose inclusion complexes generally resemble those of cyclodextrin pseudopolyrotaxanes.[124] As with cyclodextrins, complex formation is

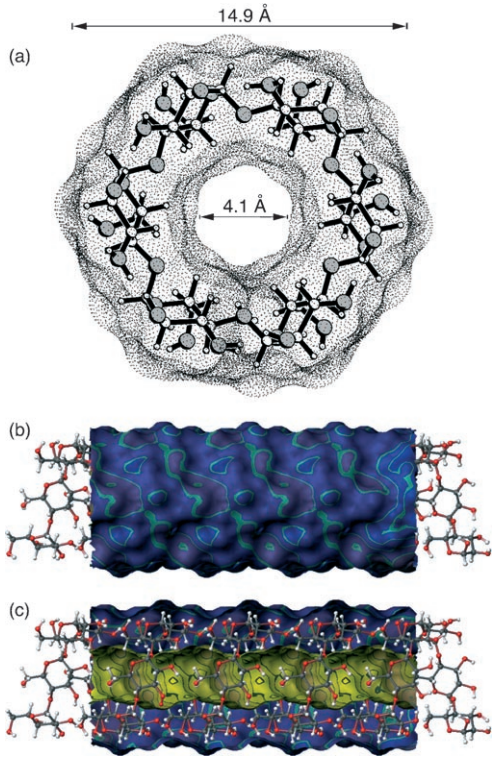

Figure 14. Crystal structure of single-helical V_H-amylose. a) View along the helix axis, which allows approximate determination of the size of the channels. b,c) Lipophilicity patterns showing the hydrophilic outer surface in blue (b) and the hydrophobic inner surface in yellow (c). The internal and external van der Waals diameters of 4.1 and 14.9 Å, respectively, are calculated from the distances of the H-5 and H-2 atoms from the helix axis, respectively, so they are directly comparable with the dimensions of α-CD (4.3 and 15.4 Å; Figure 3). Figure reprinted from Ref. [124]

driven by interactions with the hydrophobic surface of the polysaccharide (Figure 14c).[124] Although the axial cavity of V-amylose is slightly narrower than that of α-CD, amylose is very flexible and it can accommodate guests with a wide range of diameters.[125]

Kim and Choi have prepared amylose inclusion complexes of cyanine dyes of general structure DASP-C_n by adding water to solutions of the dyes and amylose in DMSO (Scheme 11).[126] These complexes can be dried and redissolved in water, even when the free dyes are not water-soluble. The hydrophobicity of the dye is important for

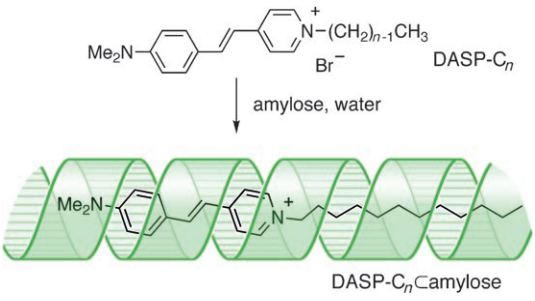

Scheme 11. Complexation of cyanine dyes DASP-C_n with amylose.[126]

complex formation, and inclusion is only observed for dyes with long alkyl tails ($n = 12$). Several spectroscopic changes demonstrate complexation: As water is added to a solution of DASP-C_{22} in DMSO in the absence of amylose, a UV/Vis absorption band corresponding to the dye aggregates appears at 420 nm. This band is absent when amylose is present, but reappears when the amylose complex is treated with cetyltrimethylammonium bromide ($CH_3(CH_2)_{15}NMe_3Br$), which is a competitive guest for the polysaccharide.[126] The DASP-C_{22}⊂amylose complex has a stability constant of $(2 \pm 1) \times 10^5\,M^{-1}$ in aqueous solution,[127] and circular dichroism measurements confirm that the dye is in a chiral environment.[126] The nonlinear optical and fluorescence behavior of these complexes are discussed in Sections 5.2 and 5.3.

Single-walled carbon nanotubes (SWNTs) with diameters of 1–2 nm form water-soluble complexes with amylose.[128,129] The binding process is believed to involve helical wrapping, thus illustrating the amazing flexibility of the amylose helix. This type of complexation process provides a way of preparing soluble SWNTs without disrupting their electronic structure, as would generally accompany covalent functionalization. SWNTs have also been solubilized with many other polymers,[130] including SPG (see Section 3.2).

3.2. Schizophyllan-Encapsulated Wires

Schizophyllan (SPG, also known as sonifilan, sizofiran, and sizofilan) is produced industrially from the fungus *Schizophyllum commune*; an identical polymer known as scleroglucan is produced by fungi of the genus *Sclerotium*.[131] It is widely used in cosmetics and as an immunotherapeutic agent in the treatment of uterine cancer.[132] In aqueous solution, SPG adopts a triple-helix structure (t-SPG), with six backbone glucose residues per helical turn in each single strand. Unlike V-amylose, t-SPG has no axial cavity. The three strands in t-SPG are held together by hydrogen-bonding interactions between the OH(2) groups of the backbone glucose units, and by hydrophobic stacking interactions between these sugar residues. The hydrophilic pendant glucose units protrude from the surface of this triple helix, thereby making t-SPG very soluble in water.[133] t-SPG is a remarkably stiff polymer in aqueous solution, with a persistence length of around 200 nm. In DMSO (and water at high pH values) it exists as a random-coil single-strand (s-SPG), which reverts to the t-SPG triplex on addition of water (at pH 7). If a hydrophobic guest is present during this renaturing process it can be trapped as an inclusion complex. SPG binds an astounding range of guests, including hydrophobic polymers, polynucleotides, and even gold nanoparticles.[134,135] The complexes probably feature helical SPG strands, but they must be different from that of native t-SPG, since it lacks a cavity.[136]

Shinkai and co-workers have explored the synthesis of conjugated polymer–SPG complexes, both by the polymerization of bound monomers and by complexation of preformed polymers.[135] One-dimensional polymerization of an SPG–monomer complex has been demonstrated using butadiyne monomer **21**.[137] Induced circular dichroism indicates

formation of the **21**$_n$⊂SPG complex when water is added to a solution of s-SPG and **21** in DMSO (Scheme 12). Photochemical 1,4-polymerization of this complex under UV irradiation appears to give an encapsulated polydiacetylene **PDA1**⊂SPG. The UV/Vis absorption spectrum of the product indicates that it is a polydiacetylene with a long conjugation length, and TEM images show a nanofibrous structure.

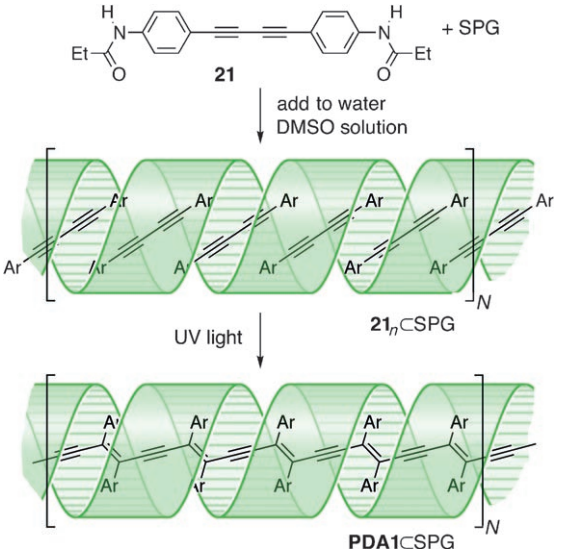

Scheme 12. "Ship-in-a-bottle" synthesis of a poly(diacetylene) SPG complex. The threaded helix structures of the SPG complexes **21**$_n$⊂SPG and **PDA1**⊂SPG have not been demonstrated experimentally.[137]

Helical wrapping by polysaccharides can provide water-soluble nanofibers of conjugated polymers that might be useful as biological sensors. Such fibers were prepared when the emeraldine base of polyaniline (PANI) was solubilized in water by complexation with SPG.[138] Amylose also forms similar polyaniline complexes, but they are less soluble in water. The circular dichroism spectra of the PANI⊂SPG complex confirm that the chromophore is in a helical environment, and TEM investigations show that the complex has a fibrous structure (unlike that of either SPG or PANI alone). The fibers have widths of 10–15 nm, which indicates that each fiber is a bundle of several PANI⊂SPG chains. Similar nanofibrous complexes have been prepared from SPG and permethyldecasilane ($Me(SiMe_2)_{10}Me$).[139] These complexes have some similarity to the $Me(SiMe_2)_{10}Me$⊂γ-CD complexes discussed in Section 2.2.8 (Figure 12).

The addition of water to a solution of SPG and polythiophene **PT3** in DMSO results in the formation of the complex **PT3**⊂SPG.[140] The circular dichroism spectrum of this complex is consistent with a right-handed helical conformation. The stoichiometry of this complex was investigated from the circular dichroism data by way of a Job plot, which led to the conclusion that two SPG strands wrap round a single polythiophene chain. AFM imaging of **PT3**⊂SPG on mica shows fibrous strands that are absent in the neat polythiophene and are different to the strands observed for neat t-SPG. The absorption spectra of **PT3**⊂SPG are discussed in Section 5.2 (Figure 22). Sanji et al. have investigated the complexes of α-sexithiophene (**6T**) with SPG and with partially carboxymethylated amylose:[141] both complexes have similar spectroscopic features but their circular dichroism spectra give Cotton effects of opposite sign, thus indicating the adoption of helical conformations of opposite handedness in the two different polysaccharide hosts.

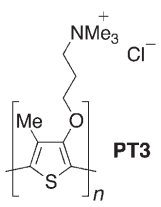

TEM and AFM images of complexes of SWNTs with SPG appear to show the first visual evidence for helical wrapping of SWNTs.[142] Fibrous structures are observed with dimensions corresponding to bundles of wrapped SWNTs. Close inspection of the bundles reveals a regular periodic structure, with inclined stripes consistent with a helical motif. A high-resolution TEM image of a fiber (Figure 15) indicates that two SPG chains are wrapped about a single nanotube, with a diameter of about 1.5 nm and helical pitch of about 10 nm.

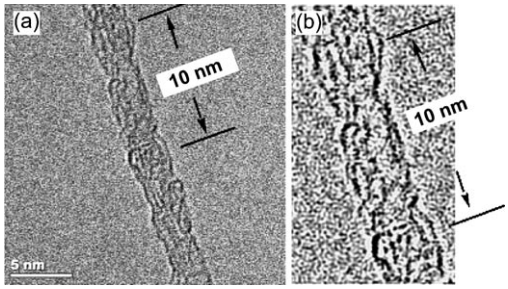

Figure 15. a) High-resolution TEM image of SWNT⊂SPG. b) Enlargement of a section of (a) by Fourier filtering. The helical pitch is marked in (a) and (b). Reprinted with permission from Ref. [142c]. Copyright 2005 American Chemical Society.

3.3. Molecular "Beanpoles"

Gladysz and co-workers have prepared polyynes insulated by α,ω-polymethylene diphosphane ligands that bridge from one end-capping organometallic terminal to the other.[143] These structures are called "beanpoles" because of their resemblance to a runner-bean plant twined round its supporting pole. The crystal structure of **22** (Figure 16) shows the polymethylene bridge units in a double-helical conformation. This approach to IMWs is unique in that it relies only on van der Waals interaction between the sp- and sp^3-hybridized carbon atoms of the chains. This study suggests a general strategy for stabilizing helically wrapped IMWs by covalently linking the ends of the conjugated polymer guest to the ends of its host polymer.

3.4. Conclusions on the Synthesis and Structural Characterization of Wrapped IMWs

The formation of supramolecular complexes by wrapping molecular wires with insulating polymers offers a simple way of forming IMWs. The great advantage of this strategy, when compared with polyrotaxane formation, is that helical hosts

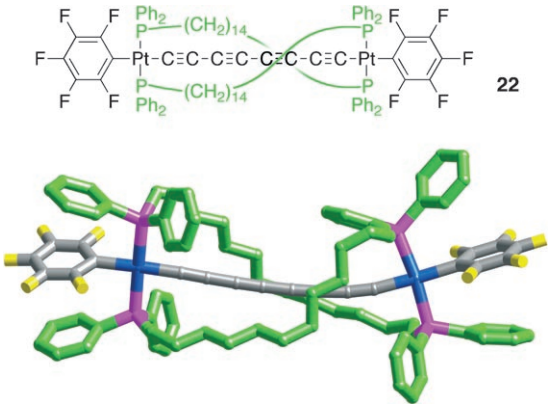

Figure 16. Structure of the molecular "beanpole" **22** in the crystal structure.[143]

are more flexible than their cyclic analogues, thus making it possible to encapsulate molecular wires with a wider range of diameters in a given host. On the other hand, polymer–polymer complexes are generally more labile and their structural characterization is extremely challenging. For example, the molecular-level structures of complexes formed from conjugated polymers and SPG are currently unknown and helical structures such as those depicted in Scheme 12 should be regarded as hypothetical working models. This field has advanced rapidly during the last few years. There is tremendous scope for extending this approach towards functional IMWs, both using natural polymers, such as amylose and SPG, and synthetic helical hosts, such as poly(*meta*-phenyleneethynylene) foldamers.[144]

4. Dendronized Conjugated Polymers

4.1. Introduction to Dendrimer Encapsulation

A dendrimer consists of a number of regularly branched substituents (dendrons) attached to a central core, with terminal groups at the surface.[145] Dendrimer topology naturally lends itself to the encapsulation and site-isolation of molecular cores. This effect is well understood in the case of small molecular cores,[146] and can be extended to encapsulate polymeric cores by attaching dendrons laterally to a polymer chain. If the core is a conjugated polymer, the material may be described as an IMW. When the dendron size and coverage are high enough, dendrimer-encapsulated polymers adopt cylindrical, rodlike geometries (Figure 17).[147] The most widely used dendrons are based on the poly(benzyl ether)s first prepared by Hawker and Fréchet[148] (Figure 18).

It is interesting to explore how the properties of an insulated π system evolve with the number of dendron substituents, the generation of the dendrons, and the length of the polymer chain. So a key parameter in the characterization of a dendronized polymer is the number-average degree of polymerization $\bar{n}_n$. It is a shame that many authors encrypt this information as $\bar{M}_n$, or as $\bar{M}_w$ in combination with the polydispersity $\bar{M}_n/\bar{M}_w$. The default technique for measuring $\bar{M}_n$ is GPC, relative to polystyrene standards, and this technique generally underestimates the molecular weight of a dendronized polymer (often by a factor of 2–3, depending on the dendron generation and the degree of polymerization; see Section 1).[147g,149–151] For this reason most of the $\bar{n}_n$ values quoted here must be regarded as very crude estimates, but even a crude estimate of $\bar{n}_n$ is vital when interpreting the behavior of these materials.

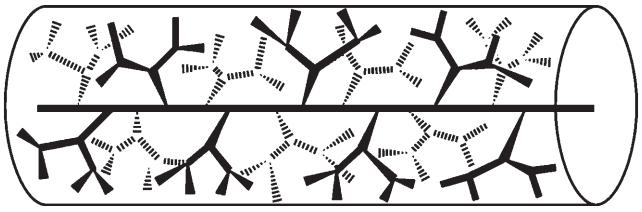

Figure 17. The dendrons can be so densely packed on a dendronized polymer that the backbone stretches out to generate a molecular cylinder (schematic representation from Schlüter and Rabe).[147c]

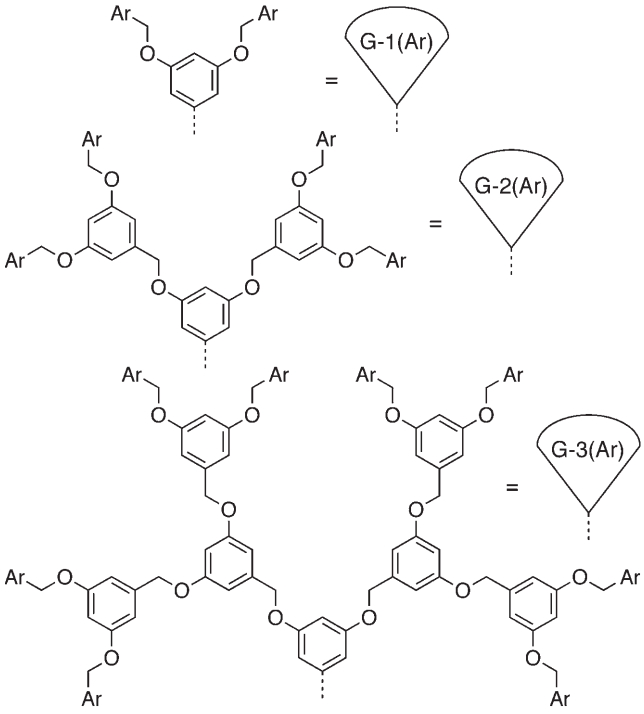

Figure 18. Fréchet-type poly(benzyl ether) dendrons G-*N*(Ar) where *N* is the generation number.[148] The representation defined here is used throughout this Review.

4.2. Dendronized Poly(para-phenylene)s from Suzuki Polycondensation

The synthesis of dendronized conjugated polymers has been achieved by two different strategies. Schlüter and coworkers have compared these two strategies for the preparation of poly(*para*-phenylene)s (PPPs) insulated by Fréchet-type poly(benzyl ether) dendrons (Scheme 13).[150] Dendro-

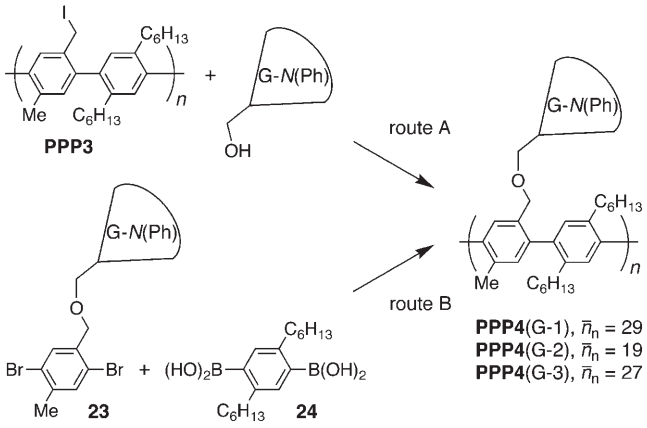

Scheme 13. Two approaches to the synthesis of dendronized poly(*para*-phenylene): by dendronization of preformed polymer (route A) and by polymerization of the macromonomer route (route B).[149] $\bar{n}_n$ is the number-average degree of polymerization (as determined by GPC) for the product of the macromonomer route.

nization of a preformed polymer (route A) has the disadvantage that steric effects hinder attachment of the bulky dendrons. These effects lead to incomplete dendron coverage, particularly for dendrons higher than the second generation. The macromonomer approach (route B) necessarily gives dendronized polymers with complete coverage, but the polymerization reaction may be retarded by steric effects. Schlüter and co-workers prepared dendronized polymers by coupling dendrons to preformed polymer **PPP3** through benzyl ether (and also urethane) linkages, and by the macromonomer route by Suzuki polymerization of 1,4-dibromophenyl-substituted macromonomers **23** with a non-dendronized diboronic acid **24**. The coverage of third-generation dendrons on polymer **PPP4**(G-3) was only 70% by route A. The degrees of polymerization ($\bar{n}_n$) for the dendronized polymers with dendrons up to the third generation from the macromonomer polymerization (route B) were comparable to those of polymers prepared by route A. Importantly, only the macromonomer route (route B) gave complete dendron coverage with third-generation dendrons, so this route has become the strategy of choice when a defect-free, dendron-insulated polymer is required.[147]

These dendronized PPPs illustrate the difficulty of determining the chain lengths of dendronized polymers. For example, GPC analysis of polymer **PPP4**(G-3) from route B gave $\bar{n}_n = 27$ ($\bar{M}_w/\bar{M}_n = 5.3$), whereas a combined light-scattering, GPC, and viscometry analysis gave $\bar{n}_n = 156$ ($\bar{M}_w/\bar{M}_n = 2.6$).[150] In this case the molecular weight seems to have been exaggerated by aggregation because, when the dendrons were cleaved from the polymer with trimethylsilyl iodide, the resulting polymer gave an average degree of polymerization by the combined analysis of $\bar{n}_n = 110$.[151] According to the Carothers equation[152] this degree of polymerization implies that the Suzuki coupling proceeded to greater than 99% conversion, which is impressive for the polymerization of a third-generation macromonomer. This degree of polymerization corresponds to a mean contour length of about 95 nm.

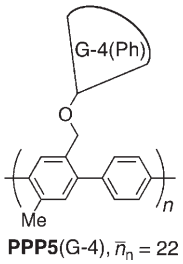

With careful optimization of Suzuki polymerization conditions, Schlüter and co-workers have applied the macromonomer approach to the preparation of poly(*para*-phenylene) **PPP5**(G-4) with fourth-generation Fréchet-type dendrons.[153] GPC analysis showed polymer **PPP5**(G-4) had $\bar{n}_n = 22$ ($\bar{M}_w/\bar{M}_n = 8.4$). This is the only report of a molecular wire insulated by dendrons as high as the fourth generation, and illustrates the difficulty in controlling the stoichiometry of a polymerization when one monomer is of substantially higher molecular weight than the other.

4.3. Dendronized Polyfluorenes from Yamamoto and Suzuki Coupling

Polyfluorenes are important for blue electroluminescence. However, they often suffer from unstable color purity because of the appearance of an emission band at about 540 nm, which arises from the oxidative formation of 9-fluorenone keto defects.[154] Encapsulation may improve the color purity by preventing this oxidation. The 9,9-methylene bridge of the fluorene monomer provides a convenient position for attachment of dendrons. Polyfluorenes bearing

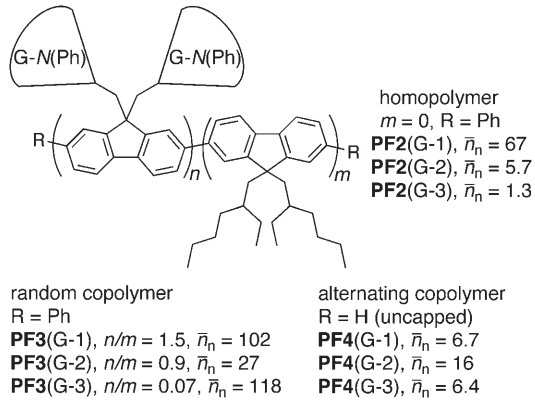

two first-, second-, or third-generation Fréchet-type dendrons per dendronized monomer were prepared by Carter and co-workers[155] as either homopolymers or as statistical or alternating copolymers with dialkyl fluorenes. The nickel-catalyzed Yamamoto homopolymerization is reasonably efficient for the first-generation macromonomer, which, after end-capping with bromobenzene, gives polymer **PF2**-(G-1) with $\bar{n}_n = 67$. This approach is much less efficient with the second-generation dendron to give **PF2**(G-2) ($\bar{n}_n = 5.7$), and with the third-generation dendron polymerization to give **PF2**(G-3) is almost completely suppressed ($\bar{n}_n = 1.3$). Fujiki and co-workers were more successful in the Yamamoto homopolymerization of dendronized polyfluorenes, and synthesized a polymer similar to **PF2**(G-2), but with 2-fluorenyl end caps, with a degree of polymerization of $\bar{n}_n = 12$.[156]

Copolymerization with nondendronized monomers reduces the steric effects. Carter and co-workers used this tactic to prepare first-, second-, and third-generation random copolymers **PF3**(G-*N*; *N*=1–3), with degrees of polymerization $\bar{n}_n = 102$, $\bar{n}_n = 27$, and $\bar{n}_n = 118$, respectively, by Yamamoto copolymerization of the dendritic macromonomers with a dibromodialkylfluorene monomer.[155,157] However, the ratio of dendronized to nondendronized monomers in these polymers was $n/m = 1.5$, 0.9, and 0.07, respectively, when equal quantities of the dibromo monomers were used, which shows that the reactivity of the macromonomers decreases with increasing generation. The same research group also prepared alternating copolymers **PF4**(G-*N*; *N*=1–3) by Suzuki cross-coupling ($\bar{n}_n = 6.7$, $\bar{n}_n = 16$, and $\bar{n}_n = 6.4$, respectively).[155]

The highly branched Müllen-type polyphenylene dendrons display shape persistency, which distinguishes them from the flexible Fréchet-type poly(benzyl ether) dendrons.[158] Consequently, site-isolation should be achieved at a low dendron generation number (for example, in polyfluorene **PF5**; $\bar{n}_n = 46$).[159]

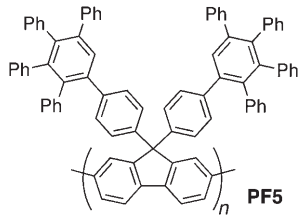

4.4. Dendronized Poly(phenylenevinylene)s

Bao et al. prepared polyphenylenevinylene **PPV2** with first-generation 3,4,5-tris(benzyloxy)benzyl ether dendrons by Heck polymerization of a 1,4-diiodobenzene-based macromonomer with 1,4-divinylbenzene ($\bar{n}_n = 15$ by GPC and light scattering).[160] Polymer **PPV2** is a thermotropic nematic liquid crystal, with a nematic–isotropic transition at 211 °C. X-ray diffraction peaks were observed for thin films of **PPV2** at 2θ spacings corresponding to the radius of the dendritic side chains (22–26 Å), which is consistent with a packing structure with interdigitated dendrons.

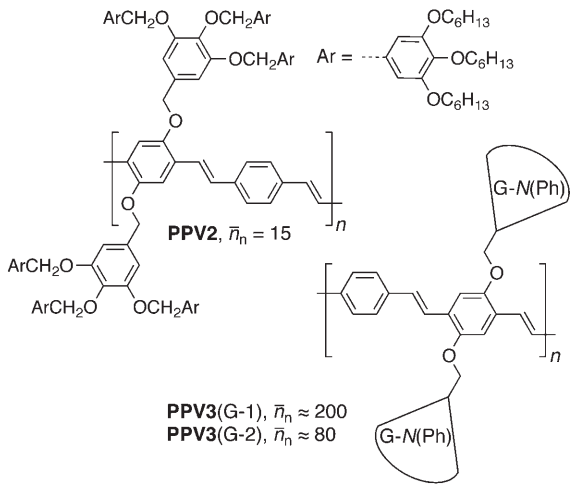

Xi and co-workers have prepared **PPV3**(G-*N*; *N*=1 and 2) by Wittig polymerization of dendronized terephthaldehyde derivatives with a 1,4-bis(xylylene)phosphonium salt.[161] Laser light scattering measurements show that the weight-average molecular weights ($\bar{M}_w$) were 400000 and 260000, respectively, for **PPV3**(G-1) and **PPV3**(G-2). If a polydispersity of $\bar{M}_w/\bar{M}_n = 2$ is assumed, this corresponds to $\bar{n}_n$ values of 200 and 80, respectively. The Gilch polymerization (Scheme 14) was also found to be an efficient route to

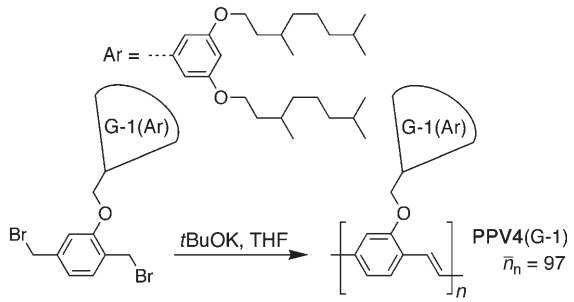

Scheme 14. Gilch route to dendronized PPVs.[162]

dendronized PPVs,[162] with GPC analysis of homopolymer **PPV4**(G-1) giving $\bar{n}_n = 97$. However, even the high degree of polymerization reported for this dendronized polymer is lower than that of the zeroth generation analogue, for which GPC analysis gave $\bar{n}_n = 320$.

4.5. Dendronized Poly(phenyleneethynylene)s from Sonogashira Coupling

Poly(phenyleneethynylene)s **PPE1**(G-*N*; *N*=1–3) and **PPE2**(G-*N*; *N*=1–3), with phenylene rings adorned with

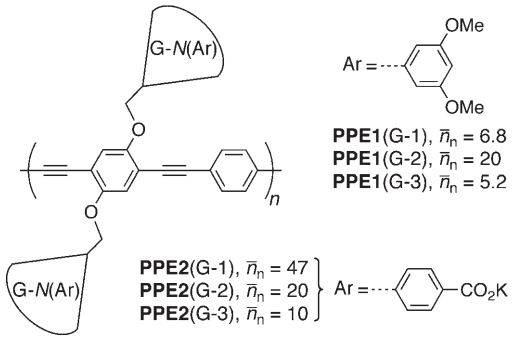

first-, second-, or third-generation Fréchet-type dendrons alternating with unsubstituted phenylene rings, have been synthesized by Aida and co-workers by Sonogashira polycondensation of dendronized 1,4-diethynylphenyl macromonomers with 1,4-diiodobenzene.[163,164]

The polymerization is optimal for the second-generation macromonomer: polymer **PPE1**(G-2) was obtained in 85 %

yield with $\bar{n}_n = 20$. The inadequate solubilizing effect of the first-generation dendrons gave a fraction for **PPE1**(G-1) of much lower molecular weight ($\bar{n}_n = 6.8$) in 30% yield, along with insoluble precipitate. The polymerization of the third-generation macromonomer was slow, and gave polymer **PPE1**(G-3) with $\bar{n}_n = 5.2$ in 90% yield. These polymers exhibit a dramatic increase in fluorescence efficiency with increasing dendron generation (see Figure 24, Section 5.3). The water-soluble polyanionic dendronized poly(phenylene-ethynylene)s **PPE2**(G-*N*; *N*=1–3) were synthesized by hydrolysis of the corresponding methyl esters. The use of these IMWs as photosensitizers for the generation of hydrogen from water is discussed in Section 5.5.

4.6. Butadiyne-Linked Oligomers from Glaser Coupling

Aida and co-workers have studied discrete dendronized oligomers **PPEB1**(G-1) and **PPEB1**(G-3) (Figure 19), which

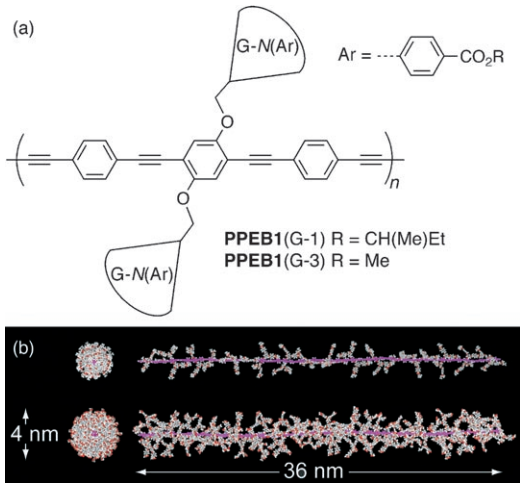

Figure 19. a) Oligomers **PPEB1**(G-1) (n=1–6, 8, 10, 12, 16) and **PPEB1**(G-3) (n=1–6, 8, 10, 12, 16, 24, 32, 64) obtained by Glaser coupling; b) calculated structures of **PPEB1**(G-1) and **PPEB1**(G-3) (n=16).[165]

were isolated by preparative GPC of Glaser-coupled acetylene-functionalized macromonomers.[165] This approach allowed the isolation of third-generation oligomers **PPEB1**-(G-3) with up to 64 repeat units. This 64-mer has an end-to-end contour length of 147 nm—an impressive length for a monodisperse IMW. Figure 19b shows calculated structures of **PPEB1**(G-1) and **PPEB1**(G-3) for $n = 16$. These models show that the third-generation cylinder has a diameter of around 4 nm, but there still appear to be gaps in the insulating layer. Analysis of the NMR spectra of these polymers and the precursor monomers provide some insights into the structure. The transverse relaxation times (T_2) of aromatic protons on the monomer unit indicate restricted conformational freedom of the focal aromatic rings in the larger dendrons. In the third-generation series, the T_2 values of the interior dendron protons decrease with oligomer length up to the decamer. This observation is consistent with increasing steric crowding of the interior dendrons with increasing oligomer chain length.

Oligo(triacetylene)s have been dendronized by Diederich and co-workers.[166] Discrete oligomers **PTA1**(G-*N*; *N*=1–3) were prepared by dendronization of (*E*)-enediynes, followed

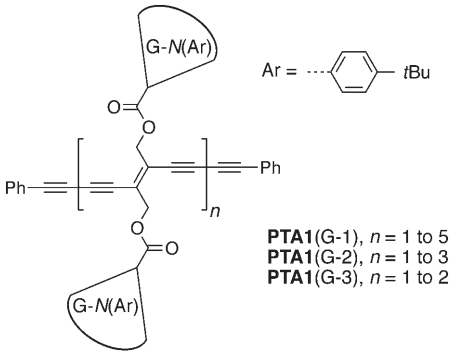

by macromonomer oligomerization by Glaser–Hay coupling in the presence of phenylacetylene as a terminator. The oligomers were separated by GPC. Oligomers with up to five repeat units were isolated (n=1–5) for the first generation. Steric suppression of the coupling reaction by higher generation dendrons meant that the largest species to be formed with the third-generation dendron was the dimer (n=2).

4.7. Dendronized Polythiophenes and Related Polymers

Polymers based on polythiophene with aliphatic polyether dendrons have been prepared by Malenfant and Fréchet by Stille coupling. Second- or third-generation dendrons were used as the only solubilizing substituents, and were placed at either every second (**PT4**) or every sixth (**PT5**) thiophene unit.[167] Polymer **PT4**(G-2) had $\bar{n}_n = 20$, while **PT5**(G-3)

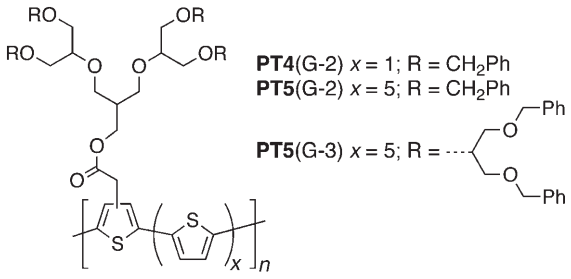

exhibited a very broad multimodal molecular-weight distribution; chains with up to 270 thiophene units (n=45) were evident in the MALDI mass spectrum of this material.

A derivative of poly(3,4-ethyenedioxythiophene) (PEDOT) with first-generation 3,4,5-tris(benzyloxy)phenyl-based dendrons was prepared by Kumar and co-workers by the electropolymerization of a dendron-substituted thiophene monomer.[168]

4.8. Nonfractal Dendronized IMWs

The geometrically repetitive, fractal nature of a dendron confers structural simplicity and aesthetic beauty, but is not essential for the site-isolation effect. Conjugated polymers encapsulated by nondendritic (that is, nonfractal) bulky substituents can also behave as IMWs. Examples include iptycene-containing poly(aryleneethylene)s such as **PPE3**,

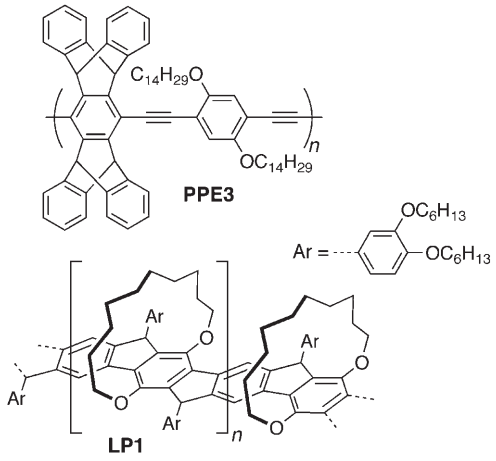

developed by Swager and co-workers,[169] as well as the "canopied" polypyrrole with a protective wing cantilevered over the face of the pyrrole units.[170] The "wrapped" ladder polymer **LP1** prepared by Scherf and co-workers is another example of a conjugated polymer sheathed by its substituents.[171] "Shish-kebab" polymers such as **25** represent a

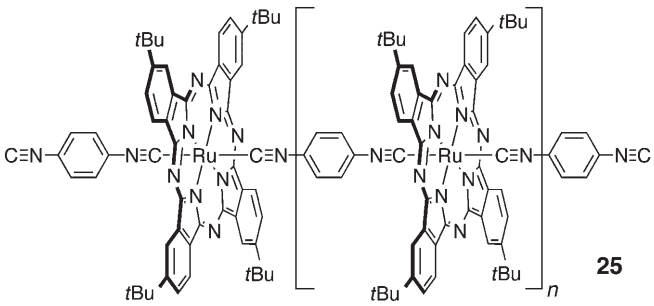

related class of IMWs,[172] as do ligand-sheathed metal–metal bonded polymers such as $\{[Rh(MeCN)_4](BF_4)_{1.5}\}_8$,[173] Ni_5^{11+} poly(pyridylamide) chains,[174] and green $[Pt(NH_2R)_4][PtCl_4]$ Magnus salts,[175] which resemble dendronized coordination polymers.[176]

4.9. Synthesis of Dendronized IMWs—Conclusions and Outlook

Dendronized conjugated polymers are the most widely investigated class of IMWs, because, in contrast to polyrotaxanes and helically wrapped systems, their synthesis requires no special supramolecular interactions. The link between these different classes of materials is illustrated by the synthesis of tubular structures by cross-linking the surface groups of a dendronized polymer by Zimmerman and coworkers, then removing the polymer core.[177] Steric hindrance is generally a limiting factor in the synthesis of dendronized polymers. The macromonomer route guarantees complete dendronization, and nearly all dendronized conjugated polymers have been synthesized this way, although it often results in a short average chain length, with number-average degrees of polymerization $\bar{n}_n$ typically in the range 5–20 for second-generation dendrons. This problem becomes more severe with higher generations, so that polymerization may be prevented before the dendron shell is compact enough to completely shield the backbone π system, or to influence the backbone conformation. Gilch polymerization and Suzuki polymerization stand out as the best reactions for the macromonomer route. Very few dendronized conjugated polymers have been synthesized by dendronization of a preformed polymer, because of concern about incomplete coverage. However, this strategy would make it easier to investigate the effects of dendronization on the optoelectronic properties of the backbone, because it would give access to materials with identical chain-length distributions, which differed only in the thickness of the dendrimer coat.

5. Function and Applications of IMWs

How does insulation change the behavior of a molecular wire, and how might this be useful? The study of IMWs is still in its infancy, and most studies have focused on synthesis and structural characterization, rather than on the functional properties of these materials. However, there is already a substantial amount of information to show how insulation can enhance the properties of a molecular wire, in ways that should lead to practical applications. Here we draw together results for all types of IMWs to highlight emerging structure–property correlations.

5.1. Stability and Chemical Reactivity of the Encapsulated π System

The delocalized electronic structures and small π–π* energy gaps of molecular wires inevitably make them vulnerable to attack, because reactions with electrophiles, nucleophiles, or radicals lead to stable delocalized intermediates. This is illustrated by the observation that the simplest conjugated polymer, polyacetylene, needs to be handled in an inert atmosphere to avoid oxidation. The environmental reactivity and operational instability of organic semiconductors is often regarded as their main limitation. Blocking this reactivity has been a key motivation for the synthesis of IMWs, and there are now many examples to demonstrate that the strategy can be highly effective.

Threading a π system inside a macrocycle to form a rotaxane can protect it from even the smallest and most reactive of species, such as singlet oxygen. For example, the cyanine rotaxane **26**⊂α-CD is 40-fold more stable towards photooxidation than the free cyanine dye (Figure 20).[67]

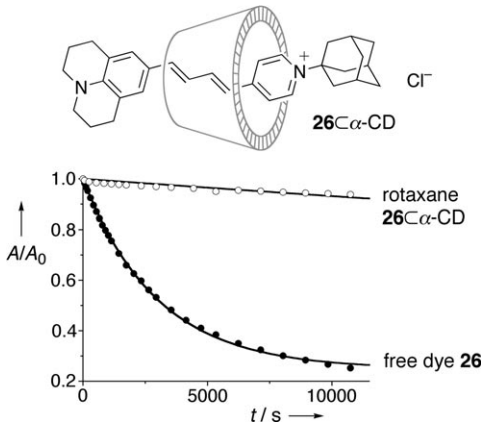

Figure 20. Photobleaching curves for rotaxane **26**⊂α-CD and free dye **26** in O_2-saturated water. A_0 is the initial absorbance and A is the absorbance after irradiation for time t with white light from a tungsten filament bulb. The data are fitted to first-order decay curves with rate constants of 7.1×10^{-6} (**26**⊂α-CD) and 3.3×10^{-4} s^{-1} (**26**).[66]

Cyanine rotaxanes also display enhanced redox reversibility as a result of the kinetic stability of their oxidized and reduced forms. This aspect is illustrated by the cyclic voltammograms of both rotaxanes **16**⊂α-CD[66] (Scheme 6). Cyanine–amylose complexes also exhibit enhanced stability; for example, thermogravimetric analysis (TGA) of solid samples of DASP-C_n and DASP-C_n⊂amylose (Scheme 11) shows that while the free dyes exhibited a major mass loss at 267 °C, the corresponding mass loss for the amylose complexes occurs at 288 °C, which is the decomposition temperature of free amylose.[178] Azo-dye rotaxanes such as **15**⊂TM-α-CD (Section 2.2.2) also exhibit enhanced chemical stability and photostability. This rotaxane is more than 100-times less reactive towards aqueous sodium dithionite than the free dye **15**.[59] As in some stilbene rotaxanes, *E*–*Z* photoisomerization is prevented by the presence of the cyclodextrin in **15**⊂TM-α-CD, whereas other stilbene rotaxanes such as **17**⊂α-CD (Section 2.2.4) undergo *E*–*Z* photoisomerization with reduced quantum yields.[179] Encapsulation prevents [2+2] cycloaddition in **17**⊂α-CD, and retards photohydration, thereby enhancing the fatigue resistance of this photochromic system. The reactivity of conjugated polyrotaxanes has not been thoroughly investigated, but Ito and co-workers have found that threading polyaniline through β-CD prevents doping with iodine.[86,94] Zeolite-encapsulated conjugated polymers frequently exhibit dramatically enhanced environmental stability:[22] for example, polyacetylene in faujasite is stable indefinitely in air,[23] and PPV encapsulated in the same zeolite is stable to laser photolysis under oxygen.[24]

The TGA data of several dendronized conjugated polymers indicate that dendronization improves the thermal stability. For example, **PPV4**(G-1) (Section 4.4, Scheme 14) has a decomposition temperature of 362 °C, which is 34 °C higher than that of the **PPV**(G-0) reference polymer.[162] Polyfluorene **PF5** (Section 4.3) shows exceptional thermal stability (decomposes at 570 °C). Energy transfer from the dendrons to the conjugated backbone (Section 5.4) can sometimes result in undesirable photosensitivity. For example, Diederich and co-workers found that **PTA1**(G-3) ($n=1$; Section 4.6), with the third-generation Fréchet-type dendrons, undergoes *E*–*Z* photoisomerization more rapidly than the corresponding unsubstituted monomer. This dendron-promoted *E*–*Z* photoisomerization also proved problematic in the dendritic encapsulation of an oligo(pentaacetylene), which when substituted with second-generation Fréchet-type dendrons could only be prepared as a mixture of *E* and *Z* isomers. Consequently, dendritic oligo(triacetylene)s were prepared with carbosilane dendrons in the place of the Fréchet benzyl ethers, and these showed no *E*–*Z* photoisomerization. Carbosilane dendrons should also give a spherical geometry at a lower generation than Fréchet-type dendrons.[166b]

5.2. Absorption Spectra, Emission Spectra, and Nonlinear Optical Properties

To a first approximation, the encapsulation of a molecular wire is not expected to perturb its electronic structure or change its π–π* energy gap, but, in principle, changes in the UV/Vis absorption and fluorescence spectra can arise as a result of three distinct classes of effects:

a) Solvatochromism: If the excited state of the molecular wire is more, or less, polar than the ground state, then the wavelengths of its absorption and emission bands will be sensitive to the polarity and polarizability of the insulating shell (just as they are to the polarity and polarizability of the solvent). A change in the polarizability of the environment around the π system can change its extinction coefficients, even if the absorption bands have no charge-transfer character.[116]
b) Conformational effects: If the encapsulating structure behaves as a long straight tube it may force the molecular wire to adopt linear and/or planar conformations, with the resulting stronger π overlap shifting the absorption and emission to longer wavelengths. In other cases insulation may favor a more twisted geometry, thus leading to a blue shift. Even when encapsulation has no effect on the conformation of the ground state, it can change the fluorescence spectrum by restricting reorganization in the excited state.
c) Aggregation: Long rigid or shape-persistent molecules such as dyes and conjugated polymers have a strong tendency to aggregate, particularly at high concentrations or in poor solvents. In this case exciton coupling between chromophores in these aggregates modifies the absorption and emission spectra. Encapsulation blocks the aggregation of the conjugated cores.

In practice spectral changes may often be due to a combination of all three of these effects, and no systems have yet been studied in sufficient detail to completely dissect out the contributions from these separate phenomena.

Cyclodextrin polyrotaxanes such as **PPP1**⊂β-CD, **PF1**⊂β-CD, **PPV1**⊂β-CD, **PDV1**⊂α-CD, and **PDV1**⊂β-CD (Section 2.2.4) generally display sharper absorption spectra, and sharper blue-shifted emission spectra, compared to the unthreaded conjugated polymers. Figure 21 a shows the

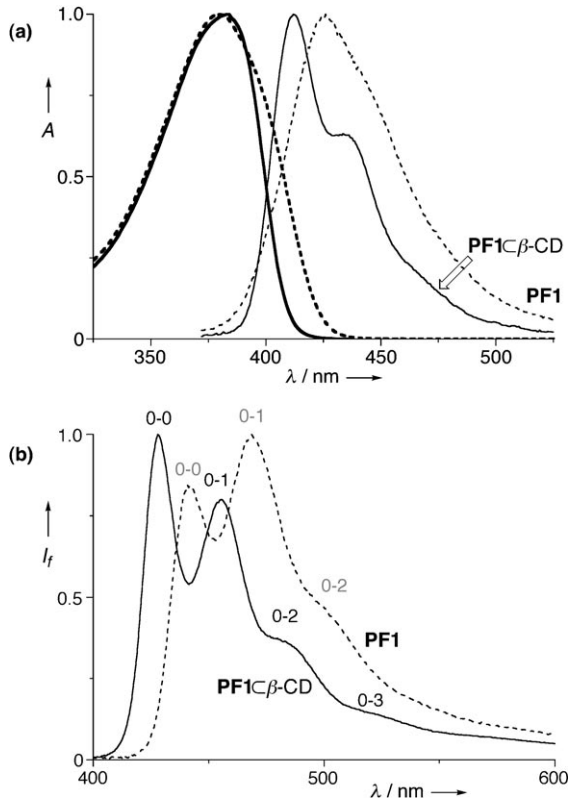

Figure 21. a) Normalized absorption spectra (bold) and emission spectra of **PF1**⊂β-CD (——) and **PF1** (-----) in aqueous solution at 298 K. b) Normalized emission spectra of **PF1**⊂β-CD (——) and **PF1** (-----) as thin films at 10 K.[73]

spectra of **PF1** and **PF1**⊂β-CD in solution.[73] The vibrationally resolved low-temperature emission spectra of this polyrotaxane (Figure 21b) show that the blue-shift in the emission can be factorized into two effects: 1) the 0–0 band is the most intense component in the emission from the polyrotaxane whereas the 0–1 band is the main component for the free polymer, and 2) the 0–0 band is blue-shifted in the polyrotaxane. Both these changes imply that encapsulation restricts reorganization in the excited state, which could include structural reorganization of the conjugated polymer and/or reorganization of the solvent shell. The crystal structures of rotaxanes such as **18**⊂α-CD (Figure 7)[70] indicate that the presence of the cyclodextrin does not significantly affect the ground-state conformation of the π system; so in these polyrotaxanes ground-state conformational effects do not appear to be relevant.

Ground-state conformational changes are thought to account for the red-shifted absorption and emission spectra of polydimethylsilane γ-CD complexes (Figure 13).[103] However, this red-shift relates to a comparison of the spectra of $Me(SiMe_2)_nMe$ in hexane with spectra of $Me(SiMe_2)_nMe$⊂γ-CD in water, so it may be partly solvatochromic. Another more apparent case of conformational control is the red-shifted emission of MEH-PPV when it threads into the linear channels of a mesoporous silica host (Figure 1).[20] Here, singlet energy transfer occurs from the free polymer molecules in solution, on the surface of the host, to polymer molecules oriented in the channels.

One might expect that the absorption and emission spectra of an IMW would be independent of the external environment, because of the screening effect of the insulation. A nice illustration of this effect is provided by the polythiophene–SPG complex **PT3**⊂SPG (Section 3.2).[140] Its absorption spectrum in aqueous solution is almost identical to that of the neat material in a solid thin film (Figure 22). In contrast,

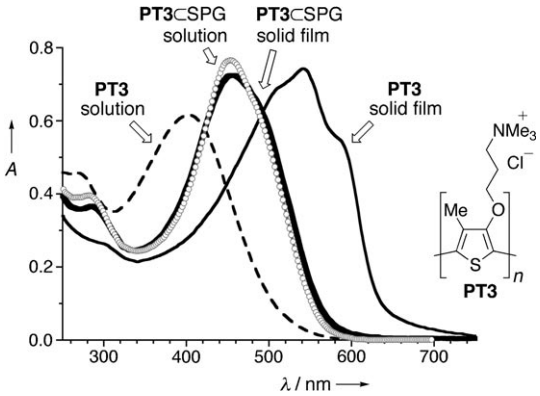

Figure 22. Absorption spectra of polythiophene **PT3** in aqueous solutions (dashed line, λ_{max} 403 nm) and as a thin film (solid line, λ_{max} = 541 nm), as well as of the **PT3**⊂SPG complex in aqueous solutions (circles, λ_{max} = 454 nm) and as a thin film (bold line, λ_{max} = 456 nm). Adapted with permission from Ref. [140]. Copyright 2005 American Chemical Society.

the absorption spectrum of a solid film of the free polythiophene **PT3** shows a red-shift of 138 nm compared to the solution spectrum, as a result of aggregation. The solution absorption and luminescence spectra of **PT3**⊂SPG are both red-shifted with respect to the neat polythiophene, which may be due to the adoption of a more planar conformation in the polysaccharide.[138]

The encapsulation of cyanine dyes such as DASP-C_{22} in amylose (Scheme 11) enhances their nonlinear optical behavior.[127,180] Solution-phase hyper-Rayleigh scattering measurements indicate that the first hyperpolarizability β of this inclusion complex is about twice that of the free dye.[127] Thin films of DASP-C_{22}⊂amylose on glass substrates exhibit spontaneous dipolar alignment, thus allowing generation of a second harmonic without external poling. These films retain their polarity for more than 100 h at 90 °C, thus demonstrating the stability of the structure.[180] Further evidence for the rigidity and robustness of this amylose–cyanine inclusion complex comes from the observation that the absorption spectra of solid thin films of these complexes are almost independent of temperature in the range 30–90 °C. In contrast, the absorption spectra of the complexes in aqueous solution become broad and shift to shorter wavelengths at higher temperature as a result of thermal conformational disorder.[181]

The effects of increasing dendrimer generation on the photophysical properties of dendronized conjugated polymers are difficult to discern because these materials are

generally synthesized by macromonomer polymerization, which results in an average chain length that decreases with increasing dendron generation (route A, Scheme 13). The problem of deconvoluting the effects of dendron generation and chain length is exacerbated by the difficulty of accurately measuring degrees of polymerization. The simplest solution to this problem is to study discrete oligomers of known chain lengths. For example, a study by Diederich and co-workers[166b] on discrete oligo(triacetylene)s **PTA1**(G-*N*) (Section 4.6), showed that the position of the absorption maximum, extinction coefficient, and fine structure for the backbone absorption band are independent of dendron generation ($N = 1$–3), despite the fact that calculations indicate that the third-generation dendrons on **PTA1**(G-3) would distort the backbone.[166b] However, this study used short chains ($n = 1$ and 2 for **PTA**(G-3)), and steric effects are expected to build up in longer oligomers. Aida and co-workers[165] compared the absorption and emission spectra of discrete oligomers with dendrons of the first generation, **PPEB1**(G-1), in dilute THF solution with those of the third generation, **PPEB1**(G-3), as a function of oligomer length for up to $n = 16$. The difference increases with increasing chain length up to $n = 8$. With the longer oligomers ($n = 8$–16), the absorption and emission spectra of **PPEB1**(G-3) are red-shifted by 11 nm (608 cm^{-1}) and 4 nm (210 cm^{-1}), respectively, compared with those of **PPEB**(G-1). This slight reduction in the π–π* gap may be due to planarization of the backbone and/or stiffening of the polymer chain in **PPEB**(G-3). A theoretical study by Stimson and co-workers[182] on dendronized **PPP4**(G-*N*) predicted that the dendrons would not alter the backbone conformation until the fourth generation is reached. An extreme case in which the dendronization must strongly influence the backbone conformation is provided by polyacetylene **PA1**(G-2) ($\bar{n}_n = 2000$

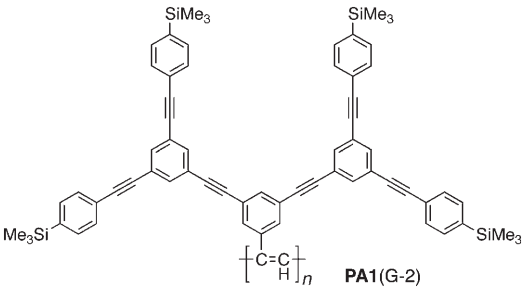

PA1(G-2)

from light scattering), although it is difficult to evaluate the effect of the dendrons on the properties of this polymer because it has a complex mixture of *cis* and *trans* double bonds.[149] Percec et al. have also prepared dendronized polyacetylenes with up to 99% of the *cis* isomer, and demonstrated that dendronization stabilizes the backbone with respect to *cis*–*trans* isomerization and electrocyclic reactions.[183]

As expected, dendronization with larger dendrons hinders aggregation. For example, the study of the aggregation of dendronized poly(phenylethynylene)s **PPE1**(G-*N*) in aqueous THF[163b] showed that the the emission spectra (λ_{max} 450 nm) of a THF solution of the second-generation polymer **PPE1**(G-2) ($\bar{n}_n = 20$) changes dramatically upon the addition of water: a dominant new band appears at 500 nm which is assigned to aggregates. The spectra of the higher generation analogue **PPE1**(G-3) ($\bar{n}_n = 5.2$) shows very little change under the same conditions; this result appears to be due to the greater dendritic encapsulation in **PPE1**(G-3), although it might just reflect its shorter chain length. An exception to the general rule that dendronization hinders aggregation is provided by **PPP4**(G-3).[150,151] As discussed in Section 4.2, this dendronized PPP aggregates strongly in THF and leads to an artificially high apparent molecular weight from light-scattering/GPC/viscometry analysis. The true degree of polymerization could only be determined by cleaving off the dendrons to prevent aggregation.

5.3. Photoluminescence Efficiency

Organic materials with high fluorescence efficiencies and minimal nonradiative decay rates are important, not just for applications directly involving light output (for example, fluorescent markers, sensors, and electroluminescent displays), but also in any application where the energy of an excited state needs to be channeled efficiently down a specific pathway (for example, photovoltaic devices, photosensors, and photochemical production of hydrogen). Many IMWs exhibit enhanced quantum yields for fluorescence compared with the corresponding free π systems. This can often be attributed to restricted conformational freedom and reduced flexibility of the excited state. Aggregation can quench fluorescence, particularly if two or more chromophores come together in a parallel face-to-face arrangement. In this H-aggregate, exciton coupling leads to low-energy non-emissive states. So encapsulation can increase the fluorescence efficiency by preventing aggregation or by modifying the geometry of the aggregate. A reduction in the polarity of the environment can also enhance the fluorescence of many chromophores. A fourth type of enhanced fluorescence efficiency arises when insulation hinders quenching by an external species, by preventing energy or electron transfer (Section 5.5).

The fluorescence efficiencies of cyclodextrin polyrotaxanes such as **PPP1**⊂β-CD, **PF1**⊂β-CD, **PPV1**⊂β-CD, **PDV1**⊂α-CD, and **PDV1**⊂β-CD (Section 2.2.4) are generally 2–3-fold higher than those of the free polymers, both in solution and in the solid state.[69,70,73,74] Like the blue-shifted emission spectra discussed above (Section 5.2), this can be attributed to reduced conformational flexibility in the excited state. A similar effect is observed in cyanine rotaxanes such as B-**16**⊂α-CD.[67] In this case fluorescence is not enhanced in water, but solvents such as dioxane, which give the highest fluorescence quantum yields for the free dye **16**, also give the strongest fluorescence enhancement in the rotaxane (up to a factor of 5). This finding demonstrates that the effect is not simply due to the nonpolarity of the cyclodextrin cavity.

Fluorescence enhancement can often be used to monitor the encapsulation of a π system. For example, the fluorescence intensity of cyanine dye **27** (which is similar to DASP-C_{16}, Scheme 11) was studied as a function of the solvent composition (DMSO/water ratio), both for the free dye and in

the presence of amylose (Figure 23).[184] The fluorescence intensity of the free dye decreases as the water content is increased, which is consistent with an increasing aggregation of the hydrophobic dye. In the presence of amylose, the

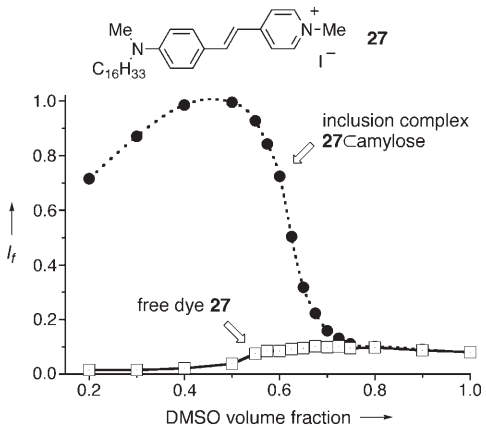

Figure 23. Variation in the relative integrated fluorescence intensity I_f (480–760 nm) versus volume fraction of DMSO in water for solutions of **27** (□) and **27**⊂amylose (●). The concentrations of **27** and amylose are 1.5×10^{-5} and 1.0×10^{-3} M, respectively. Reprinted with permission from Ref. [184]. Copyright 1998 Royal Society of Chemistry.

fluorescence intensity is unchanged when the DMSO content is $>75\,\%$, which shows the dye remains uncomplexed. When more water is added to form a solution with about 40% DMSO, the formation of a complex is evident from the sharp increase in the fluorescence. This is followed by a decrease at higher water ratios, perhaps because of swelling of the amylose helix.

Many conjugated polymers are susceptible to fluorescence quenching through aggregation; in dendronized polymers the amount of aggregation quenching is expected to decrease with increasing dendron generation. This picture is supported by the studies of poly(phenyleneethynylene)s **PPE1**(G-*N*; *N*=1–3) (Section 4.5 and Figure 24).[163a] The fluorescence quantum yield of **PPE1**(G-1) with first-generation dendrons decreases from a maximum of $\Phi_F=0.56$ as the concentration is increased (corresponding to an increase in the absorbance (A) from 0.01 to 0.1). **PPE1**(G-2) with second-generation dendrons has a higher quantum yield of $\Phi_F=1.0$ at $A=0.01$, but decreases with increasing concentration. **PPE1**(G-3) with third-generation dendrons has a quantum yield of $\Phi_F=1.0$ throughout the concentration range. The maximum efficiency of an electroluminescent device is limited by the photoluminescence efficiency of its emissive layer. Hence, fluorescence quantum yields of thin films are of great importance in evaluating the potential performance of electroluminescent polymers. The expected trend—where site isolation results in enhanced fluorescence efficiency in the solid state—is illustrated by dendronized poly(phenylenevinylene) **PPV2**[185] (Section 4.4) and dendronized polyfluorenes **PF2**(G-*N*; *N*=1–3, Section 4.3).[155]

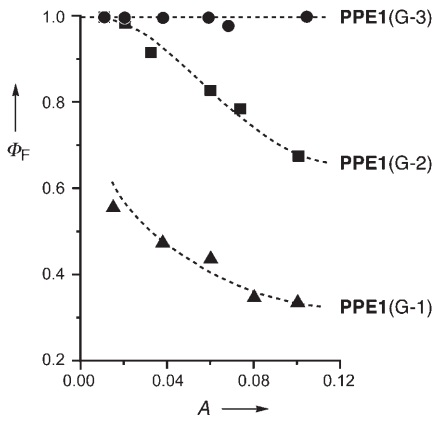

Figure 24. Fluorescence quantum yields Φ_F for **PPE1**(G-*N*; *N*=1–3) in THF solution as a function of concentration (as quantified by the absorbance, *A*). Reprinted with permission from Ref. [163a]. Copyright 1999 American Chemical Society.

5.4. Intramolecular Energy Transfer from the Sheath to the Encapsulated π System

Antenna effects, such as those involved in photosynthetic light harvesting, can occur in dendrimer systems when singlet energy migrates from the dendrons to the core.[186] This Förster-type energy transfer is favored when there is strong overlap of the emission spectrum of the dendron with the absorption spectrum of the core. For example, excitation of polymer **PPE1**(G-3) at a wavelength of 278 nm, at which benzyl ether groups in the dendrons absorb more than the polymer backbone, leads to emission from the polymer backbone only at 454 nm, which can only have occurred by energy transfer from the dendrons to the core.[163] Examination of the photoluminescence excitation spectrum confirmed that the energy transfer was approximately quantitative. Energy transfer also occurs from the Müllen-type dendrons on polymer **PF5** to the polyfluorene backbone,[159b] and this same process has been found to result in undesirable *E*–*Z* photoisomerization in the dendronized oligo(triacetylene)s with Fréchet-type dendrons synthesized by Diederich and coworkers (Section 5.1).[166b] Sheath-to-core energy transfer effects of this type are not relevant to cyclodextrin polyrotaxanes or polysaccharide-wrapped IMWs because sugar-based hosts do not have any chromophore, but they are likely to occur in any IMW where the insulation is built from aromatic units.

5.5. Intermolecular Electron Transfer with IMWs

Prevention of short-circuits is one of the most obvious (and futuristic) motivations for insulating molecular wires. Electron transfer between two IMWs has yet to be tested, but there are many situations where encapsulation has been used to control electron transfer between a molecular wire and an external redox center. These systems point to realistic applications for IMWs in photovoltaic solar-energy harvesting, photochemical evolution of hydrogen from water, and sensors for explosives.

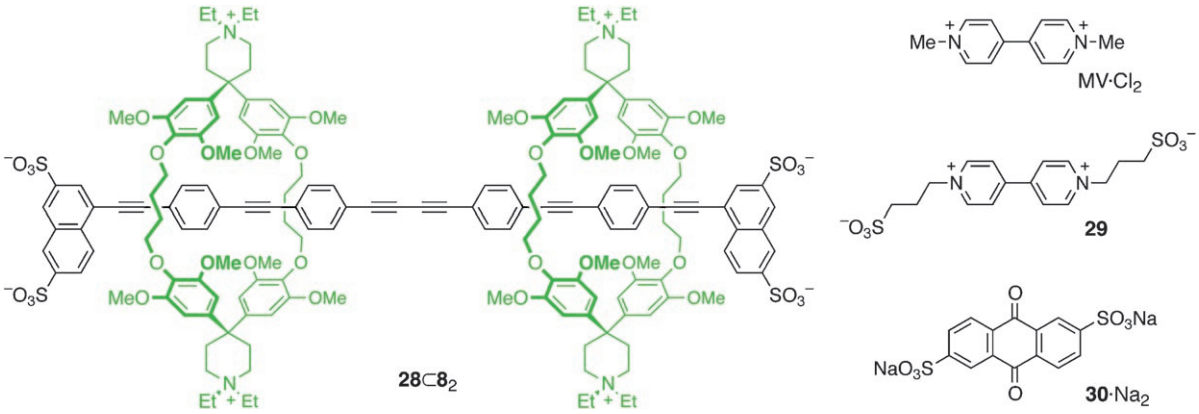

The conjugated backbone of [3]rotaxane **28**⊂**8**$_2$ illustrates how encapsulation can be used to control intramolecular electron transfer. The rotaxane is highly fluorescent, and its fluorescence can be quenched by photoinduced electron transfer to acceptors MV^{2+}, **29**, and **30**.[42] Comparison of the Stern–Volmer quenching constants of the neutral [3]rotaxane with those of the tetraanionic core **28**$^{4-}$ using these cationic, neutral, and anionic electron acceptors shows that in every case electron transfer is slower to the rotaxane than to the free π system **28**. The reduced quenching of this IMW by cationic methyl viologen MV^{2+} is partly due to electrostatic shielding by the cationic cyclophane, but there is also a substantial steric-shielding effect, as shown by the neutral and anionic acceptors; for example, the ratio of the Stern–Volmer constants with **29** is $K_{SV}(\mathbf{28})/K_{SV}(\mathbf{28}\subset\mathbf{8}_2) = 86$.

Haque et al. have demonstrated that cyclodextrin encapsulation can be used to attach dyes to nanocrystalline TiO_2 semiconductor films, and to retard interfacial charge recombination.[187] Excitation of the azo-dye rotaxane **31**⊂α-CD,

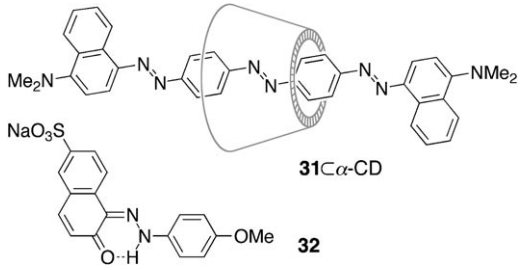

adsorbed onto TiO_2, results in rapid electron transfer from the excited state of the dye to the TiO_2 conduction band. Decay of the resulting radical cation, by electron transfer from the semiconductor in the reverse direction, was monitored by transient absorption spectroscopy. It was not possible to compare the rate of charge recombination in the rotaxane **31**⊂α-CD to that in the free dye **31**, because the free dye does not adsorb onto TiO_2, but comparison with a related azo dye, **32**, indicated that the presence of the cyclodextrin in **31**⊂α-CD retards charge-recombination by increasing the distance of the π system from the semiconductor surface. Half-times for charge recombination ($t_{50\%}$) of 300 and 4 μs were recorded for **31**⊂α-CD and **32**, respectively. The ability to control the rate of back electron transfer in these systems should be useful in the design of Grätzel-type photovoltaic cells.[188]

Dendronization of a π system can also hinder the approach of electron acceptors and reduce the rate of quenching. In other cases the dendrons can provide binding sites for small quencher molecules (either in cavities near the core or on the outer surface of the dendrons), thereby accelerating quenching.[145]

Aida and co-workers have investigated photoinduced electron transfer between polyanionic dendronized poly(phenyleneethynylene)s **PPE2**(G-*N*; *N*=1–3, Section 4.5) and methyl viologen MV^{2+}.[164] When this system is exposed to visible light in the presence of a sacrificial electron donor (triethanolamine) and a colloidal PVA/platinum catalyst, photochemical reduction of water to hydrogen is observed (Figure 25). The catalytic cycle involves the following steps (not necessarily in this chronology):

a) The MV^{2+} ions adsorb onto the anionic surface of the dendronized polymer.
b) Light is absorbed by the conjugated PPE backbone, thereby generating singlet excited states.
c) Electron transfer occurs from the excited state of the conjugated polymer to the MV^{2+} ions to generate $MV^{\bullet+}$ radical cations and radical cations (holes) on the conjugated polymer. The quenching rate constant ($k_q = 1.2 \times 10^{15}\,M^{-1}s^{-1}$) for **PPE2**(G-3) is much greater than the diffusion-controlled limit, thus demonstrating that MV^{2+} ions preassemble on the surface of the dendronized polymer.
d) The $MV^{\bullet+}$ radical cations diffuse away from the IMW and are replaced by MV^{2+} ions, which bind more strongly to the negative surface. Holes may also migrate along the molecular wire. Both these processes, together with the insulating effect of the dendron shell, reduce the probability of unproductive charge recombination by back electron transfer.
e) Holes in the conjugated polymer π system are neutralized by electrons from the sacrificial reductant (triethanolamine).
f) The $MV^{\bullet+}$ radical cations donate electrons to the colloidal platinum; this regenerates MV^{2+} and the platinum reduces water to hydrogen according to Equation (1).

$$2\,MV^{\bullet+} + 2\,H_2O \xrightarrow[\text{catalyst}]{Pt} H_2 + 2\,OH^- + 2\,MV^{2+} \qquad (1)$$

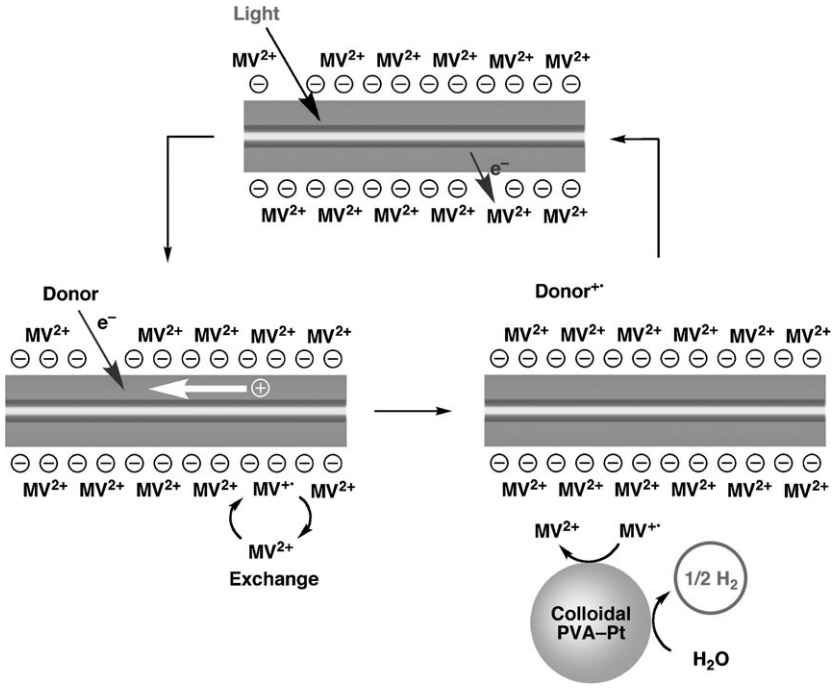

Figure 25. Schematic diagram of photoinduced hydrogen evolution from water with the dendronized poly(phenyleneethynylene) **PPE2**(G-3) as sensitizer, MV^{2+} as an electron acceptor, triethanolamine as a sacrificial electron donor, and colloidal PVA/Pt as a catalyst. Adapted with permission from Ref. [164]. Copyright 2004 American Chemical Society.

This process is remarkably efficient with polymer **PPE2**-(G-3), which has third-generation dendrons, with an overall efficiency of 13% achieved (0.13 moles of H_2 per mole of photons absorbed), compared to a maximum theoretical efficiency of 50% [two electrons are required for each molecule of hydrogen, according to Equation (1)]. **PPE2**(G-1) and **PPE2**(G-2) with lower-generation dendrons are much less efficient in hydrogen production. The dendron shell in **PPE2**(G-3) seems to enhance the efficiency of photochemical generation of hydrogen by spatially isolating the conjugated polymer cores and preventing quenching through aggregation, so that nonradiative decay does not compete with electron transfer to MV^{2+}. The high negative charge on the surface of the IMW is also crucial for binding the MV^{2+} ions. Other types of IMWs, such as polyrotaxanes and polymer-wrapped systems, have not yet been tested for this application, but it seems likely that they could be highly effective.

Another important application for fluorescence quenching by electron transfer is in sensors. Thin films of iptycene-based polymers such as **PPE3** (Section 4.8) can be used as luminescence sensors for nitro compounds commonly found in explosives.[169] The iptycene motif provides a binding site for analytes, improves the luminescence efficiency of the film by preventing close aggregation of the polymer backbone, and promotes a porous film structure that allows analytes to diffuse into the film. Fluorescence quenching occurs by photoinduced electron transfer from the polymer backbone to the analyte. The singlet excitation is able to migrate rapidly along the conjugated polymer so that a bound electron acceptor at any position along the chain can quench the whole polymer, which leads to excellent sensitivity.

5.6. Electroluminescence

Organic light-emitting diodes (OLEDs)[2,9,10] represent one of the most important applications of conjugated polymers, because of the huge demand for low-cost alternatives to liquid-crystal displays and cathode-ray tubes. The enhanced chemical stabilities and photoluminescence efficiencies of IMWs suggest that they could contribute in this area. The structure of a simple OLED is shown in Figure 26a. It consists of a thin layer of the electroluminescent material (ca. 100 nm thick) sandwiched between a transparent anode with a high work function, generally indium-tin oxide (ITO) coated glass, and a cathode with a low work function, in this case calcium capped with aluminum. When a voltage is applied, electrons are injected into the material at the cathode, to generate radical anions, and electrons are removed at the anode, thus leaving holes or radical cations. Electrons and holes migrate through the material under the influence of the electric field and combine to generate excited states, which then fluoresce.

In collaboration with the research group of Cacialli, we have shown that polyrotaxanes such as **PPP1**⊂β-CD, **PF1**⊂β-CD, **PPV1**⊂β-CD, and **PDV1**⊂α-CD (Section 2.2.4) exhibit enhanced electroluminescence efficiency, compared to the corresponding free polymers.[74] Devices with the structure shown in Figure 26a were fabricated by spin-coating an aqueous solution of the polyrotaxane onto the anode, then evaporating a layer of calcium on top of the dry polyrotaxane. Polyrotaxane OLEDs have higher turn-on voltages than those fabricated from the free polymer, as illustrated for **PDV1**⊂α-CD in Figure 26b,[74,189] but for a given current they produce more light (Figure 26c), thus reflecting their higher fluorescence quantum yields (Section 5.3).

The external electroluminescence (EL) quantum yields of these first polyrotaxane OLEDs were very low (around 0.02%), but recently we have demonstrated that the EL efficiency can be increased by a factor of up to 160 by blending the polyrotaxanes with poly(ethylene oxide) (PEO).[190] The EL efficiencies of the free polymers also increase on blending them with PEO, but remain substantially lower than those of the polyrotaxanes (see the logarithmic scale in Figure 26d). Fluorescence titrations in dilute aqueous solution as well as AFM imaging indicate that PEO binds strongly to these polyrotaxanes, presumably by complexation of the lithium counterions. The PEO probably increases the EL efficiency by wrapping round the conjugated polymer, to further insulate the π system, while also facilitating charge transport and charge injection by mobilizing the lithium cations. The dramatic enhancement in the EL efficiency in

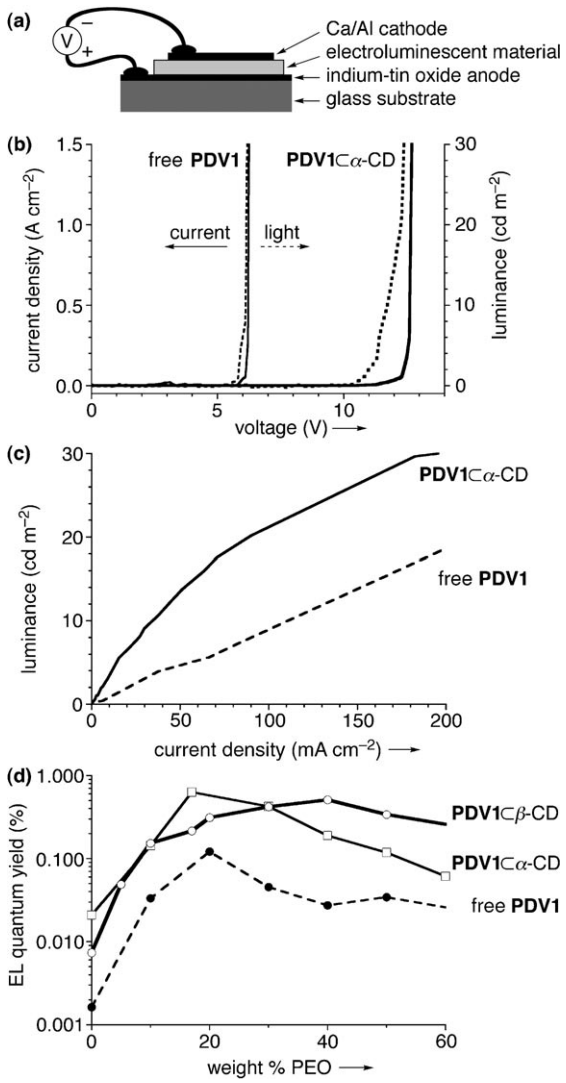

Figure 26. a) Structure of a polyrotaxane OLED. b) Variation in current density (——) and luminance (-----) with voltage for typical OLEDs fabricated from **PDV1**⊂α-CD and **PDV1**.[74,189] c) Data from Figure 26 b replotted as luminance versus current density. d) Variation in electroluminescence efficiency with the weight fraction of PEO for blends of **PDV1**⊂α-CD, **PDV1**⊂β-CD, and **PDV1**.[190]

these materials encourages us to believe that IMWs are promising materials for optoelectronic applications.

Zeolite-encapsulated conjugated polymers are generally not electroluminescent because their conductivities are too low (see Section 5.7), although Álvaro et al. have observed weak electroluminescence in an LED consisting of a 50-μm-thick film of zeolite-encapsulated PPV in polyacrylamide sandwiched between indium-tin oxide and aluminum electrodes.[24] Efficient electroluminescence has been reported in polymer–clay and polymer–metal chalogenide nanocomposites.[191,192] These nanocomposites are similar to zeolite-encapsulated polymers, except that the polymer chains are confined to two-dimensional galleries, rather than one-dimensional channels. For example, LEDs prepared from blends of MEH-PPV (Figure 1 a) and organoclay (namely, a clay in which the metal cations have been exchanged for tetraalkylammonium ions) gave external electroluminescence quantum yields of up to 0.38 %, which was about 100-times higher than that of similar devices prepared from pure MEH-PPV.[191] This result was attributed to the two-dimensional confinement of charge carriers and excitons. The results have some similarity to our work on conjugated polyrotaxanes.[74,189]

Dendronized conjugated polymers have also been used to fabricate OLEDs, and it is interesting to see how the electroluminescence behavior evolves with changing dendron generation and dendron coverage for a given polymer backbone. Carter and co-workers incorporated polyfluorene homopolymers **PF2**(G-1) and **PF2**(G-2), random copolymer **PF3**(G-2), and alternating copolymer **PF4**(G-2) (Section 4.3) into bilayer ITO/PEDOT/PF/Ca/Al devices. The homopolymer devices only started to emit light at a bias of around 16 V, while the copolymers, with lower degrees of dendron substitution, turned on at 4.5 V and 6 V, respectively. The electroluminescence efficiencies of these devices were not reported as a result of problems with reproducibility and device stability.[155] The dendronized PPVs **PPV4**(G-1) and **PPV4**(G-0) have also been tested as electroluminescent materials. The first-generation material **PPV4**(G-1) gave a similar turn-on voltage, but lower EL efficiency than the zeroth generation polymer **PPV4**(G-0).[162] Müllen and co-workers have studied OLEDs constructed from dendronized polyfluorene **PF5**. Devices with a ITO/PEDOT/**PF5**/Ca/Al structure turned on at 6–7 V, and, importantly, the emission color was more stable than for nondendronized polyfluorene devices upon continuous application of 8 V for 30 minutes.[159] This enhanced device stability may be due to the high glass-transition temperature, the high chemical stability, or the hindered diffusion of excitons to keto defects.

5.7. Conductivity and Charge Transport within IMWs

Conjugated polymers encapsulated in zeolites and mesoporous hosts exhibit negligible direct-current conductivities, even when doped, and the low conductivity of these materials is often used to test that the polymer is encapsulated, rather than coated on the surface of host particles.[22] This lack of conductivity can be attributed to the fact that the host prevents interchain charge transfer, but the host may also prevent charge carriers from moving along polymer chains. The charge-carrier mobility on isolated conjugated polymer chains can be probed using contactless microwave techniques to give the microwave dielectric constant (or polarizability) ε' and the microwave dielectric loss (or conductivity) ε'' (both of which should be high for a conductive wire). The first experiments of this type were carried out by Bein and co-workers[19] using Fe^{3+}-doped polypyrrole in mordenite (a unidirectional zeolite with 7-Å-diameter channels). The encapsulated polypyrrole gave ε' and ε'' values similar to those of the pyrrole monomer, thus indicating the absence of mobile charge carriers. The authors concluded that ions in the zeolite framework trap polarons and bipolarons on the conjugated polymer. Similar experiments on polyaniline emeraldine salt in MCM-41 mesoporous aluminosilicate

(30-Å-diameter channels) gave a microwave conductivity of 1.4×10^{-3} S cm^{-1} (compared to 5.7×10^{-3} S cm^{-1} for the free material).[18] However, the channels in this mesoporous host are wide enough to accommodate about 20 parallel polyaniline chains, so interchain contacts probably contribute to this microwave conductivity.

Some insights into how the spatially isolated conjugated polymer chains of an IMW ought to behave can be gained by studying the mobility of radical anion (electron) and radical cation (hole) centers on isolated conjugated polymer chains in dilute solution. Warman, Siebbeles, and co-workers have used pulse-radiolysis time-resolved microwave conductivity (TRMC) to address this issue.[193–195] In this technique, a pulse of electrons is used to ionize the solvent, usually benzene, thereby generating solvated electrons and benzene radical cations. Electron traps (for example, CCl_4 or O_2) or hole traps (for example, NH_3) are added to capture one type of charge carrier, while the other rapidly dopes the conjugated polymer, thus leading to a transient microwave conductivity response. The one-dimensional intrachain mobilities determined from these measurements are generally higher than those measured in bulk samples. For example, MEH-PPV (Figure 1a, Section 1) has a microwave intrachain hole mobility of 0.4 cm^2 V^{-1} s^{-1},[193] which is several orders of magnitude higher than the direct-current hole mobility in thin-films (ca. 1×10^{-4} cm^2 V^{-1} s^{-1}).[196] Even these high intrachain mobilities are smaller than predicted for a regular extended conjugated polymer chain, because of defects, conformational twists, and chain ends. Siebbeles and co-workers reported experimental and theoretical results that indicated that infinitely long PPV chains in dilute solution should have microwave intrachain hole mobilities of about 60 cm^2 V^{-1} s^{-1}.[194] Ladder polymers such as **LP1** (Section 4.8) are expected to have less torsional disorder than PPV—which lead to higher hole mobilities—and very recent results on a series of these ladder oligomers indicate that the intrachain microwave hole mobility is around 600 cm^2 V^{-1} s^{-1}.[195] Placing a molecular wire in a linear nonpolar sheath should enhance the charge mobility by reducing conformational defects and preventing charge trapping, and there is clearly much scope for exploring charge transport in IMWs by using pulse-radiolysis TRMC.

The first conductivity measurements on single IMWs were reported recently by Ito and co-workers. Strands of iodine-doped polyaniline encapsulated in α-CD-based nanotubes (Figure 12) were positioned across a 150-nm-wide gap between platinum electrodes. At 30 °C nearly ohmic behavior was observed with resistances of 17–150 GΩ;[95] these polyaniline IMWs showed no measurable conductivity without iodine doping. This exciting result provokes many questions about the mechanism of charge transport in such long IMWs, and about the contribution of junction barriers to resistance (at electrode contacts and between polyaniline segments of the chain).

The conductivities of thin films of metallo-pseudopolyrotaxanes such as **4**·M$_n$⊂**2**$_n$, **4**$_2$·M$_{2n}$⊂**7** (Schemes 2 and 3, Section 2.1.1), and **33**·M$_n$⊂**2**$_n$ have been tested as a function of the applied electrochemical potential and as a function of the metal cation (M = Cu$^+$, Zn^{2+}, or no metal ion).[34,35,38] In

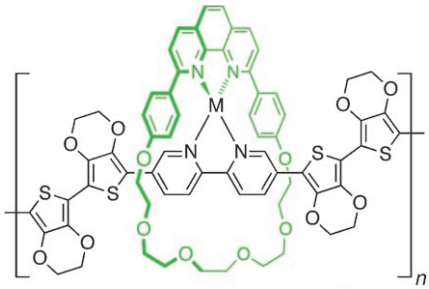

33·M$_n$⊂**2**$_n$ (M = Cu$^+$ or Zn^{2+})

general, the conductivity profiles of these polymers show peaks at each redox half-wave potential, because the conductivity is highest when the π system is partially oxidized. The presence of redox-active metal cations only makes a significant contribution to the conductivity when the M$^+$/M^{-2+} redox potential happens to match the oxidation potential of the polymer π system. Thus, zinc cations have little effect on the conductivity, because Zn^{2+} is not redox active. Copper cations have little effect on the conductivity of [**4**·Cu$_n$⊂**2**$_n$]$^{n+}$ because the first oxidation potential of the π system is much higher than that of Cu$^+$/Cu^{2+}. However, the Cu$^+$/Cu^{2+} couple in [**33**·Cu$_n$⊂**2**$_n$]$^{n+}$ happens to match the first oxidation potential of the polymer, thereby resulting in inner-sphere metal-mediated charge transport and dramatically increased conductivity.[35] A 10^6–10^7-fold increase in conductivity is observed when the metal-free polymer **33**⊂**2**$_n$ is treated with Cu^{2+} ions. A similar effect was observed when the central electron-rich strand **7** of the three-strand ladder polymer [**4**$_2$·Cu$_{2n}$⊂**7**]$^{2n+}$ is partially oxidized.[38] In this bizarre IMW, the conductive polymacrocyclic core strand **7** is isolated and insulated by the other two less conductive conjugated polymer stands **4**, which are threaded through it. The tremendous sensitivity of the conductivity of these systems to the redox activity of the coordinated metal cations suggests that they could be used in sensors, either directly for sensing redox-active cations, or for detecting small molecules which can bind to the cations or the π system and change the redox-matching.[39]

The fact that OLEDs can be fabricated from polyrotaxanes such as **PPP1**⊂β-CD, **PF1**⊂β-CD, **PPV1**⊂β-CD, and **PDV1**⊂α-CD (Section 2.2.4) shows that the presence of threaded cyclodextrins does not prevent these polymers from behaving as semiconductors.[74] The observation of electroluminescence implies that both electrons and holes can migrate through the material. However, the higher turn-on voltages of the polyrotaxanes (see, for example, Figure 26b) indicate that they have lower conductivity than the free polymers. Charge transport between the conjugated polymer backbones probably occurs through stacking of uninsulated regions of the polymer chain and/or end groups, as suggested by the crystal structures of **17**⊂α-CD,[69] **18**,⊂α-CD[70] **19**⊂α-CD, and **20**⊂α-CD[71] (Figure 7, Section 2.2.4). The mobility of the lithium counterions may contribute to charge transport in these materials, so that they behave to some extent like light-emitting electrochemical cells (LECs)[190] rather than LEDs. LECs are generally character-

ized by symmetrical current–voltage curves (at forward and reverse bias) and slow turn-on kinetics. The behavior of these polyelectrolyte polyrotaxane devices are intermediate between those of conventional LEDs and LECs, perhaps because the cations are mobile but the anions are fixed.[74,189,190]

Conductivity measurements have also been reported on cyclodextrin–polyazomethine polyrotaxanes **PAM1**⊂β-CD and **PAM2**⊂β-CD (Section 2.2.7). Four-point probe conductivity measurements on compressed pellets of the I_2-doped polyazomethine polyrotaxanes showed that the presence of the cyclodextrin has little affect on the conductivity of these polymers.[97,98]

The balance between solubility and conductivity has been explored in dendronized polythiophenes (Section 4.7). For example, polythiophene **PT4**(G-2), with a second-generation dendron on every other thiophene unit, is soluble in organic solvents but shows low conductivity when doped with iodine vapor, because the dendrons prevent interchain charge transport.[168] Polymer **PT5**(G-2), which has a second-generation dendron only on every sixth thiophene unit, was conductive when the bulk solid was doped with $NOBF_4$ but was insoluble. A soluble and conductive polymer **PT5**(G-3) was also prepared with a third-generation dendron on every sixth thiophene unit.

5.8. Single-Molecule Imaging and Manipulation

A common feature of IMWs is their suitability for single-molecule AFM imaging and manipulation. It has often been reported that when a conjugated polymer is wrapped in a polysaccharide or coated with dendrons or threaded through cyclodextrins it becomes easier to image the individual polymer chains (see, for example, Figures 10[74] and 12.[92]).[86,91,100,140] This finding must reflect the reduced tendency to aggregate and the increase in chain thickness that accompanies encapsulation, and also perhaps an increase in the persistence length. Schlüter and co-workers have presented beautiful SFM images of dendronized poly(*para*-phenylene) **PPP4**(G-3) strands oriented by the surface of HOPG.[151] Images of films of amphiphilic dendronized polymers spin-coated onto HOPG also show alignment with HOPG symmetry.[147c] Several nonconjugated dendronized polymers, such as dendronized polystyrenes with high-generation dendrons, are also highly suitable for single-molecule AFM imaging because of their shape-persistent cylindrical conformations.[147]

5.9. Processability and Solubility

Solution processability is a key advantage of organic semiconductors relative to their inorganic counterparts, because it opens up the possibility of low-cost fabrication methods such as ink-jet printing. However, conjugated polymers often tend to be insoluble and difficult to process, unless they are decorated with flexible and/or bulky substituents. Steric interactions with these solubilizing substituents can twist the π system and reduce the conjugation. In principle, threading a molecular wire in a cylindrical sheath should be a way of providing high solubility and processability, without interrupting the planar conformation of the π system. In practice, any type of insulating sheath inevitably has a dramatic effect on the solubility characteristics of a molecular wire. Most polyrotaxanes are more soluble than their free polymers. Polyaniline β-CD inclusion complexes are an exception to this trend;[86] the lower solubility of these pseudopolyrotaxanes, relative to free polyaniline, probably reflects their conformational rigidity.

6. Summary and Outlook

There are many parallels between the challenges involved in the synthesis and characterization of different types of IMWs. For example, the problem of steric congestion associated with the preparation of a highly dendronized conjugated polymer is similar to that faced in the synthesis of a highly threaded conjugated polyrotaxane. In both cases it is difficult, but possible, to achieve mean backbone contour lengths greater than 30 nm. Determining the molecular-weight distributions in these systems can also present a formidable challenge, but rapid developments in synthetic methodology and in characterization techniques such as HPLC, mass spectrometry, and surface probe microscopy are making long IMWs increasingly accessible.

One of the benefits of writing a Review of this type is that it enables one to identify the areas that appear to have been overlooked, as well as to reflect upon disruptive discoveries and opportunities for breakthroughs. The concept of the "insulated molecular wire" has developed tremendously since such systems were first mentioned by Maciejewski in the 1970s,[53] yet most of the area remains unexplored. Much of our appreciation of the possibilities latent in these materials comes from results on a small number of well-characterized IMWs. During the next few years, dramatic advances can be expected in the synthesis of the following architectures:

- cucurbituril polyrotaxanes with conjugated polymer cores,
- polysaccharide-wrapped luminescent polymers, such as PPP and PPV,
- encapsulation of highly reactive conjugated polymers, such as carbyne,
- polymer-wrapped π systems based on synthetic non-polysaccharide hosts such as foldamers,[144]
- π systems encapsulated in synthetic organic nanotubes,[197]
- attachment of IMWs to electrodes and supramolecular assembly of functional molecular electronic devices.

There are also tremendous opportunities for extending our understanding of the physical behavior of IMWs. For example, it is not clear why charge-carrier mobilities are low on isolated conjugated polymer chains in zeolites, but high in isolated conjugated polymer chains in solution (Section 5.7). The high conductivities reported for 150-nm-long polyaniline IMWs are also intriguing.[95] A profound understanding of the factors controlling charge transport within, and between, IMWs will enable us to design valuable new materials. Very

few IMWs have yet been tested as electroluminescent materials for OLEDs or as photosensitizers for hydrogen generation from water, but the first results in both these areas are extremely encouraging. IMWs could also become important as photovoltaic materials for solar cells, because they lend themselves naturally to the fabrication of diffuse heterojunctions between interpenetrating networks of *n*-type and *p*-type semiconductors of the sort that are believed to be essential for high efficiency.[12,198]

Isolated molecular wires represent just one of many supramolecular approaches to organic electronics and nanotechnology. The bottom-up synthesis of complex self-organized architectures promises to provide access to fundamentally new classes of functional materials with unprecedented properties. An illustration of how this field might generate revolutionary materials is provided by the recent invention of "metamaterials" operating at microwave frequencies.[199] These materials consist of millimeter-scale periodic lattices of metal wires and insulators, which have been designed to control the magnetic and dielectric response of the material to microwaves. Metamaterials can be constructed to exhibit unconventional electromagnetic phenomena, such as negative refractive index, and used to make "perfect lenses", which provide resolution beyond the diffraction limit. The size of the wire and insulator components of a metamaterial lattice needs to be smaller than the wavelength of the radiation, which is why it is easy to make metamaterials that operate with microwaves ($\lambda = 3$ cm at 12 GHz). Perhaps it will be possible to use IMWs to create metamaterials with negative refractive indices at visible wavelengths. The ability to position semiconducting and insulating nanocomponents accurately on the molecular scale opens up many possibilities. IMWs are set to play a central role in the supramolecular engineering of optoelectronic materials.[200]

Abbreviations

A	absorbance
AFM	atomic force microscopy
CB[*n*]	cucurbit[*n*]uril
CD	cyclodextrin
DASP	dimethylaminostyrylpyridinium
DMF	dimethylformamide
DMSO	dimethylsulfoxide
DM-β-CD	2,6-di-*O*-methyl β-cyclodextrin
EDOT	3,4-(ethylenedioxy)thiophene
EL	electroluminescence
Fc	ferrocene
FEB	frequency-domain electric birefringence
GPC	gel-permeation chromatography
HOPG	highly oriented pyrolytic graphite
HP-β-CD	2-hydroxypropyl β-cyclodextrin (complex mixture)
IMW	insulated molecular wire
ITO	indium-tin oxide
K_{SV}	Stern–Volmer constant
LEC	light-emitting electrochemical cell
LED	light-emitting diode
LP	ladder polymer
LS	light scattering
MALDI	matrix-assisted laser desorption
MCM-41	Mobil crystalline material 41 (a mesoporous aluminosilicate with a hexagonal array of channels)
MEH-PPV	poly[2-methoxy-5-(2′-ethylhexyloxy)-1,4-phenylenevinylene]
$\bar{M}_n$	number-average molecular weight
MV	methyviologen
$\bar{M}_w$	mass-average molecular weight
NMP	*N*-methyl-2-pyrrolidinone
NMWCO	nominal molecular-weight cut-off
$\bar{n}_n$	number-average degree of polymerization
NOE	nuclear Overhauser effect
OLED	organic light-emitting diode
PA	polyacetylene
PAM	polyazomethine
PANI	polyaniline
PDA	poly(diacetylene)
PDV	poly(diphenylenevinylene)
PEDOT	poly(3,4-ethyenedioxythiophene)
PEG	poly(ethylene glycol)
PEO	poly(ethylene oxide)
PF	polyfluorene
PPE	poly(phenyleneethynylene)
PPEB	poly(phenyleneethynylenebutadiynylene)
PPP	poly(*para*-phenylene)
PPV	poly(*para*-phenylenevinylene)
PT	polythiophene
PTA	poly(triacetylene)
PVA	poly(vinyl alcohol)
S_0	singlet ground state
S_1	first singlet excited state
SPG	schizophyllan glucan
STM	scanning tunneling microscopy
SWNT	single-walled carbon nanotube
T_2	transverse relaxation time
TEM	transmission electron microscopy
TGA	thermogravimetric analysis
THF	tetrahydrofuran
TM-β-CD	2,3,6-tri-*O*-methyl β-cyclodextrin
TOF	time of flight
TRMC	time-resolved microwave conductivity
XPS	X-ray photoelectron spectroscopy
λ	wavelength
Φ_F	fluorescence quantum yield
2T	2,2′-bithiophene

Our work on IMWs would not have been possible without the enthusiastic encouragement, intellectual guidance, and expertise of several collaborators, particularly Franco Cacialli (UCL, London UK), Paolo Samorì (ISIS Université Louis Pasteur, Strasbourg, France and CNR Bologna, Italy), Laura M. Herz (Oxford UK), and Richard H. Friend (Cambridge UK). We are also indebted to the key contributions to this research in Oxford made by Sally Anderson, Andrew J. Hagan, Peter N. Taylor, Michael R. Craig, Jonathan E. H.

Buston, Michael J. O'Connell, Carol A. Stanier, Jasper J. Michels, Jun Terao, and Charlotte C. Williams. We thank the EPSRC for financial support.

Received: May 6, 2006
Published online: January 16, 2007

[1] H. Shirakawa, E. J. Louis, A. G. MacDiarmid, C. K. Chiang, A. J. Heeger, *J. Chem. Soc. Chem. Commun.* **1977**, 578; H. Shirakawa, *Angew. Chem.* **2001**, *113*, 2641 – 2648; *Angew. Chem. Int. Ed.* **2001**, *40*, 2574 – 2580.
[2] J. H. Burroughes, D. D. C. Bradley, A. R. Brown, R. N. Marks, K. Mackay, R. H. Friend, P. L. Burn, A. B. Holmes, *Nature* **1990**, *347*, 539 – 541.
[3] J. E. Lennard-Jones, *Proc. R. Soc. London Ser. A* **1937**, *158*, 280 – 296.
[4] H. Kuhn, *J. Chem. Phys.* **1949**, *17*, 1198 – 1212.
[5] H. C. Longuet-Higgins, L. Salem, *Proc. R. Soc. London Ser. A* **1959**, *251*, 172 – 185.
[6] R. E. Peierls, *Quantum Theory of Solids*, Oxford University Press, Oxford, **1955**.
[7] M. Goehring, *Q. Rev. Chem. Soc.* **1956**, *10*, 437 – 450; D. Chapman, R. J. Warn, A. G. Fitzgerald, A. D. Yoffe, *Trans. Faraday Soc.* **1964**, *60*, 294 – 300; M. M. Labes, P. Love, L. F. Nichols, *Chem. Rev.* **1979**, *79*, 1 – 15.
[8] W. A. Little, *Phys. Rev. A* **1964**, *134*, 1416 – 1424.
[9] S. R. Forrest, *Nature* **2004**, *428*, 911 – 918.
[10] R. H. Friend, R. W. Gymer, A. B. Holmes, J. H. Burroughes, R. N. Marks, C. Taliani, D. D. C. Bradley, D. A. Dos Santos, J. L. Brédas, M. Lögdlund, W. R. Salaneck, *Nature* **1999**, *397*, 121 – 128; A. Kraft, A. C. Grimsdale, A. B. Holmes, *Angew. Chem.* **1998**, *110*, 416 – 443; *Angew. Chem. Int. Ed.* **1998**, *37*, 402 – 428.
[11] H. Sirringhaus, N. Tessler, R. H. Friend, *Science* **1998**, *280*, 1741 – 1744; C. D. Dimitrakopoulos, P. R. L. Malenfant, *Adv. Mater.* **2002**, *14*, 100 – 117.
[12] K. M. Coakley, M. D. McGehee, *Chem. Mater.* **2004**, *16*, 4533 – 4542; M. Granström, K. Petritsch, A. C. Arias, A. Lux, M. R. Andersson, R. H. Friend, *Nature* **1998**, *395*, 257 – 260.
[13] A. Rose, Z. G. Zhu, C. F. Madigan, T. M. Swager, V. Bulovic, *Nature* **2005**, *434*, 876 – 879; J. H. Wosnick, T. M. Swager, *Curr. Opin. Chem. Biol.* **2000**, *4*, 715 – 720.
[14] For reviews on molecular wires see: N. Robertson, C. A. McGowan, *Chem. Soc. Rev.* **2003**, *32*, 96 – 103; R. L. Carroll, C. B. Gorman, *Angew. Chem.* **2002**, *114*, 4556 – 4579; *Angew. Chem. Int. Ed.* **2002**, *41*, 4378 – 4400; J. M. Tour, *Acc. Chem. Res.* **2000**, *33*, 791 – 804; R. E. Martin, F. Diederich, *Angew. Chem.* **1999**, *111*, 1440 – 1469; *Angew. Chem. Int. Ed.* **1999**, *38*, 1350 – 1377; T. M. Swager, *Acc. Chem. Res.* **1998**, *31*, 201 – 207; M. D. Ward, *Chem. Soc. Rev.* **1995**, *24*, 121 – 134.
[15] For discussion of single-molecule conductivity see: T. Dadosh, Y. Gordin, R. Krahne, I. Khivrich, D. Mahalu, V. Frydman, J. Sperling, A. Yacoby, I. Bar-Joseph, *Nature* **2005**, *436*, 677 – 680; A. Nitzan, M. A. Ratner, *Science* **2003**, *300*, 1384 – 1389; L. A. Bumm, J. J. Arnold, M. T. Cygan, T. D. Dunbar, T. P. Burgin, L. Jones, D. L. Allara, J. M. Tour, P. S. Weiss, *Science* **1996**, *271*, 1705 – 1707.
[16] M. Parodi, B. Bianco, A. Chiabrera, *Cell Biophys.* **1985**, *7*, 215 – 235.
[17] T. Bein, P. Enzel, *Angew. Chem.* **1989**, *101*, 1737 – 1739; *Angew. Chem. Int. Ed. Engl.* **1989**, *28*, 1692 – 1694; P. Enzel, T. Bein, *J. Chem. Soc. Chem. Commun.* **1989**, 1326 – 1327; P. Enzel, T. Bein, *J. Phys. Chem.* **1989**, *93*, 6270 – 6272.
[18] C.-G. Wu, T. Bein, *Science* **1994**, *264*, 1757 – 1759.
[19] L. Zuppiroli, F. Beuneu, J. Mory, P. Enzel, T. Bein, *Synth. Met.* **1993**, *55–57*, 5081 – 5087.
[20] T.-Q. Nguyen, J. Wu, V. Doan, B. J. Schwartz, S. H. Tolbert, *Science* **2000**, *288*, 652 – 656; T.-Q. Nguyen, J. Wu, S. H. Tolbert, B. J. Schwartz, *Adv. Mater.* **2001**, *13*, 609 – 611.
[21] M. Ikegame, K. Tajima, T. Aida, *Angew. Chem.* **2003**, *115*, 2204 – 2207; *Angew. Chem. Int. Ed.* **2003**, *42*, 2154 – 2157; G. Li, S. Bhosale, T. Wang, Y. Zhang, H. Zhu, J.-H. Fuhrhop, *Angew. Chem.* **2003**, *115*, 3948 – 3951; *Angew. Chem. Int. Ed.* **2003**, *42*, 3818 – 3821.
[22] D. J. Cardin, *Adv. Mater.* **2002**, *14*, 553 – 563; T. Bein, *Stud. Surf. Sci. Catal.* **1996**, *102*, 295 – 322; E. Ruiz-Hitzky, P. Aranda, *Quim. Anal.* **1997**, *93*, 197 – 212.
[23] M. Alvaro, D. J. Cardin, H. M. Colquhoun, H. Garcia, A. Gilbert, A. K. Lay, J. H. Thorpe, *Chem. Mater.* **2005**, *17*, 2546 – 2551.
[24] M. Álvaro, A. Corma, B. Ferrer, M. S. Galletero, H. García, E. Peris, *Chem. Mater.* **2004**, *16*, 2142 – 2147.
[25] V. S.-Y. Lin, D. R. Radu, M.-K. Han, W. Deng, S. Kuroki, B. H. Shanks, M. Pruski, *J. Am. Chem. Soc.* **2002**, *124*, 9040 – 9041.
[26] C. F. van Nostrum, S. J. Picken, A.-J. Schouten, R. J. M. Nolte, *J. Am. Chem. Soc.* **1995**, *117*, 9956 – 9965; A.-M. van de Craats, J. M. Warman, K. Müllen, Y. Geerts, J. D. Brand, *Adv. Mater.* **1998**, *10*, 36 – 38.
[27] M. Kreyenschmidt, F. Uckert, K. Müllen, *Macromolecules* **1995**, *28*, 4577 – 4582; M. Grell, D. C. C. Bradley, X. Long, T. Chamberlain, M. Inbasekaran, E. P. Woo, M. Soliman, *Acta Polym.* **1998**, *49*, 439 – 444.
[28] C. J. Hawker, E. E. Malmström, C. W. Frank, J. P. Kampf, *J. Am. Chem. Soc.* **1997**, *119*, 9903 – 9904.
[29] *Molecular catenanes, rotaxanes and knots* (Eds.: J.-P. Sauvage, C. Dietrich-Buchecker), Wiley, Chichester, **1999**; F. Huang, H. W. Gibson, *Prog. Polym. Sci.* **2005**, *30*, 982 – 1018; H. Tian, Q.-C. Wang, *Chem. Soc. Rev.* **2006**, *35*, 361 – 371.
[30] *Electronic Materials: The Oligomer Approach* (Eds.: K. Müllen, G. Wegner), Wiley, Chichester, **1998**; R. E. Martin, F. Diederich, *Angew. Chem.* **1999**, *111*, 1440 – 1469; *Angew. Chem. Int. Ed.* **1999**, *38*, 1350 – 1377.
[31] E. Arunkumar, C. C. Forbes, B. D. Smith, *Eur. J. Org. Chem.* **2005**, 4051 – 4059.
[32] C. O. Dietrich-Buchecker, J.-P. Sauvage, J. P. Kintzinger, *Tetrahedron Lett.* **1983**, *24*, 5095 – 5098; C. O. Dietrich-Buchecker, J.-P. Sauvage, J.-M. Kern, *J. Am. Chem. Soc.* **1984**, *106*, 3043 – 3045; for the first application of this strategy to rotaxane synthesis see: C. Wu, P. R. Lecavlier, Y. X. Shen, H. W. Gibson, *Chem. Mater.* **1991**, *3*, 569 – 572.
[33] H. Sleiman, P. Baxter, J.-M. Lehn, K. Rissanen, *J. Chem. Soc. Chem. Commun.* **1995**, 715 – 716; P. N. W. Baxter, H. Sleiman, J.-M. Lehn, K. Rissanen, *Angew. Chem.* **1997**, *109*, 1350 – 1352; *Angew. Chem. Int. Ed. Engl.* **1997**, *36*, 1294 – 1296; H. Sleiman, P. N. W. Baxter, J.-M. Lehn, K. Airola, K. Rissanen, *Inorg. Chem.* **1997**, *36*, 4734 – 4742.
[34] S. S. Zhu, P. J. Caroll, T. M. Swager, *J. Am. Chem. Soc.* **1996**, *118*, 8713 – 8714.
[35] S. S. Zhu, T. M. Swager, *J. Am. Chem. Soc.* **1997**, *119*, 12568 – 12577.
[36] P.-L. Vidal, M. Billon, B. Divisia-Blohorn, G. Bidan, J.-M. Kern, J.-P. Sauvage, *Chem. Commun.* **1998**, 629 – 630; P.-L. Vidal, B. Divisia-Blohorn, G. Bidan, J.-M. Kern, J.-P. Sauvage, J.-L. Hazemann, *Inorg. Chem.* **1999**, *38*, 4203 – 4210.
[37] J.-P. Sauvage, J.-M. Kern, G. Bidan, B. Divisia-Blohorn, P.-L. Vidal, *New J. Chem.* **2002**, *26*, 1287 – 1290.
[38] J. Buey, T. M. Swager, *Angew. Chem.* **2000**, *112*, 622 – 626; *Angew. Chem. Int. Ed.* **2000**, *39*, 608 – 612.
[39] B. J. Holliday, T. M. Swager, *Chem. Commun.* **2005**, 23 – 36.
[40] F. Diederich in *Cyclophanes (Monographs in Supramolecular Chemistry, Vol. 2)* (Ed.: J. F. Stoddart), Royal Society of Chemistry, Cambridge, **1991**; F. Diederich, *Angew. Chem.* **1988**, *100*, 372 – 396; *Angew. Chem. Int. Ed. Engl.* **1988**, *27*,

362 – 386; S. B. Ferguson, E. M. Seward, F. Diederich, E. M. Sanford, A. Chou, P. Inocencio-Szweda, C. B. Knobler, *J. Org. Chem.* **1988**, *53*, 5593 – 5595.

[41] S. Anderson, H. L. Anderson, *Angew. Chem.* **1996**, *108*, 2075 – 2078; *Angew. Chem. Int. Ed. Engl.* **1996**, *35*, 1956 – 1959; S. Anderson, R. T. Aplin, T. D. W. Claridge, T. Goodson, A. C. Maciel, G. Rumbles, J. F. Ryan, H. L. Anderson, *J. Chem. Soc. Perkin Trans. 1* **1998**, 2383 – 2397.

[42] P. N. Taylor, A. J. Hagan, H. L. Anderson, *Org. Biomol. Chem.* **2003**, *1*, 3851 – 3856.

[43] *Comprehensive Supramolecular Chemistry*, *Vol. 3* (Eds: J. L. Atwood, J. E. D. Davies, D. D. MacNichol, F. Vögtle), Pergamon, Oxford, **1996**.

[44] K. Harata, *Bull. Chem. Soc. Jpn.* **1977**, *50*, 1259 – 1266.

[45] T. Aree, N. Chaichit, *Carbohydr. Res.* **2003**, *338*, 1581 – 1589.

[46] K. Harata, *Bull. Chem. Soc. Jpn.* **1987**, *60*, 2763 – 2767.

[47] K. Harata, *Chem. Rev.* **1998**, *98*, 1803 – 1827.

[48] The repeat distances in channel-type cyclodextrin crystal structures in Figure 4 come from a search of the Cambridge Crystallographic Database which gave the following hits: α-CD: 15 structures with a head-to-tail arrangement (8.2 ± 0.2) Å; α-CD: 6 structures with a head-to-head arrangement (15.6 ± 0.1) Å; β-CD: 20 structures with a head-to-head arrangement (15.8 ± 0.2) Å; γ-CD: 7 structures with a head-to-tail/head-to-head arrangement (23.1 ± 0.1) Å. Nonlinear zigzag channels were excluded from this analysis.

[49] C. M. Spencer, J. F. Stoddart, R. Zarzychi, *J. Chem. Soc. Perkin Trans. 2* **1987**, 1323 – 1324; K. Takeo, *Carbohydr. Res.* **1990**, *200*, 481 – 485.

[50] M. V. Rekharsky, Y. Inoue, *Chem. Rev.* **1998**, *98*, 1875 – 1917.

[51] A. Harada, M. Kamachi, *Macromolecules* **1990**, *23*, 2823 – 2824; A. Harada, J. Li, M. Kamachi, *Nature* **1992**, *356*, 325 – 327; A. Harada, J. Li, M. Kamachi, *Macromolecules* **1993**, *26*, 5698 – 5703; A. Harada, J. Li, M. Kamachi, *Macromolecules* **1994**, *27*, 4538 – 4543.

[52] G. Wenz, B. Keller, *Angew. Chem.* **1992**, *104*, 201 – 204; *Angew. Chem. Int. Ed. Engl.* **1992**, *31*, 197 – 199.

[53] Several reports of the synthesis of pseudopolyrotaxanes by polymerization of monomer–cyclodextrin inclusion complexes predate the Harada–Kamachi and Wenz–Keller systems; these include the synthesis of a material proposed to have an IMW structure: M. Maciejewski, *J. Macromol. Sci. Chem.* **1979**, *13*, 1175 – 1202.

[54] We calculated the length of these polymer repeat units by projecting onto the axis of the polymer backbone through molecular mechanics using CAChe 4.1 (Oxford Molecular Ltd.) with augmented MM2 parameters.

[55] G. Wenz, B.-H. Han, A. Müller, *Chem. Rev.* **2006**, *106*, 782 – 817; A. Harada, *J. Polym. Sci. Part A* **2006**, *44*, 5113 – 5119; F. M. Raymo, J. F. Stoddart, *Chem. Rev.* **1999**, *99*, 1643 – 1663; S. A. Nepogodiev, J. F. Stoddart, *Chem. Rev.* **1998**, *98*, 1959 – 1976.

[56] F. Cramer, W. Saenger, H.-C. Spatz, *J. Am. Chem. Soc.* **1967**, *89*, 14 – 20.

[57] K. Harata, *Bull. Chem. Soc. Jpn.* **1976**, *49*, 1493 – 1501.

[58] S. Anderson, T. D. W. Claridge, H. L. Anderson, *Angew. Chem.* **1997**, *109*, 1367 – 1370; *Angew. Chem. Int. Ed. Engl.* **1997**, *36*, 1310 – 1313; M. R. Craig, T. D. W. Claridge, M. G. Hutchings, H. L. Anderson, *Chem. Commun.* **1999**, 1537 – 1538.

[59] M. R. Craig, M. G. Hutchings, T. D. W. Claridge, H. L. Anderson, *Angew. Chem.* **2001**, *113*, 1105 – 1108; *Angew. Chem. Int. Ed.* **2001**, *40*, 1071 – 1074.

[60] H. Murakami, A. Kawabuchi, K. Kotoo, M. Kunitake, N. Nakashima, *J. Am. Chem. Soc.* **1997**, *119*, 7605 – 7606.

[61] D.-H. Qu, Q.-C. Wang, J. Ren, H. Tian, *Org. Lett.* **2004**, *6*, 2085 – 2088; Q.-C. Wang, X. Ma, D.-H. Qu, H. Tian, *Chem. Eur. J.* **2006**, *12*, 1088 – 1096.

[62] F. Sondheimer, D. A. Ben-Efraim, R. Wolovsky, *J. Am. Chem. Soc.* **1961**, *83*, 1675 – 1681.

[63] S. S. Malhotra, M. C. Whiting, *J. Chem. Soc.* **1960**, 3812 – 3822.

[64] A. Mishra, R. K. Behera , P. K. Behera, B. K. Mishra, G. B. Behera, *Chem. Rev.* **2000**, *100*, 1973 – 2011.

[65] L. M. Tolbert, X. D. Zhao, *J. Am. Chem. Soc.* **1997**, *119*, 3253 – 3258.

[66] J. E. H. Buston, F. Marken, H. L. Anderson, *Chem. Commun.* **2001**, 1046 – 1047.

[67] J. E. H. Buston, J. R. Young, H. L. Anderson, *Chem. Commun.* **2000**, 905 – 906.

[68] N. Miyaura, A. Suzuki, *Chem. Rev.* **1995**, *95*, 2457 – 2483.

[69] C. A. Stanier, M. J. O'Connell, W. Clegg, H. L. Anderson, *Chem. Commun.* **2001**, 493 – 494; C. A. Stanier, M. J. O'Connell, W. Clegg, H. L. Anderson, *Chem. Commun.* **2001**, 787.

[70] J. Terao, A. Tang, J. J. Michels, A. Krivokapic, H. L. Anderson, *Chem. Commun.* **2004**, 56 – 57.

[71] H. Onagi, B. Carrozzini, G. L. Cascarano, C. J. Easton, A. J. Edwards, S. F. Lincoln, A. D. Rae, *Chem. Eur. J.* **2003**, *9*, 5971 – 5977.

[72] The crystal structure of a fifth α-CD [2]rotaxane has been reported recently, but the coordinates are not available so we have been unable to check whether its packing arrangement resembles those of **17**⊂α-CD to **20**⊂α-CD; see J. S. Park, J. N. Wilson, K. I. Hardcastle, U. H. F. Bunz, M. Srinivasarao, *J. Am. Chem. Soc.* **2006**, *128*, 7714 – 7715.

[73] P. N. Taylor, M. J. O'Connell, L. A. McNeill, M. J. Hall, R. T. Aplin, H. L. Anderson, *Angew. Chem.* **2000**, *112*, 3598 – 3602; *Angew. Chem. Int. Ed.* **2000**, *39*, 3456 – 3460; J. J. Michels, M. J. O'Connell, P. N. Taylor, J. S. Wilson, F. Cacialli, H. L. Anderson, *Chem. Eur. J.* **2003**, *9*, 6167 – 6176.

[74] F. Cacialli, J. S. Wilson, J. J. Michels, C. Daniel, C. Silva, R. H. Friend, N. Severin, P. Samorì, J. P. Rabe, M. J. O'Connell, P. N. Taylor, H. L. Anderson, *Nat. Mater.* **2002**, *1*, 160 – 164.

[75] M. Kunitake, K. Kotoo, O. Manabe, T. Muramatsu, N. Nakashima, *Chem. Lett.* **1993**, 1033 – 1036; C. J. Easton, S. F. Lincoln, A. G. Meyer, H. Onagi, *J. Chem. Soc. Perkin Trans. 1* **1999**, 2501 – 2506.

[76] M. van den Boogaard, G. Bonnet, P. van't Hof, Y. Wang, C. Brochon, P. van Hutten, A. Lapp, G. Hadziioannou, *Chem. Mater.* **2004**, *16*, 4383 – 4385.

[77] X. Shen, M. Belletête, G. Durocher, *Chem. Phys. Lett.* **1998**, *298*, 201 – 210.

[78] C. Lagrost, K. I. C. Ching, J.-C. Lacroix, S. Aeiyach, M. Jouini, P.-C. Lacaze, J. Tanguy, *J. Mater. Chem.* **1999**, *9*, 2351 – 2358.

[79] Y. Takashima, Y. Oizumi, K. Sakamoto, M. Miyauchi, S. Kamitori, A. Harada, *Macromolecules* **2004**, *37*, 3962 – 3964.

[80] P. Hapiot, C. Lagrost, S. Aeiyach, M. Jouini, J.-C. Lacroix, *J. Phys. Chem. B* **2002**, *106*, 3622 – 3628.

[81] C. Lagrost, J. Tanguy, S. Aeiyach, J. C. Lacroix, M. Jouini, K. I. Chane-Ching, P.-C. Lacaze, *J. Electroanal. Chem.* **1999**, *476*, 1 – 14.

[82] I. Yamaguchi, K. Kashiwagi, T. Yamamoto, *Macromol. Rapid Commun.* **2004**, *25*, 1163 – 1166.

[83] R. V. Belosludov, H. Sato, A. A. Farajian, H. Mizuseki, Y. Kawazoe, *Mol. Cryst. Liq. Cryst.* **2003**, *406*, 195 – 204; R. V. Belosludov, H. Sato, A. A. Farajian, H. Mizuseki, Y. Kawazoe, *Thin Solid Films* **2003**, *438–439*, 80 – 84; R. V. Belosludov, H. Sato, A. A. Farajian, H. Mizuseki, K. Ichinoseki, Y. Kawazoe, *Jpn. J. Appl. Phys.* **2004**, *42*, 2492 – 2494; R. V. Belosludov, A. A. Farajian, H. Mizuseki, K. Ichinoseki, Y. Kawazoe, *Jpn. J. Appl. Phys.* **2004**, *43*, 2061 – 2063.

[84] J. Storsberg, H. Ritter, H. Pielartzik, L. Groenendaal, *Adv. Mater.* **2000**, *12*, 567 – 569.

[85] A. G. MacDiarmid in *Conjugated Polymers and Related Materials* (Eds.: W. R. Salaneck, I. Lundström, B. Rånby), Oxford University Press, Oxford, **1993**, chap. 7, pp. 73 – 98; F.-

L. Lu, F. Wudl, M. Nowak, A. J. Heeger, *J. Am. Chem. Soc.* **1986**, *108*, 8311 – 8313.
[86] K. Yoshida, T. Shimomura, K. Ito, R. Hayakawa, *Langmuir* **1999**, *15*, 910 – 913.
[87] R. V. Belosludov, H. Mizuseki, K. Ichinoseki, Y. Kawazoe, *Jpn. J. Appl. Phys.* **2002**, *41*, 2739 – 2741.
[88] M. Evain, S. Quillard, B. Corraze, W. Wang, A. G. MacDiarmid, *Acta Crystallogr. Sect. E* **2002**, *58*, o343 – o344; A. J. Blake, P. Hubberstey, D. J. Quinlan, *Acta Crystallogr. Sect. C* **1996**, *52*, 1774 – 1776.
[89] G. M. do Nascimento, J. E. P. da Silva, S. I. C. de Torresi, P. S. Santos, M. L. A. Temperini, *Mol. Cryst. Liq. Cryst.* **2002**, *374*, 53 – 58.
[90] G.-L. Yuan, N. Kuramoto, M. Takeishi, *Polym. Adv. Technol.* **2003**, *14*, 428 – 432; E. Subraanian, G. Anitha, M. K. Selvam, M. I. A. Braduisha, *Bull. Mater. Sci.* **2005**, *28*, 55 – 61.
[91] T. Akai, T. Abe, T. Shimomura, K. Ito, *Jpn. J. Appl. Phys.* **2001**, *40*, L1327 – L1329.
[92] T. Shimomura, T. Akai, T. Abe, K. Ito, *J. Chem. Phys.* **2002**, *116*, 1753 – 1756.
[93] A. Harada, J. Li, M. Kamachi, *Nature* **1993**, *364*, 516 – 518; M. Ceccato, P. L. Nostro, C. Rossi, C. Bonechi, A. Donati, P. Baglioni, *J. Phys. Chem. B* **1997**, *101*, 5094 – 5099.
[94] T. Shimomura, K. Yoshida, K. Ito, R. Hayakawa, *Polym. Adv. Technol.* **2000**, *11*, 837 – 839.
[95] T. Shimomura, T. Akai, M. Fujimori, S. Heike, T. Hashizume, K. Ito, *Synth. Met.* **2005**, *153*, 497 – 500; T. Akai, T. Shimomura, K. Ito, *Synth. Met.* **2003**, *135–136*, 777 – 778.
[96] A. Farcas, M. Grigoras, *J. Optoelectron. Adv. Mater.* **2000**, *2*, 525 – 530.
[97] A. Farcas, M. Grigoras, *Polym. Int.* **2003**, *52*, 1315 – 1320.
[98] A. Farcas, M. Grigoras, *High Perform. Polym.* **2001**, *13*, 201 – 210.
[99] D. Nepal, S. Samal, K. E. Geckeler, *Macromolecules* **2003**, *36*, 3800 – 3802.
[100] Y. Liu, Y.-L. Zhao, H.-Y. Zhang, X.-Y. Li, P. Liang, M.-Z. Zhang, J.-J. Xu, *Macromolecules* **2004**, *37*, 6362 – 6369.
[101] There are other reports of the synthesis of cyclodextrin rotaxanes in DMF:[76] J. W. Park, H. J. Song, *Org. Lett.* **2004**, *6*, 4869 – 4872; I. Yamaguchi, Y. Takenaka, K. Osakada, T. Yamamoto, *Macromolecules* **1999**, *32*, 2051 – 2054.
[102] N. Kobayashi, *J. Chem. Soc. Chem. Commun.* **1989**, 1126 – 1128; A. F. Danil de Namor, R. Traboulssi, D. F. V. Lewis, *J. Am. Chem. Soc.* **1990**, *112*, 8442 – 8447.
[103] H. Okumura, Y. Kawaguchi, A. Harada, *Macromol. Rapid Commun.* **2002**, *23*, 781 – 785; H. Okumura, Y. Kawaguchi, A. Harada, *Macromolecules* **2003**, *36*, 6422 – 6429.
[104] S. Mazières, M. K. Raymond, G. Raabe, A. Prodi, J. Michl, *J. Am. Chem. Soc.* **1997**, *119*, 6682 – 6683.
[105] W. A. Freeman, W. L. Mock, N.-Y. Shih, *J. Am. Chem. Soc.* **1981**, *103*, 7367 – 7368.
[106] W. L. Mock in *Comprehensive Supramolecular Chemistry*, *Vol. 2* (Ed.: F. Vögtle), Pergamon, Oxford, **1996**, pp. 477 – 493.
[107] J. W. Lee, S. Samal, N. Selvapalam, H.-J. Kim, K. Kim, *Acc. Chem. Res.* **2003**, *36*, 621 – 630.
[108] J. Lagona, P. Mukhopadhyay, S. Chakrabarti, L. Isaacs, *Angew. Chem.* **2005**, *117*, 4922 – 4949; *Angew. Chem. Int. Ed.* **2005**, *44*, 4844 – 4870.
[109] S. Liu, Y. Zavalij, L. Isaacs, *J. Am. Chem. Soc.* **2005**, *127*, 16798 – 16799.
[110] J. Kim, I.-S. Jung, S.-Y. Kim, E. Lee, J.-K. Kang, S. Sakamoto, K. Yamaguchi, K. Kim, *J. Am. Chem. Soc.* **2000**, *122*, 540 – 541; A. Day, A. P. Arnold, R. J. Blanch, B. Snushall, *J. Org. Chem.* **2001**, *66*, 8094 – 8100; A. I. Day, R. J. Blanch, A. P. Arnold, S. Lorenzo, G. R. Lewis, I. Dance, *Angew. Chem.* **2002**, *114*, 285 – 287; *Angew. Chem. Int. Ed.* **2002**, *41*, 275 – 277.
[111] W. S. Jeon, K. Moon, S. H. Park, H. Chun, Y. H. Ko, J. Y. Lee, E. S. Lee, S. Samal, N. Selvapalam, M. V. Rekharsky, V. Sindelar, D. Sobransingh, Y. Inoue, A. E. Kaifer, K. Kim, *J. Am. Chem. Soc.* **2005**, *127*, 12984 – 12989.
[112] W. Ong, M. Gómez-Kaifer, A. E. Kaifer, *Org. Lett.* **2002**, *4*, 1791 – 1794; H.-J. Kim, W. S. Jeon, Y. H. Ko, K. Kim, *Proc. Natl. Acad. Sci. USA* **2002**, *99*, 5007 – 5011.
[113] S. Y. Jon, Y. H. Ko, S. H. Park, H.-J. Kim, K. Kim, *Chem. Commun.* **2001**, 1938 – 1939.
[114] A. Flinn, G. C. Hough, J. F. Stoddart, D. J. Williams, *Angew. Chem.* **1992**, *104*, 1550 – 1552; *Angew. Chem. Int. Ed. Engl.* **1992**, *31*, 1475 – 1477; J. Zhao, H.-J. Kim, J. Oh, S.-Y. Kim, J. W. Lee, S. Sakamoto, K. Yamaguchi, K. Kim, *Angew. Chem.* **2001**, *113*, 4365 – 4367; *Angew. Chem. Int. Ed.* **2001**, *40*, 4233 – 4235; S. Y. Jon, N. Selvapalam, D. H. Oh, J.-K. Kang, S.-Y. Kim, Y. J. Jeon, J. W. Lee, K. Kim, *J. Am. Chem. Soc.* **2003**, *125*, 10186 – 10187.
[115] J. Mohanty, A. C. Bhasikuttan, W. M. Nau, H. Pal, *J. Phys. Chem. B* **2006**, *110*, 5232 – 5238; R. Wang, L. Yuan, D. H. Macartney, *Chem. Commun.* **2005**, 5867 – 5869; J. Mohanty, W. M. Nau, *Angew. Chem.* **2005**, *117*, 3816 – 3820; *Angew. Chem. Int. Ed.* **2005**, *44*, 3750 – 3754; W. M. Nau, J. Mohanty, *Int. J. Photoenergy* **2005**, *7*, 133 – 141; B. D. Wagner, N. Stojanovic, A. I. Day, R. J. Blanch, *J. Phys. Chem. B* **2003**, *107*, 10741 – 10746.
[116] C. Marquez, W. M. Nau, *Angew. Chem.* **2001**, *113*, 4515 – 4518; *Angew. Chem. Int. Ed.* **2001**, *40*, 4387 – 4390.
[117] K. Kim, *Chem. Soc. Rev.* **2002**, *31*, 96 – 107.
[118] D. Tuncel, J. H. G. Steinke, *Macromolecules* **2004**, *37*, 288 – 302.
[119] Y. Takahashi, T. Kumano, S. Nishikawa, *Macromolecules* **2004**, *37*, 6827 – 6832.
[120] A. Imberty, H. Chanzy, S. Pérez, A. Buléon, V. Tran, *J. Mol. Biol.* **1988**, *201*, 365 – 378.
[121] H.-C. H. Wu, A. Sarko, *Carbohydr. Res.* **1978**, *61*, 7 – 25.
[122] G. Rappenecker, P. Zugenmaier, *Carbohydr. Res.* **1981**, *89*, 11 – 19.
[123] W. Hinrichs, G. Büttner, M. Steifa, C. Betzel, V. Zabel, B. Pfannemüller, W. Saenger, *Science* **1987**, *238*, 205 – 208.
[124] S. Immel, F. W. Lichtenthaler, *Starch/Staerke* **2000**, *52*, 1 – 8.
[125] G. Wulff, S. Kubik, *Makromol. Chem.* **1992**, *193*, 1071 – 1080.
[126] O.-K. Kim, L.-S. Choi, *Langmuir* **1994**, *10*, 2842 – 2846.
[127] K. Clays, G. Olbrechts, T. Munters, A. Persoons, O.-K. Kim, L.-S. Choi, *Chem. Phys. Lett.* **1998**, *293*, 337 – 342.
[128] A. Star, D. W. Steuerman, J. R. Heath, J. F. Stoddart, *Angew. Chem.* **2002**, *114*, 2618 – 2622; *Angew. Chem. Int. Ed.* **2002**, *41*, 2508 – 2512.
[129] O.-K. Kim, J. Je, J. W. Baldwin, S. Kooi, P. E. Pehrsson, L. J. Buckley, *J. Am. Chem. Soc.* **2003**, *125*, 4426 – 4427.
[130] M. J. O'Connell, P. Boul, L. M. Ericson, C. Huffman, Y. Wang, E. Haroz, C. Kuper, J. Tour, K. D. Ausman, R. E. Smalley, *Chem. Phys. Lett.* **2001**, *342*, 265 – 271; Y. Lin, S. Taylor, H. Li, K. A. S. Fernando, L. Qu, W. Wang, L. Gu, B. Zhou, Y.-P. Sun, *J. Mater. Chem.* **2004**, *14*, 527 – 541.
[131] P. van der Valk, R. Marchant, J. G. H. Wessels, *Exp. Myco.* **1977**, *1*, 69 – 82; I. K. M. Morton, J. M. Hall, *Concise Dictionary of Pharmacological Agents Properties and Synonyms*, Kluwer, Dordrecht, **1999**, p. 257; T. Hongu, G. O. Phillips, *New Fibers*, Woodhead, Cambridge, **1997**, pp. 100 – 101.
[132] Y. Kimura, H. Tojima, S. Fukase, K. Takeda, *Acta Oto-Laryngol.* **1994**, *511*, 192 – 195.
[133] T. Yanaki, T. Norisuye, H. Fujita, *Macromolecules* **1980**, *13*, 1462 – 1466; Y. Deslandes, R. H. Marchessault, A. Sarko, *Macromolecules* **1980**, *13*, 1466 – 1471; T. Norisuye, T. Yanaki, H. Fujita, *J. Polym. Sci. Polym. Phys. Ed.* **1980**, *18*, 547 – 558; Y. Kashiwagi, T. Norisuye, H. Fujita, *Macromolecules* **1981**, *14*, 1220 – 1225; T. L. Bluhm, Y. Deslandes, R. H. Marchessault, *Carbohydr. Res.* **1982**, *100*, 117 – 130.

[134] K. Sakurai, S. Shinkai, *J. Am. Chem. Soc.* **2000**, *122*, 4520 – 4521; A.-H. Bae, M. Numata, T. Hasegawa, C. Li, K. Kaneko, K. Sakurai, S. Shinkai, *Angew. Chem.* **2005**, *117*, 2066 – 2069; *Angew. Chem. Int. Ed.* **2005**, *44*, 2030 – 2033.

[135] K. Sakurai, K. Uezu, M. Numata, T. Hasegawa, C. Li, K. Kaneko, S. Shinkai, *Chem. Commun.* **2005**, 4383 – 4398.

[136] Some authors have claimed that *t*-SPG has an axial cavity (see, for example, Refs. [137] and [138]), but this claim is not consisistent with the accepted structure in which the OH(2) groups of the backbone glucose units of the three strands are within van der Waals contact; see: K. Miyoshi, K. Ueza, K. Sakurai, S. Shinkai, *Chem. Biodiversity* **2004**, *1*, 916 – 924.

[137] T. Hasegawa, S. Haraguchi, M. Numata, T. Fujisawa, C. Li, K. Kaneko, K. Sakurai, S. Shinkai, *Chem. Lett.* **2005**, *34*, 40 – 41; T. Hasegawa, S. Haraguchi, M. Numata, C. Li, A.-H. Bae, T. Fujisawa, K. Kaneko, K. Sakurai, S. Shinkai, *Org. Biomol. Chem.* **2005**, *3*, 4321 – 4328.

[138] M. Numata, T. Hasegawa, T. Fujisawa, K. Sakuai, S. Shinkai, *Org. Lett.* **2004**, *6*, 4447 – 4450.

[139] S. Haraguchi, T. Hasegawa, M. Numata, F, Fujiki, K. Uezu, K. Sakurai, S. Shinkai, *Org. Lett.* **2005**, *7*, 5605 – 5608; T. Sanji, N. Kato, M. Kato, M. Tanaka, *Angew. Chem.* **2005**, *117*, 7467 – 7470; *Angew. Chem. Int. Ed.* **2005**, *44*, 7301 – 7304.

[140] C. Li, M. Numata, A.-H. Bae, K. Sakurai, S. Shinkai, *J. Am. Chem. Soc.* **2005**, *127*, 4548 – 4549.

[141] T. Sanji, N. Kato, M. Tanaka, *Org. Lett.* **2006**, *8*, 235 – 238.

[142] a) M. Numata, M. Asai, K. Kaneko, T. Hasegawa, N. Fujita, Y. Kitada, K. Sakurai, S. Shinkai, *Chem. Lett.* **2004**, *33*, 232 – 233; b) T. Hasegawa, T. Fujisawa, M. Numata, M. Umeda, T. Matsumoto, T. Kimura, S. Okumara, K. Sakurai, S. Shinkai, *Chem. Commun.* **2004**, 2150 – 2151; c) M. Numata, M. Asai, K. Kaneko, A.-H. Bae, T. Hasegawa, K. Sakurai, S. Shinkai, *J. Am. Chem. Soc.* **2005**, *127*, 5875 – 5884.

[143] J. Stahl, J. C. Bohling, E. B. Bauer, T. B. Peters, W. Mohr, J. M. Martín-Alvarez, F. Hempel, J. A. Gladysz, *Angew. Chem.* **2002**, *114*, 1951 – 1957; *Angew. Chem. Int. Ed.* **2002**, *41*, 1871 – 1876.

[144] D. J. Hill, M. J. Mio, R. B. Prince, T. S. Hughes, J. S. Moore, *Chem. Rev.* **2001**, *101*, 3893 – 4011; M. T. Stone, J. M. Heemstra, J. S. Moore, *Acc. Chem. Res.* **2006**, *39*, 11 – 20.

[145] a) E. Buhleier, W. Wehner, F. Vögtle, *Synthesis* **1978**, 155; b) D. A. Tomalia, H. Baker, J. R. Dewald, M. Hall, G. Kallos, S. Martin, J. Roeck, J. Ryder, P. Smith, *Polym. J.* **1985**, *17*, 117 – 132; c) G. R. Newkome, C. N. Moorefield, G. Vögtle, *Dendritic Molecules: Concepts, Synthesis, Perspectives*, VCH, Weinheim, **1996**; d) M. Fischer, F. Vögtle, *Angew. Chem.* **1999**, *111*, 934 – 955; *Angew. Chem. Int. Ed.* **1999**, *38*, 885 – 905; e) A. W. Bosman, H. M. Janessen, E. W. Meijer, *Chem. Rev.* **1999**, *99*, 1665 – 1688.

[146] S. Hecht, J. M. J. Fréchet, *Angew. Chem.* **2001**, *113*, 76 – 94; *Angew. Chem. Int. Ed.* **2001**, *40*, 74 – 91.

[147] a) A. D. Schlüter, *Top. Curr. Chem.* **1998**, *197*, 165 – 191; b) H. Frey, *Angew. Chem.* **1998**, *110*, 2313 – 2318; *Angew. Chem. Int. Ed.* **1998**, *37*, 2193 – 2197; c) A. D. Schlüter, J. P. Rabe, *Angew. Chem.* **2000**, *112*, 860 – 880; *Angew. Chem. Int. Ed.* **2000**, *39*, 864 – 883; d) S. Vetter, S. Koch, A. D. Schlüter, *J. Polym. Sci. Part A* **2001**, *39*, 1940 – 1954; e) A. D. Schlüter, *J. Polym. Sci. Part A* **2001**, *39*, 1533 – 1556; f) A. Zhang, L. Shu, Z. Bo, A. D. Schlüter, *Macromol. Chem. Phys.* **2003**, *204*, 328 – 339; g) H. Frauenrath, *Prog. Polym. Sci.* **2005**, *30*, 325 – 384.

[148] C. J. Hawker, J. M. J. Fréchet, *J. Am. Chem. Soc.* **1990**, *112*, 7638 – 7647.

[149] T. Kaneko, T. Horie, M. Asano, T. Aoki, E. Oikawa, *Macromolecules* **1997**, *30*, 3118 – 3121.

[150] B. Karakaya, W. Claussen, K. Gessler, W. Saenger, A.-D. Schlüter, *J. Am. Chem. Soc.* **1997**, *119*, 3296 – 3301.

[151] W. Stocker, B. Karakaya, B. L. Schürmann, J. P. Rabe, A. D. Schlüter, *J. Am. Chem. Soc.* **1998**, *120*, 7691 – 7695.

[152] W. H. Carothers, *Trans. Faraday Soc.* **1936**, *32*, 39 – 49.

[153] Z. Bo, A. D. Schlüter, *Chem. Eur. J.* **2000**, *6*, 3235 – 3241.

[154] a) U. Scherf, E. J. W. List, *Adv. Mater.* **2002**, *14*, 477 – 487; b) J. M. Lupton, M. R. Craig, E. W. Meijer, *Appl. Phys. Lett.* **2002**, *80*, 4489 – 4491; c) L. Romaner, A. Pogantsch, P. Scanducci de Freitas, U. Scherf, M. Gaal, E. Zojer, E. J. W. List, *Adv. Funct. Mater.* **2003**, *13*, 597 – 601; d) W. Zhao, T. Cao, J. M. White, *Adv. Funct. Mater.* **2004**, *14*, 783 – 790; e) L. Liu, S. Qiu, B. Wang, W. Zhang, P. Lu, Z. Xie, M. Hanif, Y. Ma, J. Shen, *J. Phys. Chem. B* **2005**, *109*, 23366 – 23370.

[155] D. Marsitzky, R. Vestberg, P. Blainey, B. T. Tang, C. J. Hawker, K. R. Carter, *J. Am. Chem. Soc.* **2001**, *123*, 6965 – 6972.

[156] H.-Z. Tang, M. Fujiki, Z.-B. Zhang, K. Torimitsu, M. Motonaga, *Chem. Commun.* **2001**, 2426 – 2427.

[157] When calculating the number-average degree of polymerization in polyfluorene copolymers **PF3**(G-*N*) and **PF4**(G-*N*) we defined $\bar{n}_n$ as the average number of fluorene units per polymer chain, that is, the average value of $(m+n)$.

[158] J. Berresheim, M. Müller, K. Müllen, *Chem. Rev.* **1999**, *99*, 1747 – 1785.

[159] a) S. Setayesh, A. C. Grimsdale, T. Weil, V. Enkelmann, K. Müllen, F. Meghdadi, E. J. W. List, G. Leising, *J. Am. Chem. Soc.* **2001**, *123*, 946 – 953; b) A. Pogantsch, F. P. Wenzl, E. J. W. List, G. Leising, A. C. Grimsdale, K. Müllen, *Adv. Mater.* **2002**, *14*, 1061 – 1064; c) A. Pogantsch, C. Gadermaier, G. Cerullo, G. Lanzani, U. Scherf, A. C. Grimsdale, K. Müllen, E. J. W. List, *Synth. Met.* **2003**, *139*, 847 – 849.

[160] Z. Bao, K. R. Amundson, A. J. Lovinger, *Macromolecules* **1998**, *31*, 8647 – 8649.

[161] J. Jiang, H. Liu, Y. Zhao, C. Chen, F. Xi, *Synth. Met.* **2002**, *132*, 1 – 4.

[162] R. Tang, Y. Chuai, C. Cheng, F. Xi, D. Zou, *J. Polym. Sci. Part A* **2005**, *43*, 3126 – 3140; Y.-H. Tseng, F.-I. Wu, P.-I. Shih, C.-F. Shu, *J. Polym. Sci. Part A* **2005**, *43*, 5147 – 5155.

[163] a) T. Sato, D.-L. Jiang, T. Aida, *J. Am. Chem. Soc.* **1999**, *121*, 10658 – 10659; b) S. Masuo, H. Yoshikawa, T. Asahi, H. Masuhara, T. Sato, D.-L. Jiang, T. Aida, *J. Phys. Chem. B* **2003**, *107*, 2471 – 2479.

[164] D.-L. Jiang, C.-K. Choi, K. Honda, W.-S. Li, T. Yuzawa, T. Aida, *J. Am. Chem. Soc.* **2004**, *126*, 12084 – 12089.

[165] W.-S. Li, D.-L. Jiang, T. Aida, *Angew. Chem.* **2004**, *116*, 3003 – 3007; *Angew. Chem. Int. Ed.* **2004**, *43*, 2943 – 2947.

[166] a) P. H. J. Schenning, R. E. Martin, M. Ito, F. Diederich, C. Boudon, J.-P. Gisselbrecht, M. Gross, *Chem. Commun.* **1998**, 1013 – 1014; b) A. P. H. J. Schenning, J.-D. Arndt, M. Ito, A. Stoddart, M. Schreiber, P. Siemsen, R. E. Martin, C. Boudon, J.-P. Gisselbrecht, M. Gross, V. Gramlich, F. Diederich, *Helv. Chim. Acta* **2001**, *84*, 296 – 334.

[167] P. R. L. Malenfant, J. M. J. Fréchet, *Macromolecules* **2000**, *33*, 3634 – 3640.

[168] K. Krishnamoorthy, A. V. Ambade, S. P. Mishra, M. Kanungo, A. Q. Contractor, A. Kumar, *Polymer* **2002**, *43*, 6465 – 6470.

[169] a) J.-S. Yang, T. M. Swager, *J. Am. Chem. Soc.* **1998**, *120*, 11864 – 11873; b) V. E. Williams, T. M. Swager, *Macromolecules* **2000**, *33*, 4069 – 4073.

[170] D. Lee, T. M. Swager, *J. Am. Chem. Soc.* **2003**, *125*, 6870 – 6871; D. Lee, T. M. Swager, *Chem. Mater.* **2005**, *17*, 4622 – 4629.

[171] R. Fiesel, J. Huber, U. Scherf, *Angew. Chem.* **1996**, *108*, 2233 – 2234; *Angew. Chem. Int. Ed. Engl.* **1996**, *35*, 2111 – 2113.

[172] M. Hanack, A. Hirsch, A. Lange, M. Rein, G. Renz, P. Vermehren, *J. Mater. Res.* **1991**, *6*, 385 – 392.

[173] G. M. Finniss, E. Canadell, C. Campana, K. R. Dunbar, *Angew. Chem.* **1996**, *108*, 2946 – 2948; *Angew. Chem. Int. Ed. Engl.* **1996**, *35*, 2772 – 2774.

[174] J. F. Berry, F. A. Cotton, P. Lei, T. Lu, C. A. Murillo, *Inorg. Chem.* **2003**, *42*, 3534 – 3539.

[175] M. G. Debije, M. P. de Haas, J. M. Warman, M. Fontana, N. Stutzmann, M. Kristiansen, W. R. Caseri, P. Smith, S. Hoffmann, T. I. Solling, *Adv. Funct. Mater.* **2004**, *14*, 323 – 328.
[176] F. Würthner, V. Stepanenko, A. Sautter, *Angew. Chem.* **2006**, *118*, 1973 – 1976; *Angew. Chem. Int. Ed.* **2006**, *45*, 1939 – 1942.
[177] Y. Kim, M. F. Mayer, S. C. Zimmerman, *Angew. Chem.* **2003**, *115*, 1153 – 1158; *Angew. Chem. Int. Ed.* **2003**, *42*, 1121 – 1126.
[178] S.-F. Lau, A. J. Sosnowik, L.-S. Choi, J. H. Callahan, O.-K. Kim, *J. Therm. Anal.* **1996**, *46*, 1081 – 1092.
[179] C. A. Stanier, S. J. Alderman, T. D. W. Claridge, H. L. Anderson, *Angew. Chem.* **2002**, *114*, 1847 – 1850; *Angew. Chem. Int. Ed.* **2002**, *41*, 1769 – 1772.
[180] O.-K. Kim, L.-S. Choi, H. Y. Zhang, X.-H. He, Y.-H. Shih, *J. Am. Chem. Soc.* **1996**, *118*, 12220 – 12221; O.-K. Kim, L.-S. Choi, H.-Y. Zhang, H.-H. He, Y.-H. Shih, *Thin Solid Films* **1998**, *327–329*, 172 – 175.
[181] L. S. Choi, O.-K. Kim, *Macromolecules* **1998**, *31*, 9406 – 9408.
[182] D. K. Christopoulos, D. J. Photinos, L. M. Stimson, A. F. Terzis, A. G. Vanakaras, *J. Mater. Chem.* **2003**, *13*, 2756 – 2764.
[183] V. Percec, J. G. Rudick, M. Peterca, M. Wagner, M. Obata, C. M. Mitchell, W.-D. Cho, V. S. K. Balagurusamy, P. A. Heiney, *J. Am. Chem. Soc.* **2005**, *127*, 15257 – 15264.
[184] W. B. Heuer, H. S. Lee, O.-K. Kim, *Chem. Commun.* **1998**, 2649 – 2650.
[185] R. Jakubiak, Z. Bao, L. Rothberg, *Synth. Met.* **2000**, *114*, 61 – 64.
[186] M. Kawa, *Top. Curr. Chem.* **2003**, *228*, 193 – 204.
[187] S. A. Haque, J. S. Park, M. Srinivasarao, J. R. Durrant, *Adv. Mater.* **2004**, *16*, 1177 – 1181.
[188] M. Grätzel, *J. Photochem. Photobiol. C* **2003**, *4*, 145 – 153.
[189] J. S. Wilson, J. J. Michels, R. H. Friend, H. L. Anderson, F. Cacialli, unpublished results.
[190] J. S. Wilson, M. J. Frampton, J. J. Michels, L. Sardone, G. Marletta, R. H. Friend, P. Samorì, H. L. Anderson, F. Cacialli, *Adv. Mater.* **2005**, *17*, 5365 – 5368.
[191] J.-W. Lee, O. O. Park, J. J. Kim, J.-M. Hong, Y. C. Kim, *Chem. Mater.* **2001**, *13*, 2217 – 2222; J. H. Park, Y. T. Lim, O. O. Park, J.-W. Yu, J. K. Kim, Y. C. Kim, *Mater. Sci. Eng. C* **2004**, *24*, 75 – 78.
[192] E. Aharon, A. Albo, M. Kalina, G. L. Frey, *Adv. Funct. Mater.* **2006**, *16*, 980 – 986.
[193] R. J. O. M. Hoofman, M. P. de Haas, L. D. A. Siebbeles, J. M. Warman, *Nature* **1998**, *392*, 54 – 56.
[194] P. Prins, F. C. Grozema, L. D. A. Siebbeles, *J. Phys. Chem. B* **2006**, *110*, 14659 – 14666.
[195] P. Prins, F. C. Grozema, J. M. Schins, S. Patil, U. Scherf, L. D. A. Siebbeles, *Phys. Rev. Lett.* **2006**, *96*, 146601.
[196] A. Kumar, P. K. Bhatnagar, P. C. Mathur, M. Husain, *J. Appl. Phys.* **2005**, *98*, 024502; M. Muratsubaki, Y. Furukawa, T. Noguchi, T. Ohnishi, E. Fujiwara, H. Tada, *Chem. Lett.* **2004**, *33*, 1480 – 1481.
[197] D. T. Bong, T. D. Clark, J. R. Granja, M. R. Ghadiri, *Angew. Chem.* **2001**, *113*, 1016 – 1041; *Angew. Chem. Int. Ed.* **2001**, *40*, 988 – 1011.
[198] G. Yu, J. Goa, J. C. Hummelen, F. Wudl, A. J. Heeger, *Science* **1995**, *270*, 1789 – 1791; J. J. M. Halls, C. A. Walsh, N. C. Greenham, E. A. Marseglia, R. H. Friend, S. C. Moratti, A. B. Holmes, *Nature* **1995**, *376*, 498 – 500.
[199] D. R. Smith, J. B. Pendry, M. C. K. Wiltshire, *Science* **2004**, *305*, 788 – 792.
[200] Note added in proof (December 2006): Since submission of the final version of this Review, the synthesis of amylose-wrapped PPV has been reported: M. Ikeda, Y. Furusho, K. Okoshi, S. Tanahara, K. Maeda, S. Nishino, T. Mori, E. Yashima, *Angew. Chem.* **2006**, *118*, 6641 – 6645; *Angew. Chem. Int. Ed.* **2006**, *45*, 6491 – 6495.

